Parametric Study on the Seismic Performance of Typical Highway Bridges in Canada

Yuling Gao

A Thesis

in

The Department

of

Building, Civil and Environmental Engineering

Presented in Partial Fulfillment of the Requirements

for the Degree of Master of Applied Science (Civil Engineering) at

Concordia University

Montreal, Quebec, Canada

September 2014

Concordia University
School of Graduate Studies

This is to certify that the thesis prepared
By: Yuling Gao

Entitled: Parametric Study on the Seismic Performance of Typical Highway Bridges in Canada

and submitted in partial fulfillment of the requirements for the degree of

Master of Applied Science (Civil Engineering)

complies with the regulations of the University and meets the accepted standards with respect to originality and quality.
Signed by the final examining committee:

Dr. A. M. Hanna Chair

Dr. A. Bhowmick Examiner

Dr. Y. Zeng Examiner

Dr. L. Lin Supervisor

Approved by _____

Chair of Department or Graduate Program Director

_____

Dean of Faculty

Date _____

Abstract

Parametric Study on the Seismic Performance of Typical Highway Bridges in Canada

Yuling Gao

Earthquakes are one of the main natural hazards that have caused devastations to bridges around the world. Given the observations from past earthquakes, substantial analytical and experimental research work related to bridges has been undertaken in Canada and other countries. The analytical research is focussed primarily on the prediction of the seismic performance of existing bridges. It includes bridge-specific investigations which are mainly conducted using deterministic approach, and investigations of bridge portfolios which are based on probabilistic approach. In both cases, nonlinear time-history analyses are extensively used. To conduct analysis on a given bridge, analytical (i.e., computational) model of the bridge is required. It is known that the seismic response predictions depend greatly on the accuracy of the input of the modeling parameters (or components) considered in the bridge model.

The objective of this study is to investigate the effects of the uncertainties of a number of modeling parameters on the seismic response of typical highway bridges. The parameters considered include the superstructure mass, concrete compressive strength, yield strength of the reinforcing steel, yield displacement of the bearing, post-yield stiffness of the bearing, plastic hinge length, and damping. For the purpose of examination, two typical reinforced concrete highway bridges located in Montreal were selected. Three-dimensional (3-D) nonlinear model the bridge was developed using SAP2000. The effects of the uncertainty of

each parameter mentioned above were investigated by conducting time-history analyses on the bridge model. In total, 15 records from the earthquakes around the world were used in the time-history analysis. The response of the deck displacement, bearing displacement, column displacement, column curvature ductility, and moment at the base of the column was considered to assess the effect of the uncertainty of the modeling parameter on the seismic response of the bridge. Recommendations were made for the use of these modeling parameters on the evaluation of the seismic performance of bridges.

Acknowledgments

I wish to express my sincere gratitude to my supervisor Dr. Lan Lin for her continuous support and guidance during my graduate study. She's the most patient advisor and one of the most diligent people I have seen. The joy and enthusiasm she has for the research work was contagious and motivational for me. I hope I would be one successful woman like her.

Thanks are also due to professors for sharing their knowledge by offering courses that helped me in my study at Concordia University.

I am grateful to the love and encouragement my family gave to me. Great appreciate is due to my mother Ms. Song, Shue. Her continuous encouragement helps me a lot whenever I have difficult times.

In regards to all my friends and staffs at Concordia University.

Table of Contents

List of Tables

List of Figures

Chapter 1

Introduction

1.1 Introduction

Bridges are key components in the transportation system of a country. They are essential for providing a safe flow of traffic along highways and enabling rescue operations during emergency situations due to natural hazards, such as earthquakes or floods. The consequences due to failures of highway bridges can be devastating in terms of human casualties and economical losses. Earthquakes are one of the main natural hazards that have caused enormous devastations to bridges around the world. Typical examples are the 1989 Loma Prieta and the 1994 Northridge earthquakes in California, the 1995 Kobe earthquake in Japan, and the 1999 Chi-Chi earthquake in Taiwan, which caused collapse of, or severe damage to, a large number of bridges. The poor behaviour of the bridges during these earthquakes was attributed to deficiencies in both the design and construction of the bridges.

The lessons from these and other earthquakes around the world in terms of the seismic behaviour of existing bridges are very important for Canada. This is because strong earthquakes can also happen in Canada. The west coast of British Columbia and the Saint Lawrence valley in eastern Canada, where there are large stocks of bridges, are known to be seismically active (NRCC, 2010). In addition, many of the existing bridges (especially those built before 1980) were designed with minimum or no seismic considerations, and are

considered vulnerable to seismic motions.

Given the observations from past earthquakes around the world, substantial analytical and experimental research work related to bridges has been undertaken in Canada and other countries. The analytical research has been focused primarily on the prediction of the seismic performance of existing bridges. It includes bridge-specific investigations which are mainly conducted using deterministic approach, and investigations of bridge portfolios which are based on probabilistic approach. In both cases, nonlinear time history analyses are extensively used for the prediction of the seismic responses of the bridges considered. To conduct a nonlinear time history analysis on a given bridge, analytical (i.e., computational) model of the bridge and seismic excitations are required. Consequently, the seismic response predictions depend greatly on both the accuracy of the modeling parameters (or components) considered in the bridge model, and the characteristics of the seismic excitations used in the nonlinear analyses.

This research is focussed on the investigation of the effects of the uncertainties of the modeling parameters on the seismic response of bridges. Specifically, the parameters that will be investigated include: superstructure mass, concrete compressive strength, yield strength of the reinforcing steel, yield displacement of the bearing, post-yield stiffness of the bearing, plastic hinge length, and damping. The uncertainties of the foregoing parameters are inevitable because of different reasons. For example, the weight of the superstructure might be larger than the design value due to the forms left inside the girders during construction; the values used to define the yield displacement and the post-yield stiffness of the bearing are not provided by the manufacture. For the seismic evaluation of the existing bridges, some of the modeling parameters mentioned above can be defined based on the construction drawings,

such as, the concrete compressive strength and the strength of the steel bars. Others, for instance, the plastic hinge length, are difficult to define. Furthermore, in most of the studies on bridge portfolios, the influence of the uncertainties of the foregoing modeling parameters is included probabilistically by specifying probability distribution functions for the parameter characteristics, which are normally based on limited information.

1.2 Objective and Scope of the Study

The objective of the study is to determine the effects of the uncertainty of the modeling parameters on the seismic response of bridges. The parameters that are considered in the research include:

- Superstructure mass,
- Concrete compressive strength,
- Yield strength of the reinforcing steel,
- Yield displacement of the bearing,
- Post-yield stiffness of the bearing,
- Plastic hinge length, and
- Damping.

The response parameters used to examine the effects are,

- Deck displacement,
- Bearing displacement including both fixed bearing and expansion bearing,
- Column displacement,
- Column curvature ductility, and
- Moment at the base of the column.

To achieve the objective of the research, the following tasks are carried out in this study:

- Select minimum two existing bridges for the study.
- Develop nonlinear models of the selected bridges for use in the time-history analysis.
- Select a set of records appropriate for the seismic analysis of the bridges.
- Define the variation of each modeling parameter considered in the study.
- Conduct nonlinear time-history analysis by subjecting the bridge model to a series of seismic excitations to cover the response from elastic to inelastic.
- Perform statistical analysis on each response parameter corresponding to the variation of each modeling parameter.

1.3 Outline of the Thesis

This thesis is organized in 6 chapters. Chapter 2 presents a review of available literature related to this study. Chapter 3 describes the selection of typical bridges for use in the analysis. In addition, nonlinear modeling of the selected bridges is presented in detail in this chapter. Review of seismic hazard in Montreal and selection of appropriate earthquake records for the time-history analysis of bridges are provided in Chapter 4. The results from the nonlinear time-history analysis are discussed in Chapter 5 along with the discussion on the effects of the uncertainty of the modeling parameters on the seismic response of bridges. Finally, Chapter 6 presents the main observations and conclusions resulting from the study. Recommendations for further research are also included in the chapter.

Chapter 2

Literature Review

2.1 Introduction

The server damage to building structures and infrastructure due to 1971 magnitude 6.8 San Fernando Earthquake brought attention to the earthquake engineering community, in which seismic loads should be considered in the structural design. This earthquake may be considered as the starting point of the ongoing research and development in the earthquake safety of structures.

Many of bridges in Canada were built before 1970, and have been in service for more than 40 years. These bridges were designed with no seismic consideration. The bridges built between 1970 and 1985 also might be considered deficient for seismic resistance, because the seismic hazard levels they were designed for were much lower than those based on the current understanding of the seismic hazard. Given the forgoing considerations, it is wise to evaluate the seismic performance of the existing bridges in Canada. Two methods are currently used for such purpose. One is called deterministic approach; the other is called probabilistic approach. The former is used to conduct investigation on a specific bridge with a given number of spans, span length, types of bearings, foundation types, and so on. The latter is used to evaluate the seismic performance of bridge portfolios. In both methods, fragility curves are commonly used to evaluate the seismic performance of bridges.

2.2 Development of Fragility Curves

Fragility curves present the probabilities of a structure or a structure component reaching and/or exceeding different damage states under a series of ground motions. A simple expression of the fragility curves is given in Nielson (2005),

$$Fragility = P\,[LS \mid IM = y] \tag{2.1}$$

where,

P = damage probability

LS = limit state (i.e., a given damage state)

IM = intensity measure for the ground motion (e.g., PGA)

y = a given level of the ground motion (e.g., PGA = 1.0g)

The peak ground acceleration (PGA) of a ground motion was a commonly used IM in the past for the development of fragility curves of bridges (Nielson, 2005; Pan et al., 2007 and 2010; Tavares et al., 2012). It was based on the assumption that the period of bridges was generally quite short. According to HAZUS (FEMA, 2003), the limit state (also known as damage state) is defined as slight damage, moderate damage, extensive damage, and complete damage. Definitions of damage states mentioned above are given in Table 2.1. For illustration, Figure 2.1 shows fragility curves of a typical multi-span continuous concrete bridge in centre and southeastern U.S. developed by Nielson (2005).

Table 2.1 Definitions of damage states given in HAZUS (FEMA, 2003).

No damage	No damage to the structure.
Slight/minor damage	Minor cracking and spalling of the abutments, cracks in shear keys at abutments, minor spalling and cracks at hinges, minor spalling of the column (damage requires no more than cosmetic require), or minor cracking of the deck.
Moderate damage	Any column experiencing moderate (shear cracks) cracking and spalling (column still sound structurally), moderate movement of the abutment (<50 mm), extensive cracking and spalling of shear keys, any connection having cracked shear keys or bent bold, keeper-bar failure without unseating, rocker-bearing failure, or moderate settlement approach.
Extensive damage	Any column degrading without collapse – shear failure – (column structurally unsafe), significant residual movement at connections, or major approach settlement, vertical offset of the abutment, differential settlement at connections, shear-key failure at abutment.
Complete damage	Any column collapsing and connection losing all bearing support, which may lead to imminent deck collapse or tilting of substructure due to foundation failure.

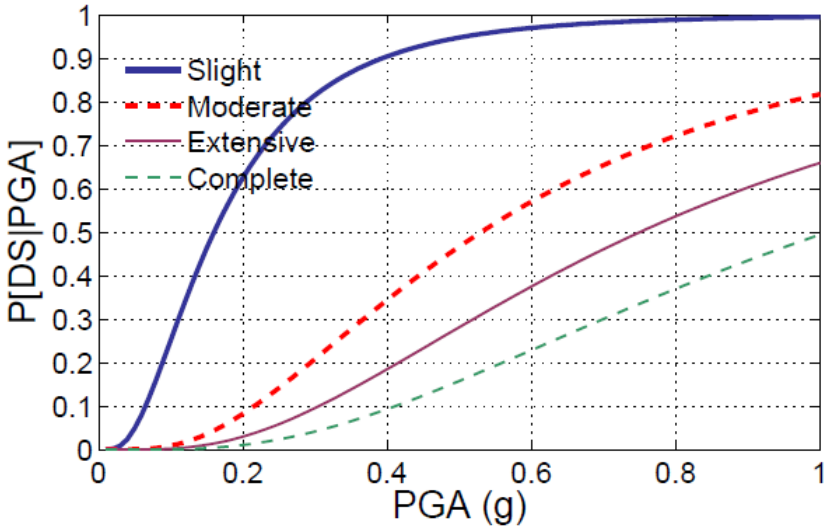

Figure 2.1 Fragility curves for a typical multi-span continuous concrete bridge (Nielson, 2005).

A complete mathematical function of the fragility curves can be found in the literature, such as, Shome (1999), Melchers (2001), Miranda & Aslani (2003), Baker & Cornell (2005), etc. As an example, the function used in Melchers (2001) is given in Equation 2.2,

$$P_f = \Phi\left[\frac{\ln S_d / S_c}{\sqrt{\beta_d^2 + \beta_c^2}}\right] \tag{2.2}$$

Where,

$\Phi[\cdot]$ = the standard normal distribution function,

S_d = the median value of seismic demand in terms of a chosen ground motion intensity parameter, $S_d = aIM^b$ (Cornell et al., 2002) in which a and b are the regression coefficients,

S_c = the median value of the structural capacity defined for the damage state,

β_d = logarithmic standard deviation for the demand,

β_c = dispersion or lognormal standard deviation of the structural capacity.

The major sources of uncertainties in the development of fragility curves using deterministic method include the ground motion records used as seismic excitations, properties of the materials, and the modeling parameters, such as, stiffness of the bearing, plastic hinge length of the column, etc. It is very clear that the deterministic approach cannot be used to evaluate the performance of bridge portfolios in a region because it is not realistic to conduct structural analysis on each bridge given a wide variety of bridge configurations.

To overcome the disadvantage of using the deterministic approach on the seismic assessment of bridges in a large population, the probabilistic approach was established recently (Neilson, 2005). To apply this approach, bridges in a region are first divided into several

groups. This can be done by considering the following structural characteristics (FEMA, 2003) (i) span continuity: simply supported, continuous; (ii) number of spans: single- or multiple-span; (iii) material of construction: concrete, steel; (iv) pier type: multiple-column bents, single-column bents, and pier walls; (v) abutment type: monolithic, non-monolithic; and (vi) bearing type: high rocker bearings, low steel bearings and neoprene rubber bearings, such that bridges in each group are represented by *a generic bridge*. Then each generic bridge will be analysed individually based on the typical values of the modeling parameters of the group. The corresponding fragility curves for each generic bridge can be developed using Eq. 2.2. The effects of the modeling parameters of each individual bridge, such as, material properties, span length, thickness of the superstructure, height of the pier, etc. are taken into account probabilistically by using Monte Carlo method. It can be seen that the probabilistic approach is not only more complicated than the deterministic method, but also larger uncertainties are involved in the analysis.

2.3 Review of Previous Studies

A number of parametric studies were conducted in the past to evaluate the effects of several modeling parameters on the seismic response of bridges in North America. Hwang et al. (2001) selected a four-span continuous concrete girder bridge in Central United States to investigate the sensitivity of characteristics of ground motions including the earthquake magnitude and distance, soil properties, properties of materials (concrete and reinforcing bars), stiffness of springs used to model the foundation and abutments. The column curvature and bearing displacement were selected as global response parameters to exam the performance of bridges. They reported that bearings and columns are very sensitive to earthquake ground motions.

Choi et al. (2004) conducted a study on the effects of the material properties on four typical bridges in Central and Southeastern United States. The bridges considered in the study were multi-span simply supported steel girder bridge, multi-span continuous steel girder bridge, multi-span simply supported pre-stressed concrete girder bridge, and multi-span continuous pre-stressed concrete girder bridge. They concluded that fixed bearing in multi-span simply supported steel girder-type bridges is more vulnerable to earthquake than any other components. They also suggested that all major components including the deck, bearing, expansion joint, and column should be taken into consideration in the development of fragility curves.

Nielson (2005) carried out a comprehensive study on development of fragility curves for nine generic highway bridges. They are (i) multi-span simply supported concrete girder bridge, (ii) multi-span simply supported concrete box-girder bridge, (iii) multi-span simply supported slab bridge, (iv) multi-span continuous concrete girder bridge, (v) multi-span continuous slab bridge, (vi) multi-span simply supported steel girder bridge, (vii) multi-span continuous steel girder bridge, (viii) single span concrete girder bridge, and (ix) single span steel girder bridge. A number of uncertainties considered were in the study, such as, bearing stiffness, coefficient of friction of the bearing, translational and rotational stiffness of the foundation, direction of seismic excitation, gap width, etc. These uncertainties were considered in the development of so-called system fragility curves by using Monte-Carlo simulation. The fragility curves show that steel girder-type bridge is the most vulnerable bridge among all the nine bridges considered followed by concrete girder-type bridge.

Padgett et al. (2007) performed analysis on multi-span simply supported steel girder bridge located in Central and Southeastern United States. The purpose of the study was to

investigate the effects of the restrainer cables (e.g., yield strength of cable, slack in restrainer cable, and restrainer cable length), effective stiffness of elastomeric bearings, yield strength of the steel jackets, and the reinforcing of the shear keys on the behaviour of the bridge. They found that the direction of the seismic excitation has significant effects on the bridge response in addition to the bearing stiffness, rotational stiffness of the foundation, and the gap width.

Pekcan et al. (2008) compared analysis results using a detailed finite element model (FEM) and a simplified beam-stick model on a three-span continuous concrete box-girder bridge. They reported that the simplified model was better than the FEM if the skew angle of the bridge is larger than 30 degrees. On the other hand, FEM is preferable for analyzing bridges with relatively larger skew angle (i.e., skew > 30 degrees) in order to capture higher mode effects. In addition, they evaluated the bridge performance under different skew angles from 0 to 60 degrees, and concluded that bridge response would increase significantly if the skew angle is larger than 30 degrees. In general, the structural response changes slightly when the skew angle is less than 30 degrees. Similarly, Abdel-Mohti (2010) investigated the effect of skew angle on the seismic response of three reinforced concrete box-girder bridges. However, the observations are different from those given in Pekcan et al. (2008). Abdel-Mohti (2010) reported that the bridge deformations and forces increase with the increasing of the skew angle.

Very recently, Pan et al. (2010) conducted a parametric study on a 3-span simply supported steel girder bridge (it is a generic bridge) in New York using a set of artificial accelerograms. The parameters considered in the sensitivity analysis were the superstructure weight, gap size, concrete compressive strength, yield strength of the reinforcement, fraction coefficient of the expansion bearing. It is necessary to mention that only one response parameter, i.e., pier curvature ductility, was used to exam the effect of each of the parameters

mentioned above on the response of the bridge. They reported that increasing the superstructure weight would lead to larger curvature ductility. In addition, the pier curvature ductility decreases with the concrete compressive strength and the yield strength of the reinforcing bars. They also found that the bridge response is less sensitive to the concrete compressive stress as compared to the yield strength of the steel.

Few studies on the development of fragility curves of typical highway bridges in Canada were performed in the last decade. The latest one was conducted by Tavares et al. (2012), which provides the fragility curves of typical highway bridges in Quebec. Five generic bridges including the multi-span continuous slab bridge, multi-span continuous concrete girder bridge, multi-span continuous steel girder bridge, multi-span simply supported concrete girder bridge, and multi-span simply supported steel girder bridge were considered in the analysis. This study is very similar to the one carried out by Neilson (2005) in which the uncertainties of the modeling parameters were taken into account by using Monte-Carlo method. It was concluded that the stiffness of abutment (both rotational stiffness and translational stiffness) did not have significant effect on the seismic response of the bridge. Both columns and elastomeric bearings would sustain severe damage at lower excitation levels which suggests higher ductility of these two components is required for the design. Another finding given in Tavares et al. (2012) is the abutment wing wall became fragile at relatively high intensity levels compared to other components in the bridge.

Some studies focused on investigation the effects of a specific modeling parameter on the seismic response of bridge. For example, Dicleli & Bruneau (1995) assessed the effect of number of spans on the response of bridges. Two continuous bridges were used in the study. One had two spans, and the other had three spans. Dynamic analysis was conducted using only

one earthquake record given the earlier stage of research on earthquake engineering. Therefore, further research is needed by considering other types of bridges (such as simply-supported bridges) and using more records in the time-history analysis in order to draw a solid conclusion on the effect of number of spans on the seismic response of bridges.

Aviram et al. (2008a) conducted a comprehensive study on the modeling abutments. In their study, three types of abutment model were developed, which are designated as roller, simplified, and spring abutments, respectively. The simple roller abutment model consists of only single-point constraints (in the vertical direction). The comprehensive spring abutment model contains discrete representations of the behaviour of backfill, bearing pad, shear key, and back wall. The simplified model is a compromise between the simple roller model and the comprehensive spring model. They recommend using a spring model for abutments for short-span bridges. In most of the research on the seismic assessment of bridges, the stiffness of abutments was determined based on the recommendations given in Caltrans Seismic Design Criteria (SDC) (2013). Willson & Tan (1990) also proposed simple formulae for determining translational and rotational stiffness of abutment in both longitudinal and transverse directions.

Avşar (2009) investigated the effects of the incident angle of seismic motions on the bridge response and reported that for two-component horizontal excitations, the largest response of typical (non-curved) bridges is obtained when one component acts in the longitudinal direction of the bridge and the other component acts in the transverse direction. In another word, there is no need for assuming a random incident angle of the seismic excitation, as used in some studies.

Chapter 3

Description and Modeling of Bridges

3.1 Introduction

It is known that bridges can be categorized into different groups according to

- Span continuity, i.e., simply-supported or continuous,
- Number of spans, such as, single-span or multi-span,
- Material of construction, e.g., concrete, steel or composite material,
- Pier type, such as, wall-type pier or column bent,
- Abutment type, i.e., U-type abutment, seat-type abutment, etc.,
- Bearing type, e.g., steel bearing, elastomer bearing, etc.

Given the variety of bridges in Canada and for the purpose of this study, it is important to select bridges that are representative of typical highway bridges for the analysis. Note that the typical highway bridges are referred to the short- and medium-span bridges, not the long-span bridges in which the maximum span length is greater than 150 m according to the Canadian Highway Bridge Design Code (CHBDC, 2006). As reported by Tavares et al. (2012), there are about 2672 multi-span bridges in Quebec in which 25% of them are multi-span simply supported (MSSS) concrete girder-type bridges, 21% are multi-span continuous (MSC) concrete girder-type bridges, 11% are multi-span continuous (MSC) slab bridges, 7% are multi-span continuous (MSC) steel girder-type bridges, and 8% are multi-span simply supported (MSSS) steel girder-type bridges. The typical cross section of the superstructure of each type of bridges

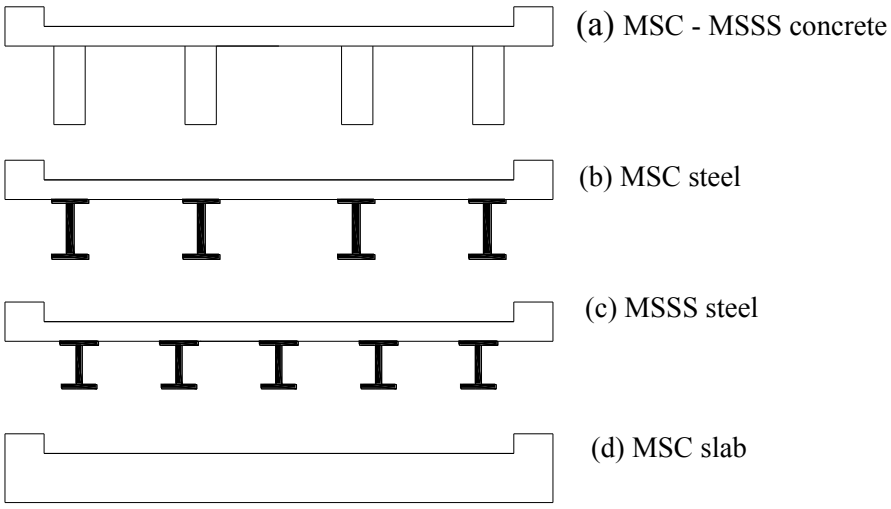

Figure 3.1 Typical bridge classes in Quebec (Adopted from Tavares et al., 2012).

mentioned above is shown in Fig. 3.1. It is necessary to mention that seismic analysis is not required for one-span simply supported bridges according to CHBDC (2006) due to the fact that the seismic forces are resisted by abutments which have quite large lateral stiffness. Consequently, the superstructure of these bridges is not vulnerable to the seismic loads. Tavares et al. (2012) also found that most of the bridges in Quebec have three spans with seat-type abutments sitting on shallow foundations. In terms of the column bents, they reported that wall-type columns, circular columns, and rectangular columns are commonly used. Given these, two bridges located in Montreal were selected for this study. The first bridge is a three-span continuous concrete girder-type bridge, and the second one is a three-span continuous concrete slab bridge. For ease of discussion, these two bridges are referred to as Bridge #1 and Bridge #2 in the study, respectively. Figures 3.2 and 3.3 show the geometric configurations of two bridges. Detailed characteristics of the selected bridges are described hereafter.

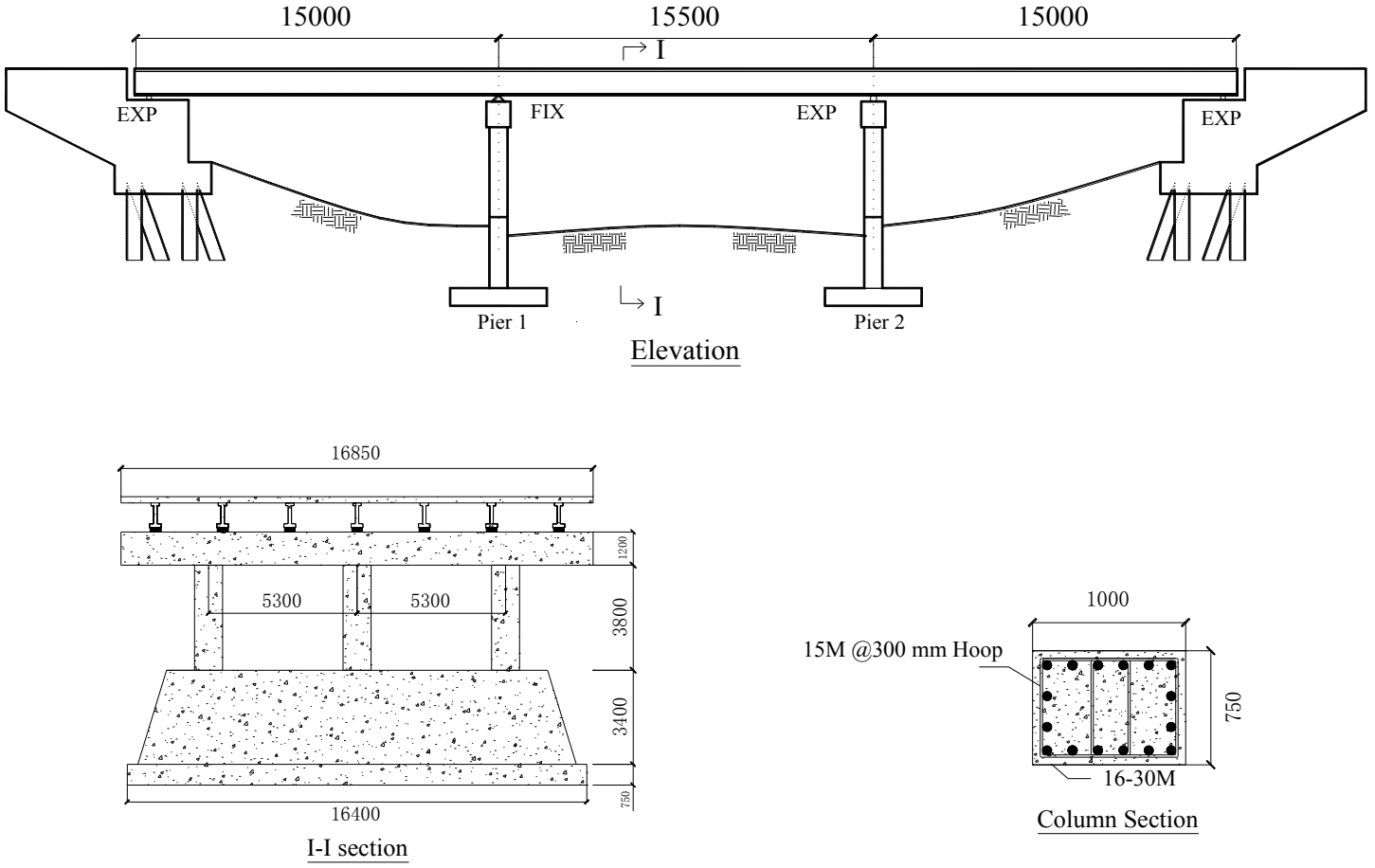

Figure 3.2 Geometric configuration of Bridge #1.

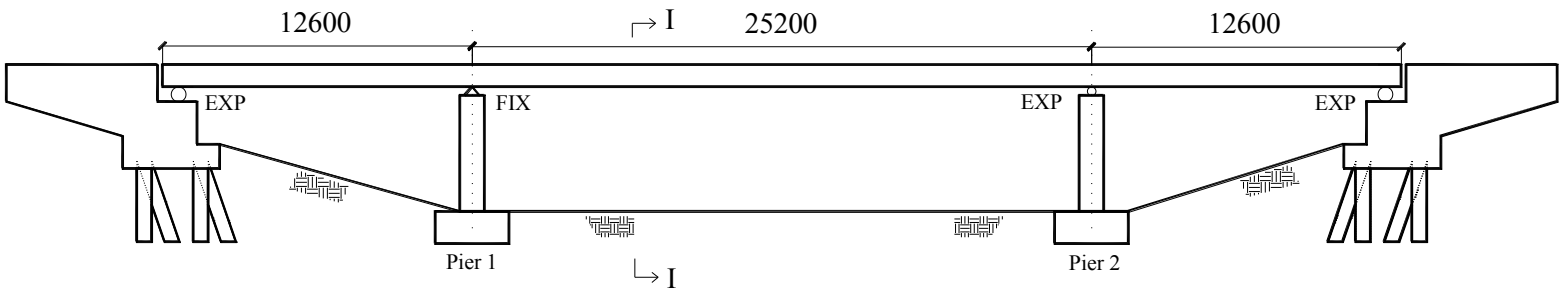

Elevation

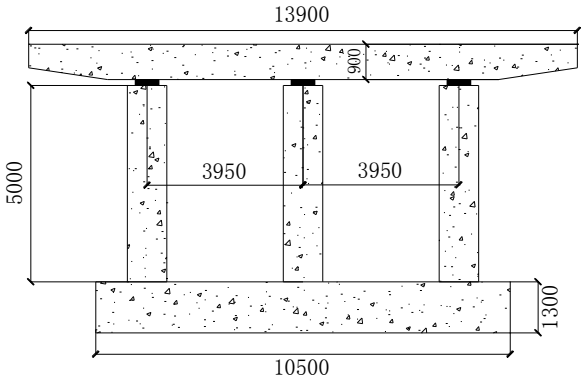

I-I section

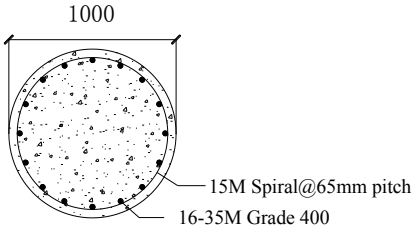

Column Section

Figure 3.3 Geometric configuration of Bridge #2.

3.2 Description of Bridges

3.2.1 Bridge #1

Bridge #1 was built in the 1980s and consists of three continuous span without skew. As presented in Fig. 3.2, the middle span of the bridge is 15.5 m, and the two end spans are 15 m. The overall deck width is 16.85 m. The superstructure consists of a 0.225 m thick reinforced concrete slab and seven 0.9 m C.P.C.I (Canadian Precast Prestressed Concrete) prestressed girders at a spacing of 2.4 m. The concrete deck is reinforced with 30M bars on the top and the bottom. Each C.P.C.I girder consists of 6 straight tendons and 8 parabolic tendons on the bottom across each span. Each prestressing tendon is composed of 7 Grade-1860 wire strands. The jacking force per strand at the final stage is 145 kN, and it is lowered down to 116 kN when the losses are considered. Such losses include the losses due to elastic shortening, creep, shrinkage, friction loss, etc.

The cross section of the cap beam is 1 m wide, and 1.2 m deep. The multi-column bents consist of three rectangular columns. The center-to-center spacing between columns is 5.3 m. The dimensions of each column are 1 m (in the transverse direction) x 0.75 m (in the longitudinal direction). The average height of the column is 3.8 m. Each column is reinforced with 16-30M bars providing longitudinal reinforcement ratio of 1.49%. Column ties with 15M at a spacing of 300 mm were used as transverse reinforcement. The transverse reinforcement ratio is about 0.24%. Strip footing is used for the column bents.

Seat-type abutments are on pile foundations as shown in Fig.3.2. The width of the abutment back wall is 16.85 m, which is as wide as the superstructure. The height of the back wall is 1.5 m, and the length of the wing wall is 5 m.

For the deck and columns, the compressive strength of concrete is 30 MPa. For the girders, it is 35 MPa whereas it is 20 MPa for the cap beam. No information could be obtained from the original bridge drawings on the stress of the reinforcing steel used in the structure. Therefore, the yield strength of the reinforcement is assumed to be 400 MPa.

As shown in Fig. 3.2, expansion bearings, which allow both translation and rotation, are used on the abutments and pier 2. Fixed bearings, which allow translation only (i.e., not rotation), are used on the pier 1. Due to the lack of information on the type of bearings used in the bridge, elastomeric bearings are considered given their good performance against the seismic loads (Pan et al., 2010; Fu, 2013), and they were designed according to CHBDC (2006). The requirements specified in AASHTO (2014) are also used to finalize the bearing design. More specifically, the bearings designed satisfy the following requirements:

- Maximum instantaneous compressive deflection,
- Bearing maximum rotation,
- Bearing combined compression and rotation including uplift requirement and shear deformation requirement,
- Bearing stability.

Rectangular elastomeric bearing (450 mm x 350 mm x 100 mm) is used on the bottom of each girder at the abutments and piers. Each bearing consists of 4 layers of the steel plate and 6 layers of elastomer. The thickness of the steel plate is 2 mm, and the total thickness of the elastomer is 80 mm. It is necessary to mention that both fixed bearings and expansion bearings have the same size. As illustrated in Figs. 3.2 and 3.3, the fixed bearing and expansion bearing are drawn as triangle and circular shapes, respectively.

3.2.2 Bridge #2

Bridge #2 was also built in the mid-1980s. It has three spans which are 12.6 m, 25.2 m, and 12.6 m, respectively for a total length of 50.4 m, as shown in Fig. 3.3. The bridge has no skew (i.e., it is a straight bridge). The overall width of the bridge is 13.6 m. The superstructure consists of a continuous, voided prestressed concrete slab. The thickness of the slab is 90 cm. The prestressing force is provided by 14 parabolic cables in the longitudinal direction of the bridge, each cable consists of 19-0.5 inch diameter strands and 16-0.6 inch diameter strands. The slab is also prestresses in the transverse direction using 9 cables at the end span, and 20 cables at the middle span, in which each cable is composed of 4-0.5 inch diameter strands and 16-0.6 inch diameter strands. The jacking force of each cable at the final stage is 1100 kN.

The column bent has three circular columns. The diameter of each column is 1 m, and the average height of the column is 5 m. the distance between center to center of columns is 4.25 m. As illustrated in Fig.3.3, the longitudinal reinforcement of the column consists of 16-35M (d_b = 35.7 mm) bars which provide a reinforcement ratio of 2.95%. The transverse reinforcement consists of a No. 15 (d_b = 16 mm) spiral with a pitch of 65 mm. The confinement steel ratio is 1.33%.

Seat-type abutments are also used at the ends of the bridge. The width of the abutment back wall is 9.9 m and the height is 1.5 m. the length of the wing wall is 5.9 m. the foundations of both the column bents and abutments are strip footing on rock.

The compressive strength of the concrete used for the slab is 35 MPa, while for the columns and foundations is 30 MPa. Like Bridge #1, the yield strength of the steel is also assumed to be 400 MPa.

Rectangular elastomeric bearings with 600 mm x 600 mm x 130 mm are chosen to place on the top of each column at the abutments and piers. The bearing consists of 5 layers of the steel plate with the thickness of 2 mm each layer. The total thickness of the elastomer is 40 mm. Fixed bearings are used on the Pier 1, and expansion bearings are used on the abutments and Pier 2 (Fig. 3.3). The fixed bearings and the expansion bearings also have the same size like Bridge #1.

3.3 Modeling of Bridges

In this study, three-dimensional finite element models were developed by using the structural analysis software SAP2000 (CSI, 2012) for the purpose of analyses. SAP2000 has been used in a number of studies on the evaluation of bridges subjected to seismic loads (Shafiei-Tehrany, 2008; Pan et al., 2010; Waller, 2010; etc.). The advantage of SAP2000 is a number of elements (e.g., link element) are available which can be used to model the nonlinearity of different components of a bridge system including bearings and plastic hinges during seismic excitations. It is necessary to mention that another program OpenSees (McKenna & Feneves, 2005) can also be used for the nonlinear analysis of bridges. However, a study conducted by Aviram et al. (2008a) showed that these two programs provide very similar results. SAP2000 was selected for this study due to its simplicity in modeling and less time-consuming in the analysis compared with OpenSees.

3.3.1 Superstructure

A spine model shown in Fig. 3.4 was used to model the superstructure for each bridge considered in this study. According to the capacity design method specified in AASHTO (2014) and CHBDC (2006), the superstructure of the bridge system should remain elastic during

earthquake events. Therefore, the superstructure was modeled using elastic beam elements located along the centroid of the superstructure. Each span of the bridge is discretized into 10 equal segments in order to achieve higher accuracy of the results. It is necessary to mention that a minimum number of four elements per span are required for modeling the superstructure according to ATC-32 (1996). The properties of superstructure (i.e., the cross-sectional area, moment inertia, shear area, torsional constant, etc.) of each bridge were defined using "Section Designer" which is an integrated utility built into SAP2000. For illustration, Figures 3.5a and 3.5b show the typical geometric properties of the Bridge #1 and Bridge #2 considered in this study, respectively. It is known that both the flexural moment of inertia and the torsional moment of inertia have significant effects on the bridge response. In this study, a factor of 0.75 was used to reduce the moment of inertia of the deck section, and no reduction factor was applied to the girder sections as recommended by Caltrans SDC (2013). Reduction of the torsional moment of inertia was not considered given the regularity of the bridge according to Caltrans SDC (2013).

The total mass of the bridge was lumped to the nodes of the superstructure. It is necessary to mention that the weight of the cap beams (for Bridge #1) and the half weight of the column bents were lumped to the nodes of the superstructure (i.e., nodes in the longitudinal direction X-X, Fig. 3.4) at the Piers 1 and 2. Note that the translational mass lumped to each node can be calculated by the program itself, and it is assigned to each of the three global axes (X, Y, and Z as shown in Fig. 3.4). However, the rotational mass (i.e., the rotational mass moment of inertia) cannot be calculated by the program itself, i.e., it must be calculated manually. The rotational mass moment of inertia of the superstructure can be determined using Equation 3.1,

$$M_{xx} = (Md_w^{\,2})/12 \tag{3.1}$$

Where

M_{xx} = mass of moment inertia of superstructure in the global X-X direction,

M = total tributary mass of the superstructure segment,

d_w = width of the superstructure.

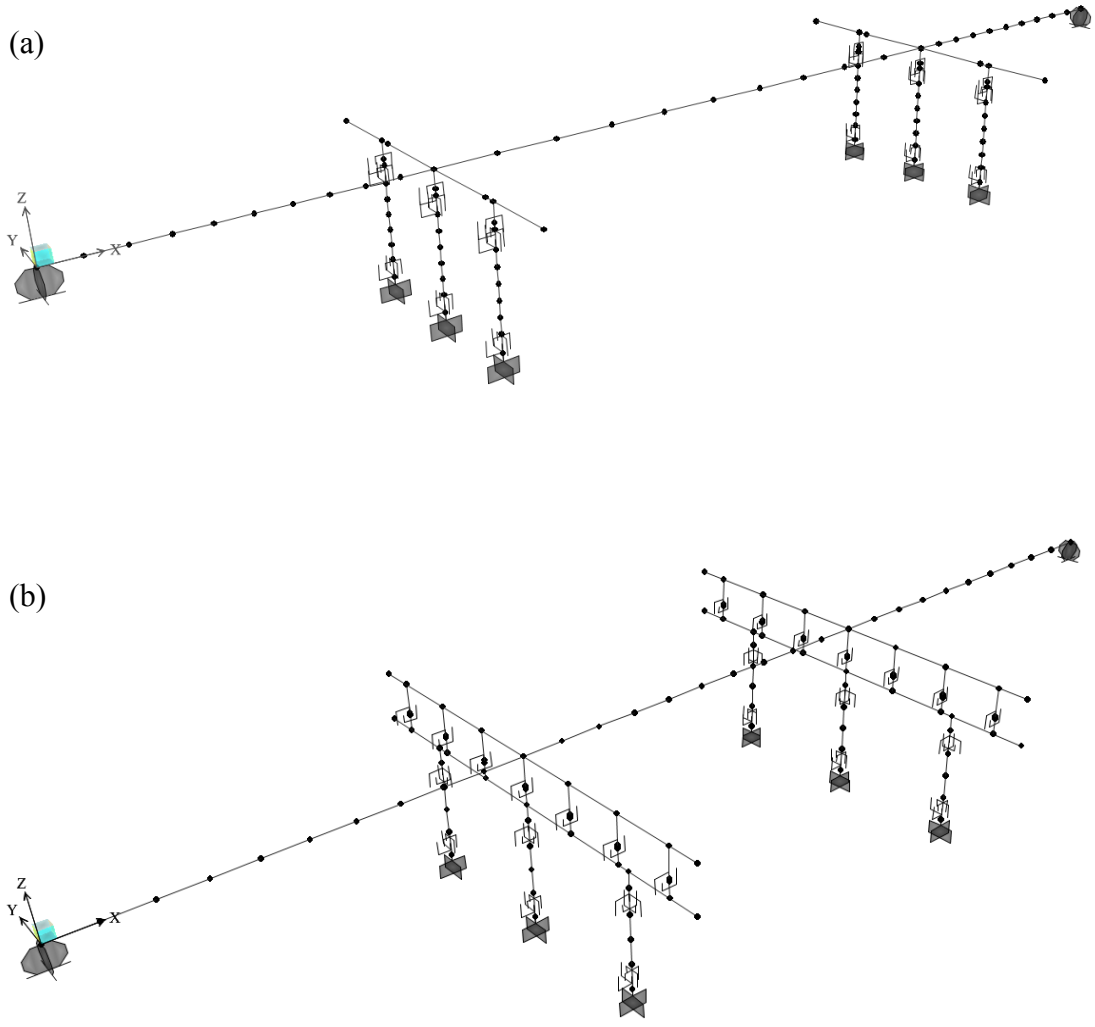

Figure 3.4 Scheme of the spine models in SAP2000, (a) Bridge #1; (b) Bridge #2.

(a)

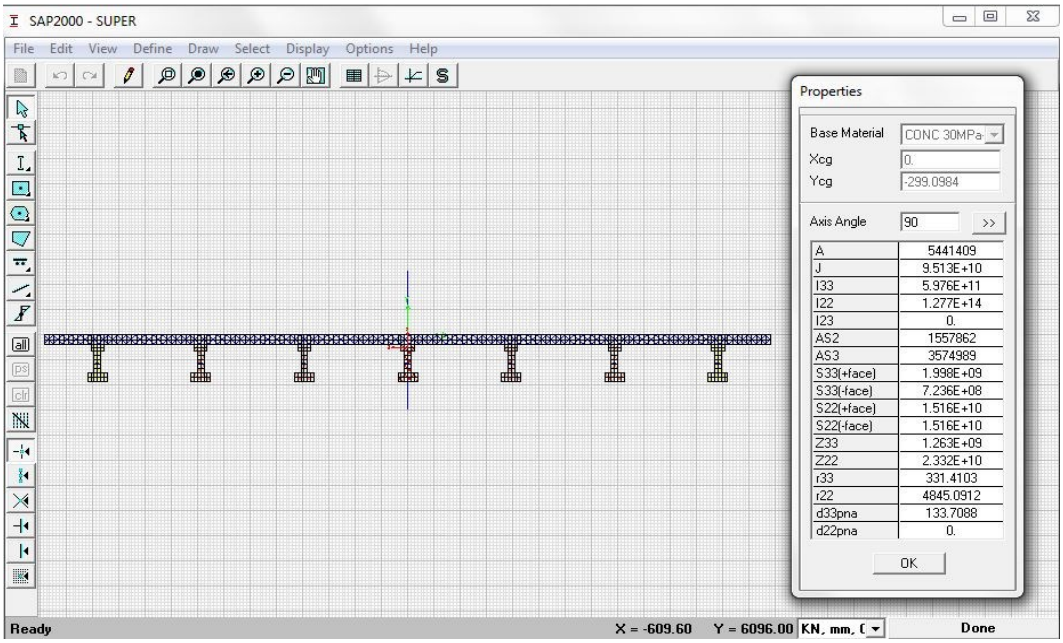

(b)

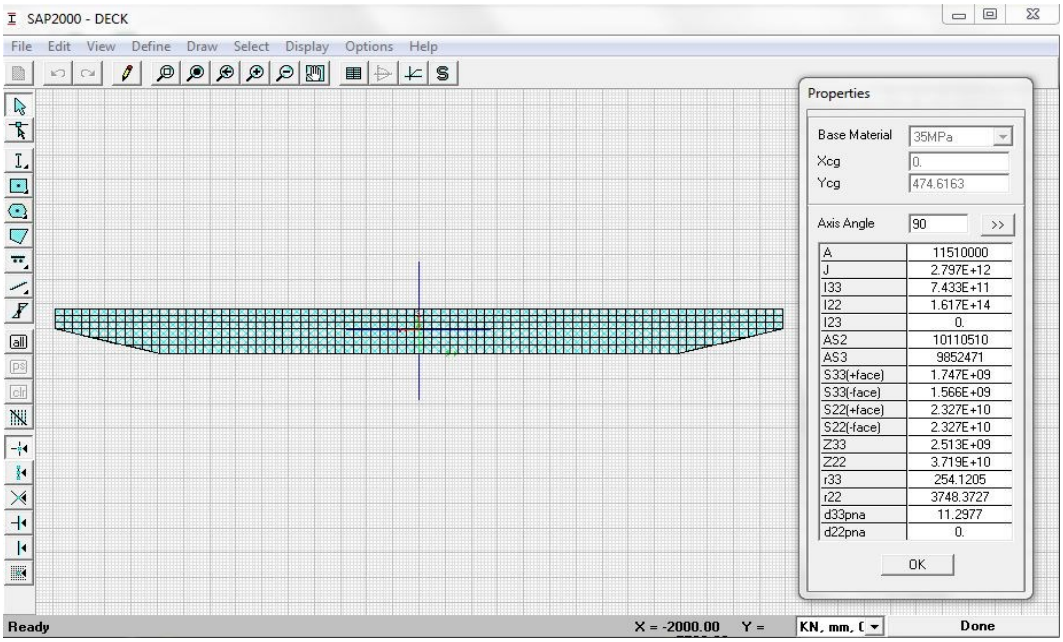

Figure 3.5 Determination of the geometric properties of the superstructure of bridge models using Section Designer in SAP2000, (a) Bridge #1; (b) Bridge #2.

3.3.2 Bearing

As described in the Section 3.1 "Description of Bridges", two types of elastomeric bearings are used in the bridges, they are fixed bearings and expansion bearings. Fixed bearings only allow the rotation of the superstructure relative to the substructure, while expansion bearings allow both rotation and translation movements. In this study, behavior of the bearing is represented by the Link Element in SAP2000. The initial lateral (K_H), vertical (K_v), and rotational (K_θ) stiffnesses of the elastomeric pads are determined using Equations 3.2, 3.3, and 3.4, respectively.

$$K_H = GA / H_r \tag{3.2}$$

$$K_V = EA / H \tag{3.3}$$

$$K_\theta = EI / H_r \tag{3.4}$$

Where

G = shear modulus, and it is taken as 0.80 MPa in this study following the recommendation of Caltrans SDC (2013),

E = modulus of elasticity of the rubber,

I = moment of inertia of the bearing,

A = plan area of the elastomeric pad,

H = thickness of the bearing,

H_r = total thickness of the rubber.

The nonlinear behavior of the elastomeric bearing in the longitudinal direction is modeled using bilinear hysteretic rule as shown in Fig. 3.6 following the recommendations made by Kelly (1997) and DesRoches et al. (2003). In Figure 3.6, K_1 and K_2 represent the

initial lateral stiffness (i.e., elastic stiffness) and the plastic stiffness, respectively. The plastic stiffness K_2 is taken as 1/3 K_1 in this study as suggested by Mander et al. (1996). In Fig. 3.6, the notations D_y and D_u in Fig. 3.6 represent the yield displacement and the maximum displacement of the bearing, respectively. Following the recommendation given in DesRoches et al. (2003) and Akogul & Celik (2008), D_u is assumed to be equal to the height of the elastomer and D_y is assumed to be 10% of D_u. In this study, the stiffness of the bearing in transverse direction is assumed to be infinite, i.e., the stiffness is about 100 times larger than that in the longitudinal direction. The parameters used to model the expansion bearings in Bridge #1 and Bridge #2 are given in Table 3.1.

Table 3.1 Parameters used in the modeling of the bilinear behavior for the expansion bearings.

Bridge No.	Bearing Size	D_y (mm)	F_y (kN)	D_u (mm)	F_u (kN)
#1	450 x 350 x 100 mm	8.0	12	75	47
#2	600 x 600 x 130 mm	5.0	35	50	142

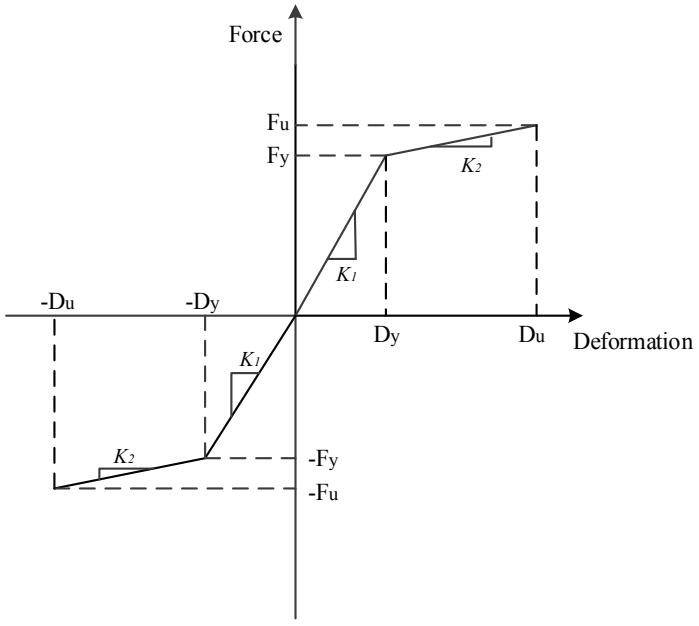

Figure 3.6 Bilinear behavior of elastomeric bearings in the longitudinal direction.

3.3.3 Columns and Cap Beams

It is expected that plastic hinges would form on the bottom and/or top of a column during larger earthquake events (Paulay & Priestley, 1992). In this study, plastic hinges were assumed on both the bottom and top of the column in accordance with the seismic provisions of the New Zealand Code (TNZ, 2003). It should be noted that the current edition of the CHBDC (2006) does not specify the location of the plastic hinge. The plastic hinge zones are modeled with nonlinear elements while the rest part of the column is modeled by elastic elements. The detail description on the modeling of the columns and cap beams is given hereafter.

3.3.3.1 Modeling the plastic hinge zone

Plastic Hinge Length

According to CHBDC (2006), the plastic hinge length L_p shall be taken as the maximum value of (i) the maximum cross-sectional dimension of the column, (ii) one-sixth of the clear height of the column, and (iii) 450 mm. Therefore, the plastic hinge length L_p of the columns for Bridge #1 is considered as 1 m, and for Bridge #2 is 0.72 m (see Fig. 3.2 and 3.3), respectively. In this study, the plastic hinge length of the column was also determined using the formula provided by Caltrans SDC (2013) which is expressed in Eq. 3.5.

$$L_p = 0.08L + 0.022 f_{ye} d_{bl} \geq 0.044 f_{ye} d_{bl} \tag{3.5}$$

Where

L = height of column, in mm

f_{ye} = expected yield strength of the steel bar, in MPa

d_{bl} = diameter of a longitudinal rebar, in mm

Using Eq. 3.5, it was found that the plastic hinge length of the column of Bridge #1 was 720 mm while it was 610 mm for Bridge #2. Based on the calculation following the specifications of CHBDC and Caltrans, plastic hinge length of the column of 1.0 m was used in the model of Bridge #1, and 0.72 m was used in the model of Bridge #2.

Moment-curvature relationship for column section

For the purpose of defining the link Element which is used to simulate the behavior of the column in the plastic hinge region during larger earthquakes, moment-curvature relationships for the end sections of the column were determined using fiber analyses of the cross sections. The concrete stress-strain relationship included the effect of confinement was determined based on the model proposed by Mander et al. (1988) as shown in Fig. 3.7. This model is also recommended by ATC-32 (1996), Caltrans SDC (2013) and FHWA (2012). As shown in Fig. 3.7, the major parameters that are used to define the confined concrete stress-strain relationship are, the compressive strength of confined concrete (f_c'), the compressive stress of confined concrete (ε_{cc}), and the ultimate compressive strain (ε_{cu}). The formulas for determining these parameters can be found in Paulay and Priestley (1992).

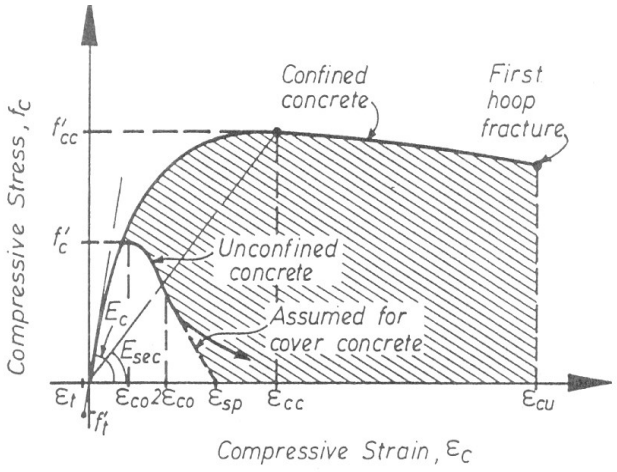

Figure 3.7 Mander Model for confined and unconfined concrete (Adopted from Paulay & Priestley, 1992).

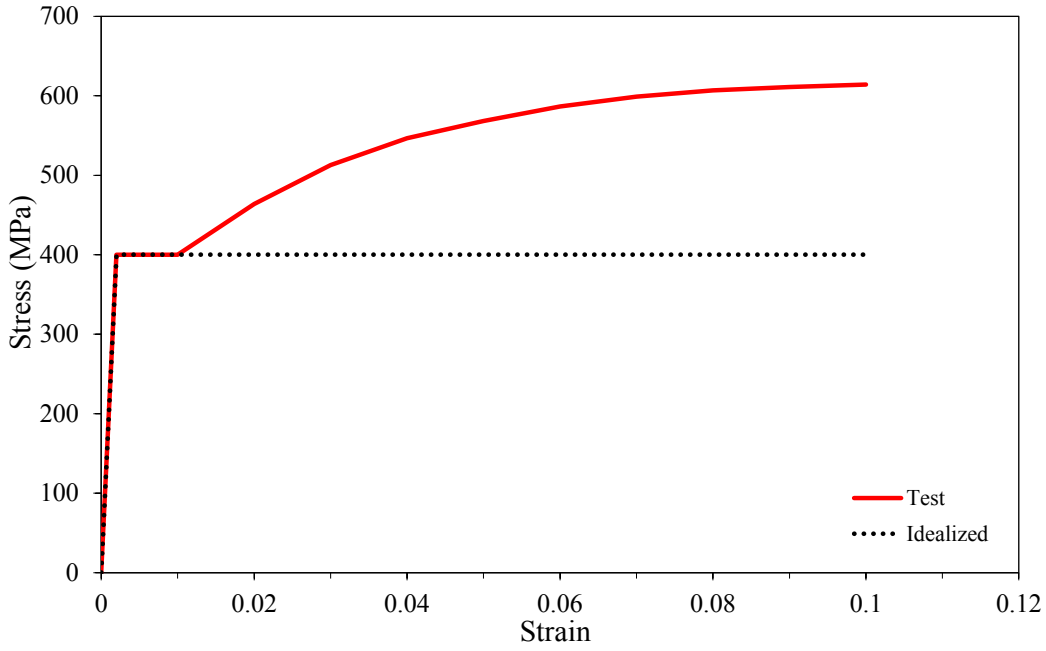

Figure 3.8 Steel stress-strain relationship given in Naumoski et al. (1993).

Figure 3.8 illustrates a typical stress-strain relationship for steel bars reported by Naumoski et al. (1993) including the strain hardening. The results from the preliminary analysis show that the strain hardening does not have effects on the response of the two bridges. Given this, an idealized bilinear stress-stain curve (dotted line in Fig. 3.8) was used in this study to model the behaviour of the steel bar.

Nominal values for the material strengths (i.e., concrete and reinforcement resistance factors $\Phi c = \Phi s = 1$) were used in the fiber analysis. The axial force used in the fiber analysis included the force resulting from the dead load only. For illustration, Figures 3.9a and 3.9b show the moment-curvature relationships for modeling the plastic hinges of the columns of the Bridge #1 and Bridge #2, respectively. The computed moment-curvature relationship was idealized by two linear segments representing the pre- and post-yielding ranges. Based on the shape of the moment-curvature relationship, a bilinear hysteretic model (i.e., Multi-linear

Kinematic Plasticity model) was selected from a number of models available in SAP2000, as shown in Fig. 3.10.

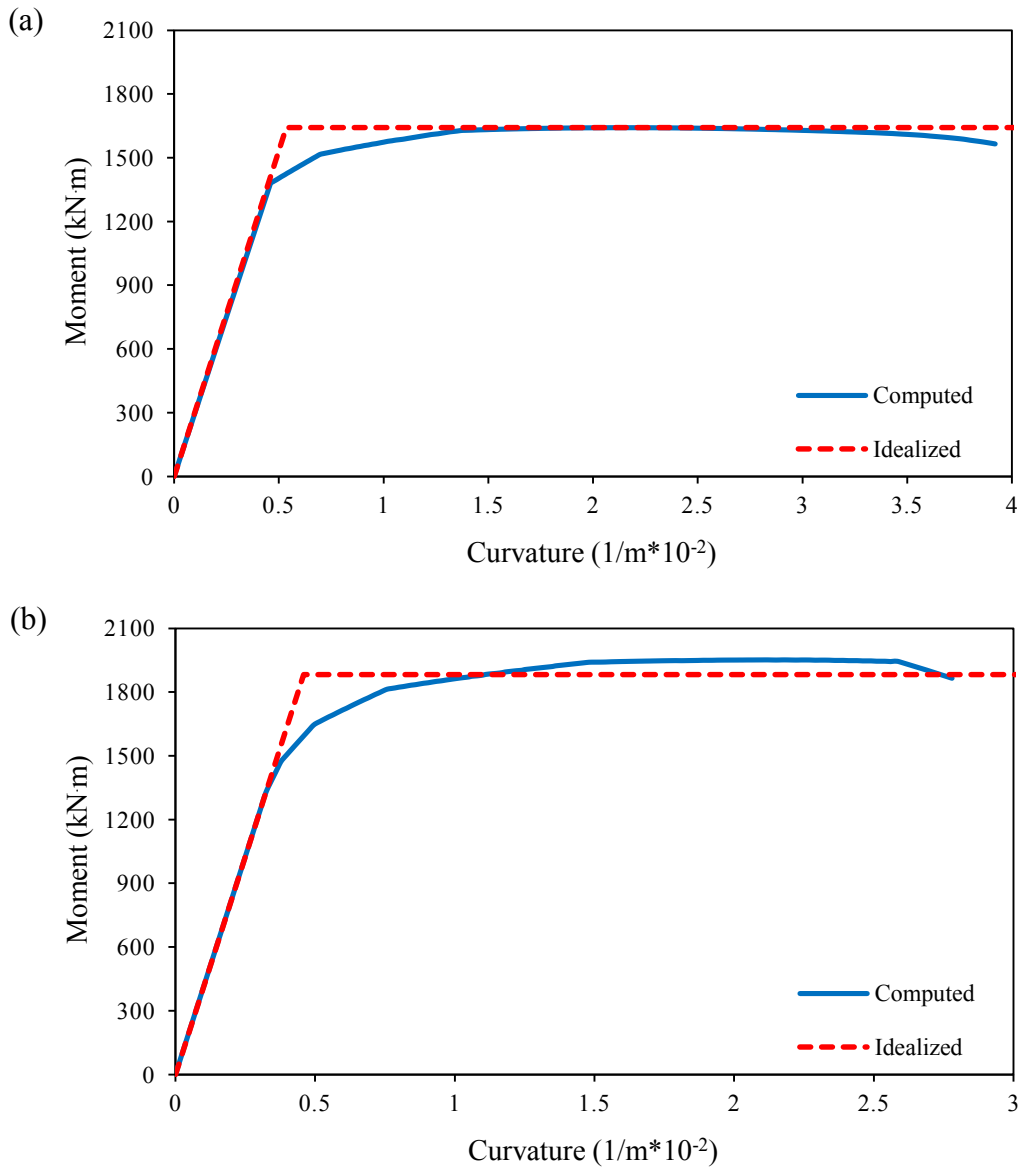

Figure 3.9 Moment-curvature curves of the column section, (a) Bridge #1; (b) Bridge #2.

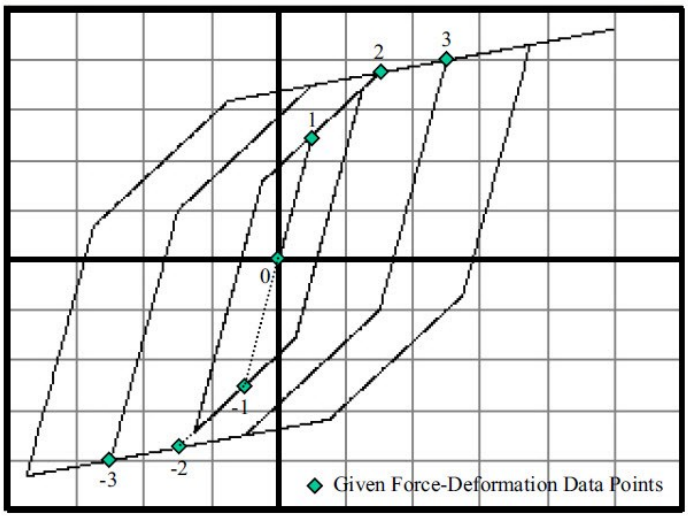

Figure 3.10 Multi-linear Kinematic Plasticity model (Adapted from CSI, 2012).

3.3.3.2 Modeling columns and cap beams

The columns are assumed to behave elastically outside the plastic hinge regions. In total, each column was divided into 5 equal length segments (See Figs. 3.4). Cap beams (for Bridge #1) were modeled as elastic beam elements, and the connections between cap beams and bearings; cap beams and columns were modeled using rigid elements as shown in Fig. 3.11.

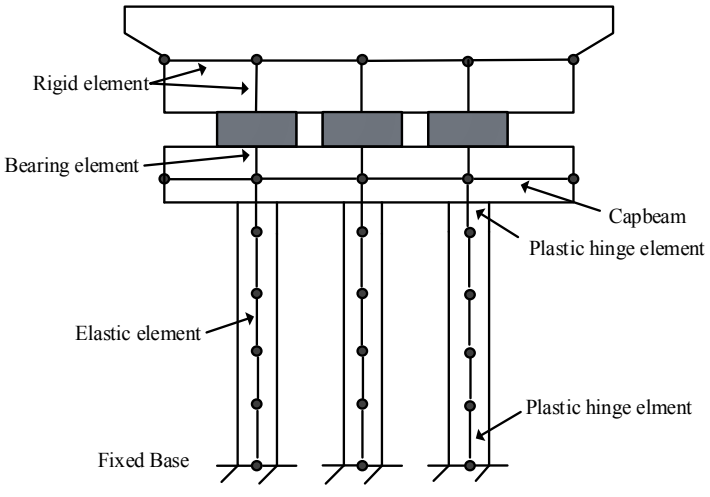

Figure 3.11 Detailed modeling of a column bent.

3.3.3.3 Material properties

In order to take into account the effect of the combined flexure and axial force, the effective shear area of the ductile concrete column was estimated by using a reduction factor of 0.8 to its gross shear area (i.e., $A_{v,\,eff} = 0.8\,A_{v,g}$) in accordance with Caltrans SDC (2013). In addition, the effective moment of inertia (I_{eff}) of column shall be calculated using Eq. 3.6 to account for the effect of concrete cracking. The two parameters for each of the two bridge models, i.e., M_y and ϕ_y, can be determined based on the idealized moment-curvature curve presented in Fig. 3.9. In this study, it was found that the effective moment inertias of the columns in Bridge #1 and Bridge #2 are about $0.331I_g$ and $0.492I_g$, respectively. Moreover, Caltrans SDC (2013) recommend a factor of 0.2 shall be applied to the torsional stiffness of column members with respect to its gross area.

$$I_{eff} = \frac{M_y}{E_c \phi_y} \tag{3.6}$$

Where

M_y = Moment corresponds to the first steel bar yields

ϕ_y = Curvature corresponds to the first steel yields

E_c = Modulus of elasticity of concrete, it is calculated by $4500\sqrt{f_c'}$

3.3.4 Abutment

Abutment modeling has a significant impact on the nonlinear response of bridges during earthquake events (Wilson & Tan, 1990). Recently Aviram et al. (2008a) conduced a comprehensive investigation of the effect of the abutment modeling on the seismic response of bridges. Three approaches for the modeling of the abutment were considered in their study,

and they were designated as roller abutment model, simplified abutment model, and spring abutment model (Fig. 3.12). For the purpose of this study, a brief description of these models is given hereafter, the detailed explanations for each of the modeling techniques can be found in Aviram et al. (2008a and 2008b).

As seen in Fig. 3.12a, the roller abutment model consists of a boundary condition that applies only constrains against the vertical displacement, i.e., the abutment is free for the translation in the longitudinal direction and rotation. Therefore, the response of this bridge model is dominated by the formation of the plastic hinges and the capacity of the columns. It is the simplest model among the three abutment models proposed by Aviram et al. (2008a).

Figure 3.12b illustrates a general scheme of the simplified abutment model. The model consists of a rigid element with its length equal to the width of the superstructure and a series of springs in the longitudinal, transverse, and vertical directions. The rigid element is connected to the centerline of the superstructure through a rigid joint. In the longitudinal direction, the simplified abutment model consists of three elements, i.e., a rigid element in which both shear and moment are released at the end, a gap element which is used to represent the gap between the superstructure and the abutment in the longitudinal direction, and a zero-length element used to represent the response of the embankment fill. The nonlinear behavior of the embankment fill is modeled using an elastic-perfectly-plastic curve, which can be defined according to Caltrans SDC (2013). In the transverse direction, a zero-length element is defined at each end of the rigid element (see Fig. 3.12b), it is used to present the response of the backfill and wing wall. Generally speaking, the nonlinear response curve of the zero-length element is similar to that defined in the longitudinal direction, however, the stiffness of abutment is modified due to the different behavior of the abutment in the longitudinal and transverse

directions. In the vertical direction, elastic spring is defined at each end of the rigid element. The stiffness of the spring is equal to the stiffness of the total bearing pads.

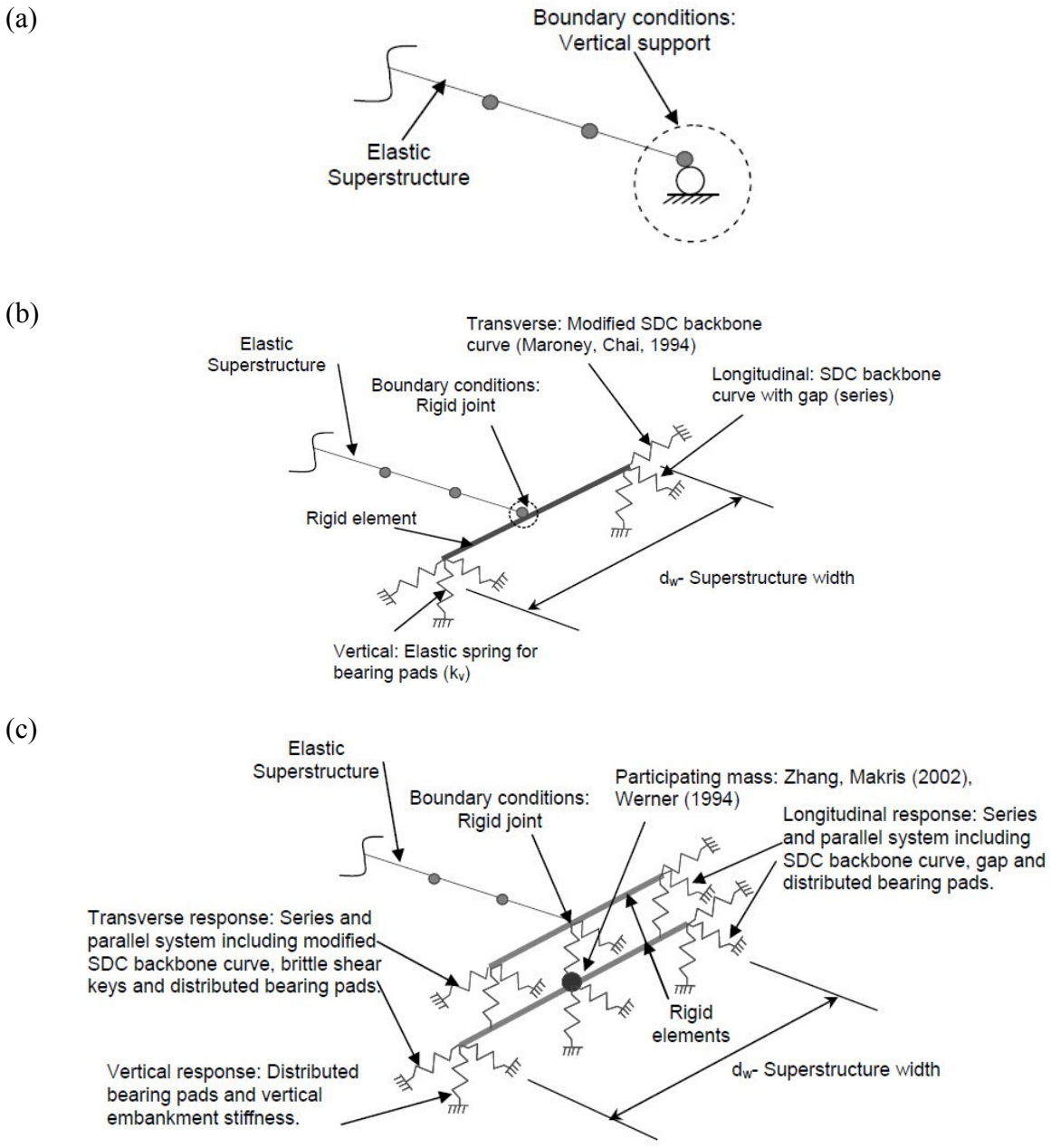

Figure 3.12 Abutment models, (a) Roller model; (2) Simplified model; (3) Spring model (Adopted from Aviram et al., 2008a).

The spring abutment model is an improved model based on the simplified abutment model, and a general scheme of the model is presented in Fig. 3.12c. The spring model considers the nonlinear response of the abutment in the longitudinal, transverse, and vertical directions while the simplified abutment model considers the nonlinear response of the abutment in the longitudinal and transverse directions (i.e., the simplified model assumes the response of the abutment in the vertical direction is linear). As shown in Fig. 3.12c, the responses of both bearing pads and embankments are considered in the modeling.

Aviram et al. (2008a) used six different types of bridges for the investigation. Nonlinear time-history analyses were conducted on each bridge by using the three abutment models described above. They concluded that the roller model provided relatively conservative results while simplified model and the spring model provided very similar longitudinal displacement. The dominant periods of the bridge obtained from these three abutment models are relatively close except that the first mode period of the bridge from the spring model is significantly smaller than that from the roller model and the simplified model. Given these and the objective of this study (i.e., selection appropriate records for use for the nonlinear time-history analysis of bridges), the roller abutment model was selected due to its lowest model complexity.

3.4 Dynamic Characteristics of the Bridge Models

In this study, modal analysis was conducted first on the bridge models in order to understand the dynamic characteristics of the two bridges. In total, 12 modes were considered in the modal analysis for each bridge. Rayleigh damping of 5% of critical was assigned to all the 12 modes of each bridge model. The damping was specified to be proportional to the initial stiffness of the models.

Table 3.2 provides the natural periods of the first three vibration modes of Bridge #1 model and Bridge #2 model, respectively. The mass participation factor and the modal participation factor resulting from the modal analysis are also included. It can be seen in the table the first mode period of the Bridge #1 is about 0.99 s and that of the Bridge #2 is about 0.89 s, which are very close. This is because the substructure system of the two bridges is very similar, i.e., both have two column bents in the longitudinal direction, and each column bent has three columns in the transverse direction. It can also be seen in Table 3.2 that the 2nd and 3rd mode participation factors of the Bridge #1 and the Bridge #2 model are about 0 which indicates the response of the two bridges is dominated by the first mode. Moreover, the results in Table 3.2 show that for Bridge #1, the mass participation factor is about 0.93 for longitudinal direction, while for Bridge #2, is about 0.98, i.e., for both bridge models, more than 90% of the mass participated in the dynamic analysis.

Figure 3.13 illustrates the mode shapes of the first three modes for Bridge #1 and Bridge #2. It can be seen clearly in Fig. 3.13 that the first mode shape is dominated by the vibration in the longitudinal direction for both bridges. Regarding the second mode shape, both bridges are dominated by torsion, in which the vibration periods are 0.41 s and 0.80 s for Bridge #1 and Bridge #2, respectively. In terms of the third mode shape, both bridges are dominated by vibrations in transvers direction, with vibration periods of 0.27 s and 0.71 s respectively.

Table 3.2 Dynamic characteristics of the bridge models from modal analysis.

	Bridge #1					Bridge #2				
Mode	Period (sec)	MPR UX	MPR UY	MPF UX	MPF UY	Period (sec)	MPR UX	MPR UY	MPF UX	MPF UY
1	0.99	0.93	0	8.78	0	0.89	0.98	0	1.19	0
2	0.41	0	0	0	0.02	0.80	0	0	0	0
3	0.27	0	0.97	0	8.99	0.71	0	0.99	0	1.19

Note: MPR-Mass participation ratio; MPF-Modal participation factor.

(a)

Mode 1:
Longitudinal $T_1 = 0.99$ s

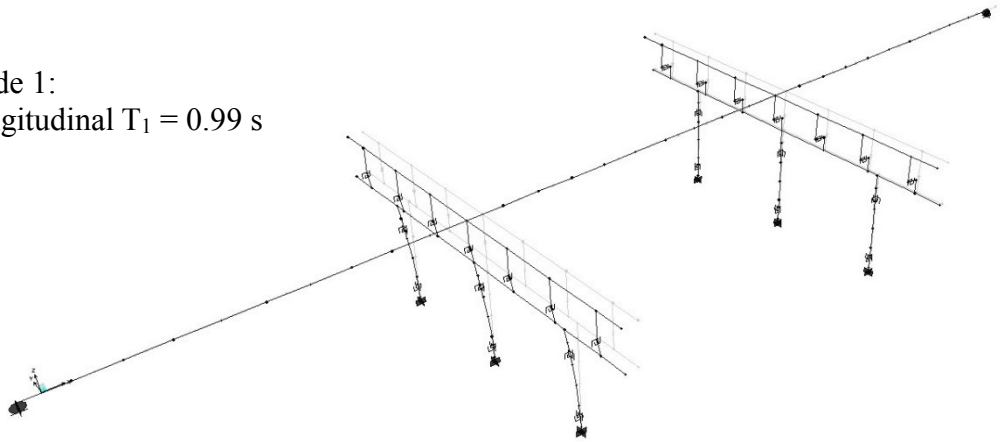

Model 2:
Torsional $T_2 = 0.41$ s

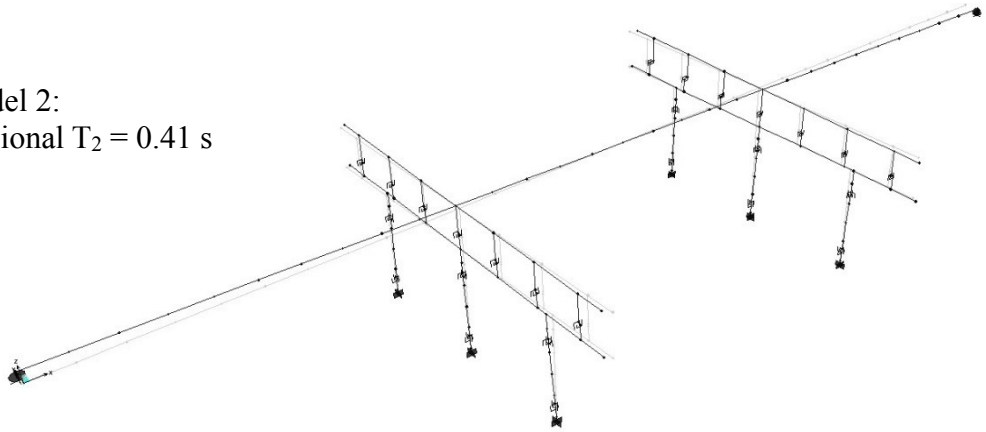

Mode 3:
Transverse $T_3 = 0.27$ s

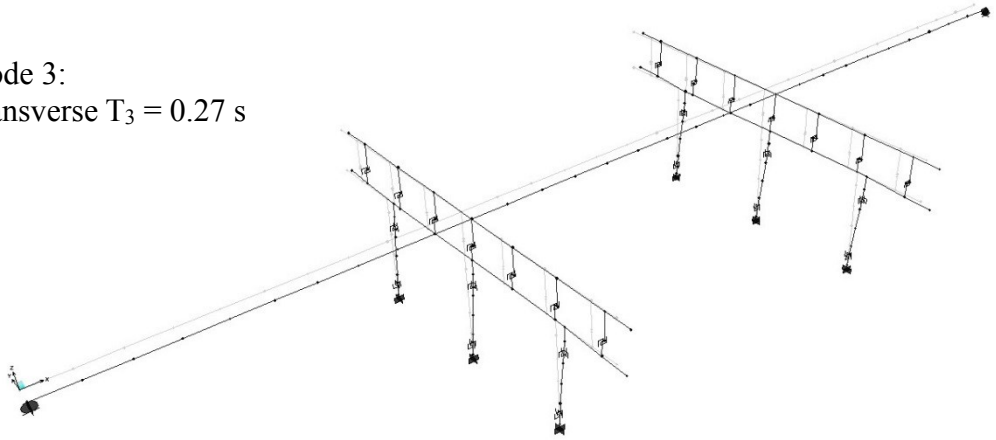

(b)

Mode 1:
Longitudinal $T_1 = 0.89$ s

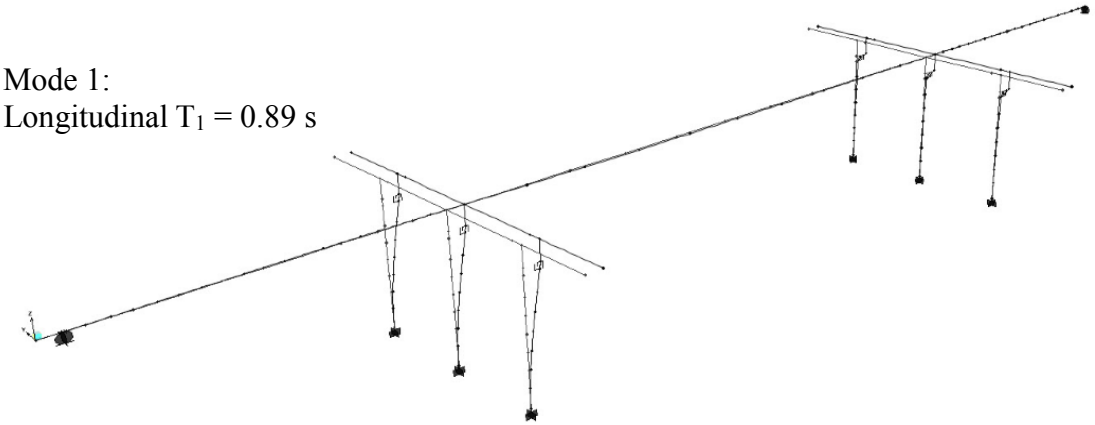

Mode 2:
Torsional $T_3 = 0.80$ s

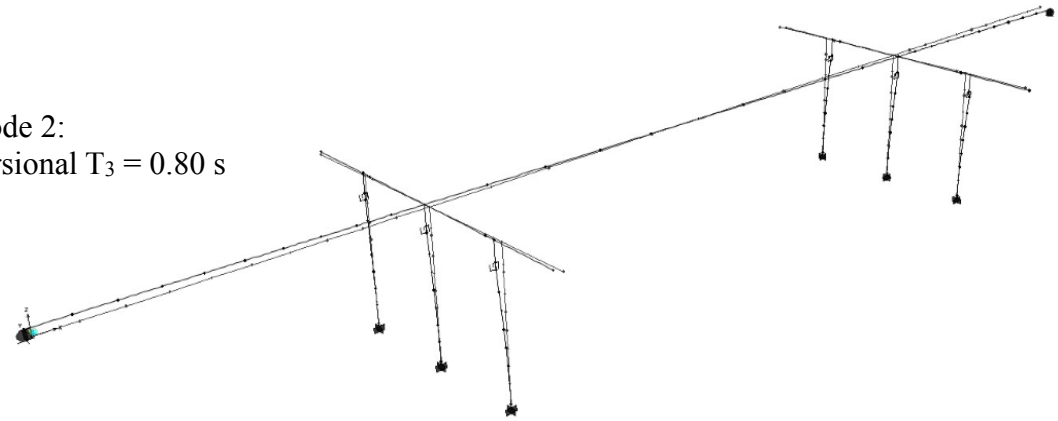

Mode 3:
Transverse $T_2 = 0.71$ s

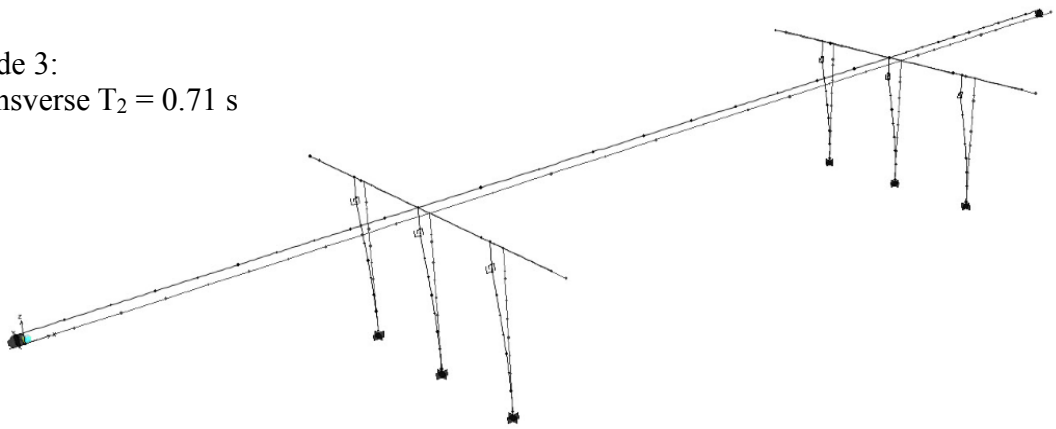

Figure 3.13 Mode shapes of the first three modes from the modal analysis, (a) Bridge #1; (b) Bridge #2.

Chapter 4

Selection of Earthquake Records

4.1 Seismic Hazard for Montreal

With improvement on our knowledge, currently the seismic hazard for a given site is represented by a uniform hazard spectrum rather than by the peak ground acceleration or peak ground velocity which was used about 20 years ago. A uniform hazard spectrum represents an acceleration spectrum with spectral ordinates having the same probability of exceedance. Uniform hazard spectra can be computed for different probabilities (e.g., 2% in 50 years, 10% in 50 years, etc.) and different confidence levels. Two typical confidence levels used to define uniform hazard spectra are 50% and 84% which represent the confidence in percentage that the spectral values will not be exceeded for the specified probability. Figure 4.1 shows the 50% and 84% levels uniform hazard spectrum (UHS) for the probability of exceedance of 10% in 50 years (i.e., annual probability of exceedance of 0.002) for 5% damping for soil class C while the spectral values were provided by Geological Survey of Canada. The soil class C is referred to the soil with the shear wave velocity between 360 m/s and 750 m/s according to the National Building Code of Canada (NRCC 2010). It is necessary to mention that the probability of exceedance of 10% in 50 years is the design earthquake level specified in CHBDC (2006).

The seismic response coefficient (i.e., seismic design spectrum) for Montreal was determined using Equation (4.1) in accordance with CHBDC (2006),

$$C_{sm} = \frac{1.2AIS}{T_m^{2/3}} \leq 2.5AI \tag{4.1}$$

Where ,

A = zonal acceleration ratio,

I = importance factor,

S = site coefficient,

T_m = period of vibration of the m^{th} mode.

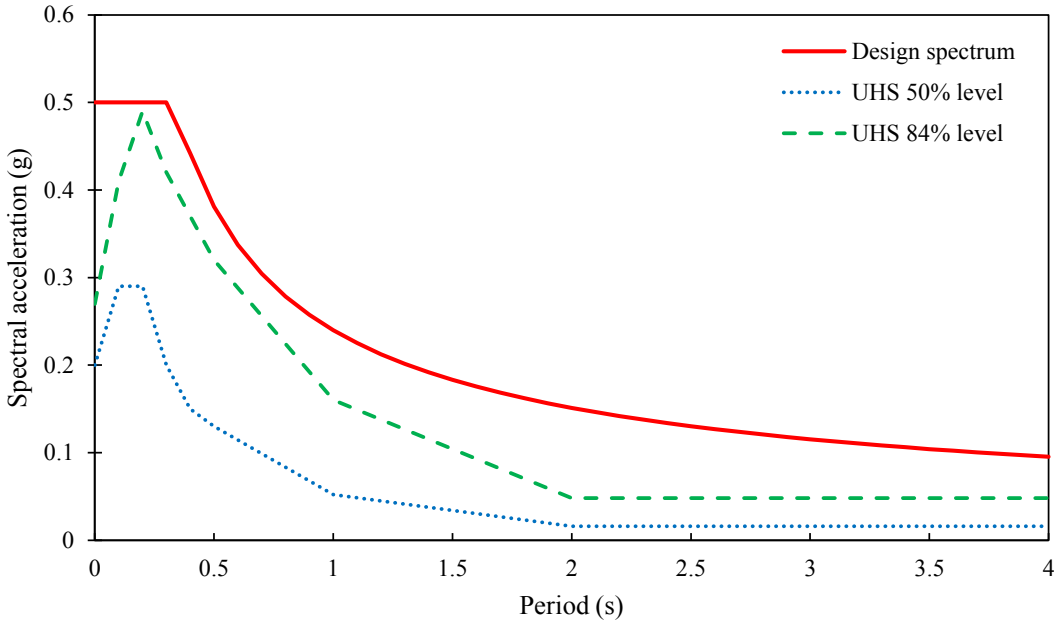

Figure 4.1 Design and uniform hazard spectra for Montreal, 5% damping.

The zonal acceleration ratio A for Montreal is 0.2 for probability of exceedance of 10% in 50 years as given in Table A3.1.1 in CHBDC (2006). The importance factor I is taken as 1.0 for normal importance. The value of 1.0 is used for the site coefficient S based on the assumption that the foundation sits on soil type I which is rock or stiff soil according to CHBDC. For the purpose of comparison, the design spectrum for Montreal is superimposed

in Fig. 4.1. The spectral acceleration at the period of 4.0 s is taken as half of the value at the period of 2.0 in accordance with CHBDC.

4.2 Scenario Earthquakes for Montreal

The seismic hazard at a given site represents the sum of the hazard contributions of different earthquakes at different distances from the site. For each site, however, there are a few earthquakes that have dominant contributions to the hazard. These earthquakes are normally referred to as scenario or predominant earthquakes. The shape of the uniform hazard spectrum for a given site, representing the seismic hazard for the site, depends on the magnitudes of the scenario earthquakes and the distances of these earthquakes from the site. In general, the dominant contribution to the short period ground motion hazard is from small to moderate earthquakes at small distances, whereas larger earthquakes at greater distance contribute most strongly to the long period ground motion hazard.

For the purpose of the selection of earthquake ground motions for use in the seismic analyses, it is necessary to know the magnitude (M) and the distance (R) of the earthquakes that have the largest contributions to the seismic hazard. This can be done by computing the seismic hazard contributions of selected M-R ranges that cover all possible magnitude-distance combinations, which is also called seismic hazard deaggregation analysis. Figure 4.2 provided by Geological Survey of Canada shows the M-R contributions for Montreal for probability of exceedance of 10% in 50 years. Figure 4.2(a) shows the contributions to the seismic hazard for period of 0.2 s, representing the short period ground motion hazard. Similarly, Figure 4.2(b) shows the contributions for period of 1.0 s, representing the long period ground motion hazard. The contributions are computed for magnitude intervals of 0.25, and distance intervals of 20 km. It can be seen in Fig. 4.2(a) that the dominant M-R values corresponding to the seismic

hazard of 10% in 50 years probability of exceedance are $M_w = 5.65$ and R = 55 km for period of 0.2 s, and $M_w = 6.5$ and R = 134 km for period of 1.0 s. Note that these M and R values are the *mean* (or weighted average) values for each period.

(a)

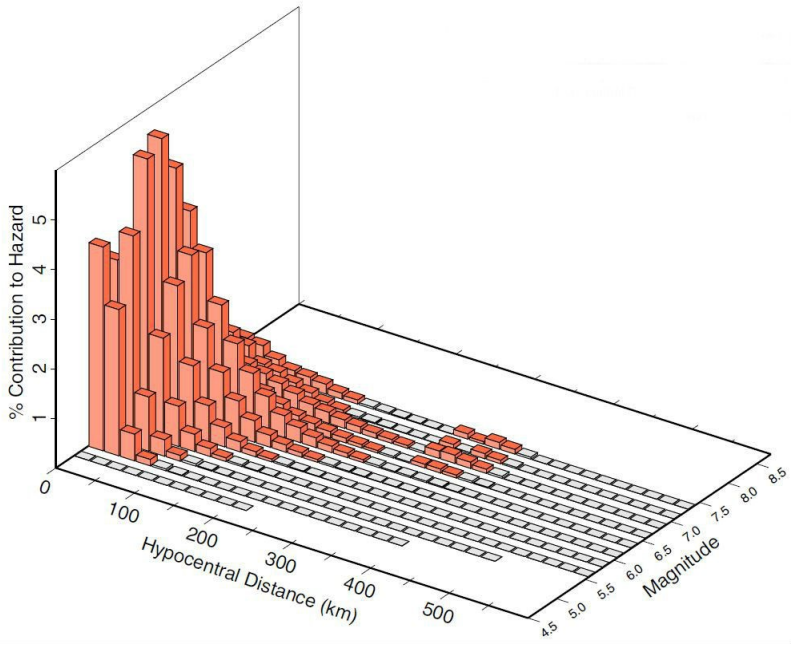

(b)

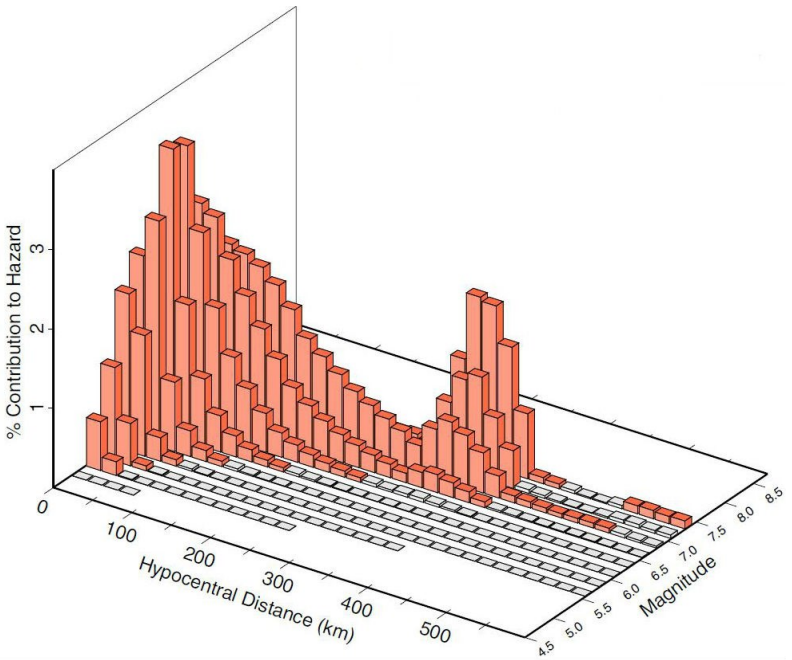

Figure 4.2 Seismic hazard deaggregation results for Montreal for probability of exceedance of 10% in 50 years: (a) Sa(0.2s); (b) Sa(1.0s).

4.3 Selection of Records

Ground motion records from earthquakes in Montreal would be the most appropriate for the time-history analysis of the bridges considered in this study. Since such records are not available, the records complied by Naumoski et al. (1988 and 1993) were selected.

Due to lack of strong ground motion records in eastern Canada, Naumoski et al. (1988 and 1993) compiled a number of records obtained from earthquakes around the world which are representative of the characteristics of ground motions in eastern Canada. The records are grouped into three ensembles, i.e., high A/V set, intermediate A/V set, and low A/V set, according to the ratio of the peak ground acceleration (in g) to peak ground velocity (in m/s). The average A/V ratios of the high A/V, intermediate A/V, and low A/V sets are about 2.0, 1.0, and 0.5, respectively. According to Naumoski et al. (1988), seismic motions from small to moderate earthquakes at short distances are represented by high A/V ratios while those from large earthquakes at large distances are characterized by low A/V ratios. In terms of the frequency content, high A/V motions normally have a high frequency content, and low A/V motions have a low frequency content. Seismic motions with a high frequency content are characterized by predominant frequencies higher than approximately 2 Hz (i.e., periods lower than 0.5s), and seismic motions with a low frequency content are characterized by predominant frequencies lower than 2 Hz (i.e., periods longer 0.5 s).

As reported by Adams and Halchuk (2003); Naumoski et al. (1988), ground motions in eastern Canada are typically characterized by high frequency content and high A/V ratios. Given this, the ensemble of the records with high A/V ratios in Naumoski et al. (1988) was adopted for the analysis. In total, the ensemble consisted of 13 pairs of the horizontal and vertical components. It is necessary to mention that only horizontal components were used in

this study, and the characteristics of the records are presented in Table 4.1. Note that the last two records in the table were selected from the intermediate ensemble given in Naumoski et al. (1988). It can be seen from the table that the magnitudes of the earthquakes of the selected records are between 5.25 to 6.9, and the distances range from 4 km to 26 km. These magnitudes

Table 4.1 Characteristics of records used in the study (Naumoski et al., 1988).

Rec No.	Earthquake	Date	Magn	Recording site	Epic. dist. (km)	Comp.	A (g)	V (m/s)	A/V	Soil type
1	Parkfield California	June 27 1966	5.6	Temblor No. 2	7	N65W	0.269	0.145	1.86	Rock
2	Parkfield California	June 27 1996	5.6	Cholame, Shandon No. 5	5	N85W	0.434	0.255	1.70	Rock
3	San Francisco California	Mar. 22 1957	5.25	Golden Gate Park	11	S80E	0.105	0.046	2.28	Rock
4	San Francisco California	Mar. 22 1957	5.25	State Bldg., S.F.	17	S09E	0.085	0.051	1.67	Stiff soil
5	Helena Montana	Oct. 31 1935	6.0	Caroll College	8	N00E	0.146	0.072	2.03	Rock
6	Lytle Creek	Sep. 12 1970	5.4	Wrightwood, California	15	S25W	0.198	0.096	2.06	Rock
7	Oroville California	Aug. 1 1975	5.7	Seism. Station Oroville	13	N53W	0.084	0.044	1.91	Rock
8	San Fernando California	Feb. 9 1971	6.4	Pacoima Dam	4	S74W	1.075	0.577	1.86	Rock
9	San Fernando California	Feb. 9 1971	6.4	Lake Hughes Station 4	26	S21W	0.146	0.085	1.72	Rock
10	Nahanni, NWT, Canada	Dec. 23 1985	6.9	Site 1, Iverson	7.5	LONG.	1.101	0.462	2.38	Rock
11	Honshu Japan	Apr. 5 1966	5.4	Hoshina-A	4	N00E	0.270	0.111	2.43	Stiff soil
12	Monte Negro Yugoslavia	Apr. 9 1979	5.4	Albatros Hotel Ulcinj	12.5	N00E	0.042	0.016	2.63	Rock
13	Banja Luka Yugoslavia	Aug. 13 1981	6.1	Seism. Station Banja Luka	8.5	N90W	0.074	0.032	2.31	Rock
14	Central Honshu, Japan	Feb. 26 1971	5.5	Yoneyama Bridge	27	TRANS	0.151	0.059	2.56	Stiff soil
15	Near E. Coast of Honshu, Japan	May. 11 1972	5.8	Kushiro Central, Wharf	33	N00E	0.146	0.06	2.43	Stiff soil

and distances cover the dominate magnitude and distance ranges that have the largest contribution to the seismic hazard at the bridge location (Huang, 2014). The selected records have A/V ratios between 1.67 and 2.63 with an average A/V of 2.12.

For illustration, Figure 4.3 shows the response spectra of the selected records scaled to the design spectral acceleration at the fundamental period of the Bridge #1, $Sa(T_1) = 0.24g$, in which $T_1 = 0.99$ s. Note that the design spectrum for Montreal for the probability of exceedance of 10% in 50 years is also superimposed in the figure. As can be seen in the figure, the mean spectrum of the records is below the design spectrum for the period longer than 0.99 s, and it is above the design spectrum for the period shorter than 0.99 s.

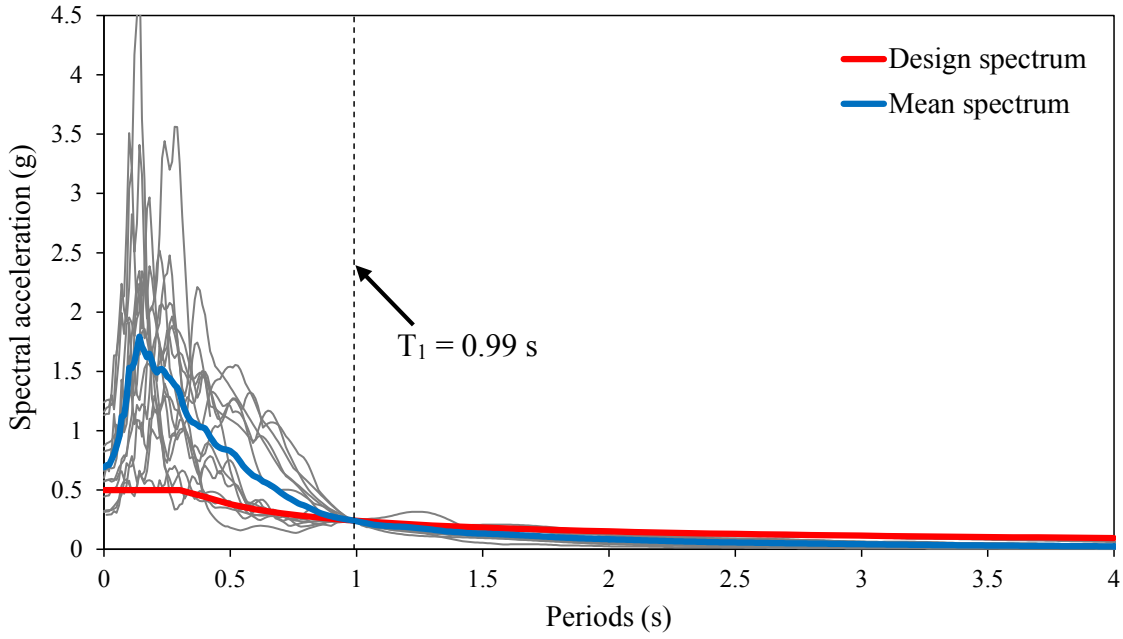

Figure 4.3 Scaled response spectra of the records based on $Sa(T_1)$, Bridge #1, 5% damping.

Chapter 5

Analysis Results

5.1 Overview

In this study, nonlinear time-history analyses were conducted by subjecting the two bridge models to the selected records. In order to determine the structural response due to ground motions with different intensities, the records were scaled to a range of intensity levels according to $Sa(T_1)$. In total, eleven excitation levels were used for the analysis ranged from 0.05 g to 1.20 g for Bridge #1, from 0.05 g to 1.30 g for Bridge #2. Expressed in terms of the reference spectral acceleration Sa_{ref} which was determined based on the design spectrum for Montreal according to CHBDC (2006), the seismic excitations are from $0.2Sa_{ref}$ to $5.0Sa_{ref}$. These intensity levels were selected to cover a wide range of the structural response from elastic to inelastic in order to assess the effects of the structural modeling parameters on the seismic response of bridges. The fundamental periods T_1 of Bridges #1 and #2 were 0.99 s and 0.89 s, respectively, as described in Chapter 3.

According to the current seismic provisions of the bridge design codes CHBDC (2006) and AASHTO (2014), all the inelastic deformations during earthquake events should occur in the substructure while the superstructure should remain elastic. Given this, response parameters used for the purpose of the study included those representing the behavior of the superstructure and substructure, respectively. More specifically, a number of response parameters selected for the study were:

- deck displacement,
- bearing displacement,
- column displacement,
- column curvature ductility, and
- moment at the base of the column.

The deck displacement is a "global" deformation parameter and has been used in a number of studies for the evaluation of the seismic performance of bridges (e.g., Hwang et al., 2001; Tavares et al., 2012, etc.). In addition, the gap size between the deck and the abutment can also be used to represent the displacement of the superstructure (e.g., Pan et al., 2010). Since the abutments of the two bridges considered in the study were modeled as rollers, gap size was not used for the investigation.

As reported by Choi et al. (2004), Nielson & DesRoches (2007), and Tavares et al. (2012), the seismic performance of a bridge depends very much on the behavior of the bearing which works as a connection between the superstructure and substructure. From the structural point of view, the displacement of the deck (i.e., displacement of the superstructure) is equal to the sum of the displacements of the bearing and the column (i.e., displacement of the substructure). Clearly, the bearing displacement is a "local" response parameter, and it was used in this study to examine the shear response of the bearing due to the seismic loads. It is necessary to mention herein that both fixed and expansion bearings were used in the two bridges, and the fixed bearing only allows the rotation (i.e., translation is not allowed) while the expansion bearing allows both rotation and translation. The different behavior of the two types of bearings is discussed in detail in the sections below.

The column top displacement is another response parameter used in this investigation. In knowing the displacement, one can determine the column drift ratio. Unlike the seismic design of buildings in which the interstorey drift ratio should be limited to 2.5% according to the National Building Code of Canada (NRCC, 2010), the current edition of CHBDC (2006) does not specify any limitation on the drift ratio of bridges. It is believed that the results of the column displacement from this study would be helpful in understanding this issue. In this study, the displacement of the columns of the two piers in each of bridges were considered. This is because bearings used on the top of the two piers were different, i.e., fixed bearings were used on pier 1, while expansion bearings were used on pier 2 (see description in Chapter 3).

The curvature ductility of the column is also a "local" deformation parameter and represents the extent of inelastic deformations at a specified section of a structural member. The curvature ductility for a given section of a member represents the ratio of the maximum curvature (ϕ_u) experienced during the response to the yield curvature (ϕ_y) of the section. This response parameter has been used extensively on the seismic evaluation of bridges, because it is an indicator of the nonlinearity of the column during earthquake events (e.g., Nielson & DesRoches, 2006; Pan et al., 2010; Avşar et al., 2011; and Tavares et al., 2012).

The bending moment on the bottom of the column represents one of the "global" force demands used to design the bridge substructure subjected to seismic loads. A larger moment indicates that larger seismic force is applied to the column. Please note that shear force was not considered in the investigation because the nonlinear behavior of the column was defined using the moment-curvature relation as discussed in Chapter 3.

Overall, the response parameters selected in the study covered the responses of both the superstructure and substructure. They represent both the deformation and force of a given member during seismic excitations at different levels.

For each excitation motion considered in the study, maximum value of each of the response parameters mentioned above was computed. Given a large number of analyses conducted in this study, it is not practical to consider the maximum response from a single time-history analysis. Therefore, the responses resulting from the set of excitations were statistically analysed to compute the mean (M) value. The use of the mean values is considered appropriate because these values are more "stable" (i.e., they have smaller variations) than the mean plus one standard deviation (M+SD) values.

As given in Chapter 1 (Introduction), the main objective of the study was to investigate the effects of the different modeling parameters on the seismic response of bridges. More specifically, the following modeling parameters were considered in the analysis,

- Superstructure mass,
- Concrete compressive strength,
- Yield strength of the reinforcing steel,
- Yield displacement of the bearing,
- Post-yield stiffness of the bearing,
- Plastic hinge length, and
- Damping.

Nonlinear time-history analyses were conducted by changing the nominal value of each modeling parameter by a range of factors. The nominal value of each parameter along with its

variation is given in Table 5.1. The observations of the results from the sensitivity analyses on the foregoing modeling parameters are described in the sections below.

5.2 Effects of the Superstructure Mass

It is well known that the mass of the structure will affect the fundamental period of the structure as well as the inertial force. The benefit of increasing the structure mass is that the dominant period of the structure will be lengthened which will, in turn, reduce the spectral acceleration. As a result, the inertia force applied to the structure might be reduced as well.

The total weight of the structure built might be different than the design value due to unforeseen reasons during construction. In this study, the superstructure mass (weight) was varied by 0.7 to 1.3 times the nominal value. The nominal mass was determined based on the geometry of the superstructure, as illustrated in Figs 3.2 (for Bridge #1) and 3.3 (for Bridge #2) in Chapter 3.

Figure 5.1 shows the results of the deck displacement corresponding to the different superstructure mass at 11 intensity levels considered in this study, in which Figs. 5.1a and 5.1b present the results for Bridge #1 and Bridge #2, respectively. Each point in the figure represents the maximum mean displacement at a given excitation level. The main observation of the results is that the deck displacement increases with the increasing of the superstructure mass. Note that the change of the superstructure mass by ± 30%, with respect to its nominal value, shifts the fundamental period of the bridge slightly, i.e., the spectral acceleration will not change too much. As a result, the inertia force is directly proportional to the mass, such that larger mass leads to larger inertia force. It can be seen in the figures that the superstructure mass does not affect the deck displacement for the excitations lower than about 0.50 g (i.e., $2.0Sa_{ref}$). The effect is noticeable when the excitation level is higher than 0.50 g, and it

increases with the intensity level. Table 5.2 presents the maximum differences of the deck displacements resulting from the variation of the superstructure mass with respect to the reference response at typical intensity levels. The reference response refers to the response based on the nominal mass, which is designated as "100% Super mass" in the figures in this section (Figs. 5.1 to 5.8). The results in Table 5.2 show that the change of the superstructure mass by 30% causes the change of the displacement by 9.4% of the reference response at the highest intensity level, $5.0Sa_{ref}$. It indicates that the superstructure mass does not have significant effect on the deck displacement.

The findings of the results for the maximum moment on the base of the column (Fig. 5.2) are similar to those of the deck displacement, i.e., larger mass leads to larger moment. Like for the deck displacement, the effects of the superstructure mass on the bending moment are noticeable starting at the intensity level about 0.50 g (i.e., $2.0Sa_{ref}$). By comparing the resulted differences for the moment with those for the deck displacement shown in Table 5.2, it can be concluded that the effect of the change of the superstructure mass on the bending moment on the base of column is relatively larger compared to that on the deck displacement.

The results for the bearing displacements of Bridge #1 and Bridge #2 are illustrated in Figs. 5.3 and 5.4 respectively, in which Fig. 5.3 presents the results for the fixed bearing and Fig. 5.4 for the expansion bearing. The results in the figures show that the bearing displacement increases with the increasing of the superstructure mass, except for the fixed bearing on Bridge #1 (Fig. 5.3a) where the displacement from the 85% of the nominal superstructure mass is significantly larger than the reference value. This might be due to the redistribution of the seismic force during nonlinear behavior of the bridge. Another observation of the results in Fig. 5.3 is that the superstructure mass has noticeable effect starting at 0.24 g for Bridge #1,

and at 0.26 g for Bridge #2, which both correspond to $1.0Sa_{ref}$. This is because the bearing already yielded, yield displacement is 0.5 mm defined in the modeling. By comparing the fixed bearing displacements of the two bridges, it was found that the superstructure mass has different effects on the two bridges. More specifically, for the two bridges, the ratio of the total difference between the displacements resulting from 70% and 130% of the superstructure mass to the reference value was about 1.5 for Bridge #1 while 1.1 for Bridge #2. The results in Table 5.2 show that the superstructure mass has more effects on the displacement of the fixed bearing on Bridge #1 than those on Bridge #2, while for the expansion bearing the effects are similar. In general, the variation of the superstructure mass with 30% with respect to the nominal value led to the difference about 5 ~ 10% of the reference value (Table 5.2). Based on the results shown in Fig. 5.4, it was found that the expansion bearings on the two bridges reach their ultimate displacement (75 mm for Bridge #1, 50 mm for Bridge #2) when the excitation is at about $1.3Sa_{ref}$. Given the finding in Heidebrecht & Naumoski (2002), i.e., earthquakes at twice of the design level would also occur, the bearings on these two bridges might be replaced by those with larger shear resistance.

Figures 5.5 and 5.6 show the displacements of the column of the two bridges at piers 1 and 2, respectively. The results in the figures clearly show that the displacement of the column at pier 1 (Fig. 5.5) is much larger than at pier 2 (Fig. 5.6). This is because fixed bearings were used on the top of pier 1 and expansion bearings were used on the top of pier 2. As a result, the resultant lateral stiffness of the fixed bearing and column of pier 1 is much larger than that of the expansion bearing and column of pier 2, which yields larger lateral force applied to pier 1. It is interesting to notice that the change of the superstructure mass has negligible effect on the displacement of the column of pier 2 in which the expansion bearings were used (Fig. 5.6).

Based on the results shown in Table 5.2, it was found that on average the change of the superstructure mass by 30% will change the displacement of the column of pier 1 by about 8%, where fixed bearings were installed.

The results for the column curvature ductility are presented in Figs. 5.7 and 5.8, in which Fig. 5.7 is for the column at pier 1 (fixed bearings were used) and Fig. 5.8 is for the column at pier 2 (expansion bearings were used). By comparing the results shown in the figures, it can be seen that the change of the superstructure mass has less effect on the column at pier 2 (Fig. 5.8 and Table 5.2). This is because pier 1 takes a greater amount of the total seismic load than pier 2, due to the larger resultant lateral stiffness of pier 1 as discussed above. The results in the figures also show that all the fixed bearings on the two bridges yield at the excitation level of about 0.25 g which corresponds to $1.0Sa_{ref}$ (i.e., the design earthquake level) because the ductility is greater than 1.0. Therefore, it is wise to increase the size of the bearings such that they can sustain during larger earthquakes that might occur in the future. As given in Table 5.2, for Bridge #1, the 30% changing of the superstructure mass creates on average about 5% difference of the pier ductility.

5.3 Effects of the Concrete Compressive Strength

The uncertainty of the material property is one of the factors that is taken into account in the assessment of the seismic fragility of bridges as given in Choi et al. (2004), Pan et al. (2010), and Tavares et al. (2012). In terms of the nonlinear time-history analysis, it is known that the concrete compressive strength (f_c') would affect the result of the moment-curvature or moment-rotation relationship of a given reinforced concrete section in addition to its capacity. For illustration, Figure 5.9 shows the moment-curvature relationships of an end section on the bottom of the column at pier 1 on Bridge #1 using f_c' = 20 MPa and f_c' = 40 MPa, respectively.

It can be seen in the figure that the curves determined using the two different concrete strengths are different. Given this, sensitivity analyses were conducted in this study based on different concrete compressive strength for the column. Specifically, the nominal strengths of f_c' considered in the analysis were 20 MPa, 25 MPa, 30 MPa, 35 MPa, and 40 MPa, in which the response corresponding to $f_c' = 30$ MPa was considered as a reference.

The results of the deck displacement using different f_c' are presented in Fig. 5.10 in which Fig. 5.10a is for the Bridge #1 and Fig. 5.10b is for Bridge #2. The results in the figures show that smaller f_c' provides larger deck displacement while larger f_c' gives smaller deck displacement, but the variation among the responses is quite small (i.e., less than 5% for the highest intensity level of $5.0Sa_{ref}$, Table 5.3). Such results were expected because the variations of the concrete strength were only assigned on the column and not on the deck/girder. In addition, the superstructure should behave elastically according to the capacity design principle for bridges specified in CHBDC (2006). The small difference between the responses was due to the change of the stiffness of the substructure arising from different f_c'.

Figure 5.11 illustrates the results of the bending moment at the base of the column of the two bridges considered. It can be seen in the figure (also in Table 5.3), the variations in the moments due to different f_c' for Bridge #2 were slightly larger than those for the Bridge #1. The calculation shows that for Bridge #1, at the excitation level of $5.0Sa_{ref}$, the difference between the moments using f_c' of 20 MPa and 30 MPa (reference strength) was about 3%; the difference between the moment using f_c' of 40 MPa and 30 MPa (reference strength) was about 5.3%. While for Bridge #2 and for the same excitation level, these differences were about 5.2% and 8%, respectively. In general, it can be reported that the difference between the moment using f_c' of 20 MPa (or 40 MPa) and the reference moment using f_c' 30 MPa is about 6% (Table

5.3). It can also be assumed that the variation in the moments is proportional to the f_c', for example, the difference between the moment using f_c' of 30 MPa (or 35 MPa) and the reference moment using f_c' 30 MPa would be about 3%.

The results of the displacement of the fixed bearing are shown in Fig. 5.12, and of the expansion bearings in Fig. 5.13. By comparing the results in the figures, it can be noticed that the concrete compressive strength f_c' does not affect the expansion bearing displacement, i.e., all f_c' provide the same displacement. However, it has significant effects on the fixed bearing displacement especially for the Bridge #1. For example, for Bridge #1, at the intensity level of $2.0Sa_{ref}$, the difference between the response using f_c' of 20 MPa and the reference response of using f_c' of 30 MPa was about 13.8%; while for Bridge #2, for the same intensity level, the difference was about 8.1% (Table 5.3). When the excitation level was increased to $5.0Sa_{ref}$, for Bridge #1, the difference became 23.7%, but for Bridge #2, the difference was still 8% which is the same as that for the excitation level of $2.0Sa_{ref}$. Detailed calculation show that for Bridge #1 the average variation in the responses associated with f_c' of 20 MPa and 30 MPa based on all the intensity levels considered in the study was about 16%, and that associated with f_c' of 40 MPa and 30 MPa was about 9%. For Bridge #2, the variations were about 8% using f_c' of 20 MPa and 30 MPa and 5% using f_c' of 40 MPa and 30 MPa.

Given the observations of the results of the deck displacement, fixed bearing (used on Pier 1) displacement, and expansion bearing (used on pier 2) displacement, one would expect that the change of f_c' will not have any effect on the displacement of the column at pier 1, and it will have effect on the column at pier 2 as shown in Figs. 5.14 and 5.15. It is necessary to mention that from theoretical point of view, the deck displacement is equal to the sum of the bearing displacement and the displacement of the column. Therefore, if the effects of f_c' are

shown in the results of the fixed bearing, they will not be shown in the results of the column (compare Fig. 5.12 to 5.14). Similarly, if there are no effects on the expansion bearing displacement, then there will be effects on the column (compare Fig. 5.13 to 5.15). The results in Fig. 5.15 show that f_c' has more effects on Bridge #2 than Bridge #1 because the lateral stiffness of Bridge #2 is larger than that of Bridge #1. As given in Table 5.3, for Bridge #1 the variations in the displacement with respect to the reference displacement using f_c' of 20 MPa and 40 MPa at $5.0Sa_{ref}$ are 4.3% and 2.3%, respectively; for Bridge #2, the variations are 12.1% and 6.6%, respectively.

The major findings of the results of the curvature ductility (illustrated in Figs. 5.16 and 5.17) are similar to those for the column displacement, i.e., f_c' does not have effects on the curvature ductility of the column at pier 1, where fixed bearings were used. This is because a large amount of the lateral force was carried by the bearing due to its relatively larger lateral stiffness. In addition, the results in Fig. 5.17 show that f_c' does not have significant effect on the curvature ductility of the column at pier 2 where expansion bearings were used. As seen in Table 5.3, the maximum difference between the curvature ductility using the variable f_c' and the reference ductility is about 7.1% (it is for Bridge #2 at $2.0Sa_{ref}$). The results in Table 5.3 also indicate that f_c' has more effects on a stiffer column (the column on Bridge 2) than a softer column (the column on Bridge #1).

5.4 Effects of the Yield Strength of the Reinforcing Steel

The effects of the yield strength of the reinforcing steel (f_y) on the seismic response of the two bridges were also investigated in this study. The typical values of f_y considered were 300 MPa, 350 MPa, 400 MPa, 450 MPa, 500 MPa, and 550 MPa in which the response obtained using f_y of 400 MPa was used as a reference.

The results of the deck displacement due to different f_y are presented in Fig. 5.18. It can be seen clearly that f_y does not have effects on the lateral displacement of the superstructure due to the mechanism of the bridge as explained in the previous section. Figure 5.19 shows the results of the bending moment at the base of the column based on different f_y. A general conclusion of the results is that a smaller f_y provides larger moment, while a larger f_y provides smaller moment. For example, for Bridge #1, at the intensity level of $1.0Sa_{ref}$, the moment resulting from f_y of 300 MPa was about 4% larger than the reference moment using f_y of 400MPa. As given in Table 5.4, the variation of the response using f_y of 300 MPa or 550 MPa for the two bridges is about 5% with respect to the reference value at each excitation level considered in this study. Furthermore, it was found in the study that the change of f_y by 50 MPa would change the moment on the base of the column by about 2%.

By comparing the results of the fixed bearing displacement (Fig. 5.20) to those of the expansion bearing displacement (Fig. 5.21), it can be found that for Bridge #1, f_y has a significant effect on the fixed bearing while it does not have an effect on the expansion bearing. It is interesting to notice in Fig. 5.20 that for Bridge #1, the effect of f_y depends on the excitation level. More specifically, for the intensity levels between 0.24 g (i.e., $1.0Sa_{ref}$) and 0.72 g (i.e., $3.0Sa_{ref}$), the bearing displacement using f_y of 550 MPa is larger than the reference displacement associated with f_y of 400 MPa. However, when the intensity level is at 1.20 g (i.e., $5.0Sa_{ref}$), the observation is opposite to that described above. In general, for Bridge #1, when the excitation level is larger than 0.72 g (i.e., $3.0Sa_{ref}$), it can be seen in Fig. 5.20 that smaller f_y tends to provide larger displacement which is consistent with the finding of the results of the Bridge #2. For Bridge #1, at the excitation level of 1.20 g, the difference between the displacements using f_y of 300 MPa and 400 MPa is about 15%, as given in Table 5.4. The same

amount of variation was also observed using f_y of 550 MPa and 400 MPa. However, the variations in the fixed bearing displacement of Bridge #2 resulting from f_y of 300 MPa and 550 MPa compared with the reference displacement using f_y of 400 MPa were about 5% (Table 5.4). In terms of the displacement of the expansion bearing, it can be seen in Fig. 5.21 and Table 5.4 that reducing f_y does not change the displacement, i.e., the displacement using f_y of 300 MPa is almost the same as that using f_y of 400 MPa. But increasing f_y leads to a slightly larger response, the displacement based on f_y of 550 MPa is about 5% larger than the reference value.

Similar to the findings of the effects of the f_y on the column displacement, the results in Figs. 5.22 and 5.23 show that f_y does not affect the displacement of the column at the pier 1 where the fixed bearings were used, while it affects the displacement of the column at the pier 2 where the expansion bearings were used. In Fig. 5.23a, for Bridge #1, the effects of f_y are only observed at the moderate levels of the excitation from 0.36 g (i.e., $1.5Sa_{ref}$) to 0.96 g (i.e., $4.0Sa_{ref}$). The maximum difference between the responses using a differential f_y and the reference value was about 7% (i.e., $3.0Sa_{ref}$, Table 5.4) which corresponds to f_y of 550 MPa. There are no effects at the extreme high levels (> 0.96 g). For Bridge #2, the maximum difference between the responses using differential f_y and the reference value is about 7.9% (Table 5.4).

The results of the curvature ductility of the column at pier 1 and pier 2 are presented in Figs. 5.25 and 5.26, respectively. As expected, f_y has significant effects on the column curvature ductility. This is because the moment-curvature relation of a member depends very much on the yield strength of the steel bar f_y. For illustration, Figure 5.24 shows moment-curvature curves of a bottom section of the column at pier 2 corresponding to f_y of 300 MPa

and 550 MPa. In the figure it can be seen that the curve using f_y of 300 MPa is well below that using f_y of 550 MPa, which indicates that a reinforced concrete member with smaller f_y has relatively smaller stiffness than that with larger f_y. Therefore, smaller f_y creates larger curvature ductility as shown in Figs. 5.25 and 5.26. Table 5.4 summarizes the variations in the column curvature ductility with respect to the reference ductility using f_y of 400 MPa. It can be reported that the yield strength of 300 MPa would lead to the maximum about 30% larger ductility than that of 400 MPa.

5.5 Effects of the Yield Displacement of the Bearing

As discussed in Section 5.2, yielding of the bearing occurred at a quite low excitation level, i.e., $1.0Sa_{ref}$, and the displacement of the bearing linearly increased with the increase of the intensity of the ground motion. Given this, it is worth assessing the effects of the yield displacement of the bearing (D_y) on the seismic response of the bridge. The reference value of D_y for Bridge #1 was 8 mm and for Bridge #2 was 5 mm, which were assumed to be 10% of the ultimate bearing displacement D_u as a minimum yield displacement following the recommendation made by DesRoches et al. (2003). It is necessary to mention that the test results of the yield displacement of bearings are currently not available. Therefore, additional values of D_y which are 15%, 20%, 25%, 30%, and 35% of the D_u were used for the sensitivity analysis. More specifically, the values used in the analysis of D_y for Bridge #1 were 8 mm, 12 mm, 16 mm, 20 mm, 24 mm, and 28 mm; for Bridge #2 the values were 5 mm, 8 mm, 10 mm, 13 mm, 15 mm, and 18 mm.

The results of the deck displacement, moment at the base of the column, displacement of the fixed bearing, displacement of the expansion bearing, column displacement, and the column curvature ductility resulting from the different values of D_y of the two bridges are

presented in Figs. 5.27 to 5.34. It can be seen in the figures that the change of D_y does not affect the response parameters mentioned above except the displacement and the curvature ductility of the column at pier 2 where the expansion bearings were used. This is because the initial elastic stiffness of the bearing does not depend on D_y, it depends on the geometry of the bearing including the plan area of the bearing pad, and the total thickness of the elastomer. In other words, the elastic stiffness K_1 of the bearing (Fig. 3.6, Chapter 3) was kept constant in the analysis, in which K_1 was 1500 kN/m for Bridge #1, 7000 kN/m for Bridge #2 as provided in Table 3.1, Chapter 3 These values were determined by using D_y of 8 mm for Bridge #1, 5 mm for Bridge #2, respectively. If the stiffness of the bearing does not change, the total lateral stiffness of the bridge will not change as well. In addition, it was assumed that no stiffness degradation occurred during nonlinear behavior of the bearing, i.e., the degrading stiffness of the bearing is the same as the initial elastic stiffness (Fig. 3.10, Chapter 3). As a result, the deck displacement, the fixed bearing displacement and the expansion bearing displacement did not change with D_y. As illustrated in Fig. 5.32 and 5.34, the change of D_y only affects the displacement and curvature ductility of the column at pier 2 Bridge #2, where the expansion bearings were used. This is due to the fact that the column at the pier 2 behaved elastically (curvature ductility is less than 1.0, Fig. 5.34). Therefore, the response increased linearly with D_y. For both parameters, the response resulting from D_y of 18 mm was about 40% (38.3% and 43.1% for the column top displacement, and column curvature ductility at pier 2, respectively) larger than the reference value at the excitation level of $1.0Sa_{ref}$, and was about 10.1% at the excitation level of $5.0Sa_{Ref}$ (Table 5.5).

5.6 Effects of the Post-yield Stiffness of the Bearing

As described in Chapter 3, the post-yield stiffness (K_2) was considered to be 1/3 times the initial elastic stiffness (K_1) in modeling the nonlinear behavior of the bearing. The factor 1/3 was suggested by on Hwang et al. (2001) and DesRoches et al. (2003). In order to assess the effects of the post-yield stiffness K_2 of the bearing on the response of the bridge, different values for the K_2 were used in the investigation which were 0, 0.3, 0.5, and 0.7. It is necessary to mention that K_2 of 0 represents elastic-perfectly-plastic hysteretic behavior of the bearing during earthquake events. Among the four values considered, 0.3 was used as a reference.

The results of the deck displacement, moment at the base of the column, displacement of the fixed bearing, displacement of the expansion bearing, column displacement, and the column curvature ductility associated with different values of K_2 of the two bridges are illustrated in Figs. 5.35 to 5.42. It can be seen in the figures that the effects of K_2 on the deck displacement (Fig. 5.35), moment at the base of the column (Fig. 5.36), displacement of the fixed bearing (Fig. 5.37), displacement of column at pier 1 (Fig. 5.39), and curvature ductility of the column at pier 1 (Fig. 5.41) are very similar, i.e., for each of the parameters mentioned above, the responses provided by K_2 of 0.3, 0.5, and 0.7 are very close. The response using K_2 of 0 is larger than the reference response using K_2 of 0.3, in which the maximum difference is about 7% for the intensity level of 5.0Sa(T_1).

In this study, it was found that K_2 had significant effects on the displacement of the expansion bearing (Fig. 5.38), displacement and curvature ductility of the column at pier 2 (Figs. 5.40 and 5.42, respectively) where expansion bearings were installed. In terms of the expansion bearing displacement, the results showed that K_2 of 0 provided the largest response and K_2 of 0.7 provided the smallest response. The calculation shows that for Bridge #1, for the

excitation level of $1.0Sa_{ref}$, the bearing displacement corresponding to K_2 of 0 is about 17.1% larger than the reference response using K_2 of 0.3; and for the excitation level of $5.0Sa_{ref}$, is about 37% larger than the reference displacement. These differences became 15.6% and 20.4% when K_2 of 0.7 was used as listed in Table 5.6. As shown in Fig. 5.38 and Table 5.6, the variations in the displacement due to different values of K_2 for Bridge #2 are smaller than those for Bridge #1. In general, for Bridge #2, the difference between the displacements using K_2 of 0 or K_2 of 0.7 with respect to the reference value is about 10 ~ 20%.

The observations of the results of the displacement and curvature ductility of the column at pier 2 (Figs. 5.40 and 5.42, respectively) are very similar, i.e., for Bridge #1, K_2 of 0.3, 0.5, and 0.7 created almost the same response, while K_2 of 0 provided relatively larger response, which is about 40% greater than the reference value using K_2 of 0.3 at the intensity level of $5.0Sa(T_1)$ (Table 5.6). However, for Bridge #2, K_2 of 0.7 provided the largest response; K_2 of 0 provided the smallest response, while the response using K_2 of 0.3 is approximately in-between those using K_2 of 0.7 and K_2 of 0. As given in Table 5.6, for all the excitation levels considered in the study, the response including displacement and curvature ductility of the column at pier 2 resulting from K_2 of 0.7 is 66.9 ~ 89.3% larger than the reference value from K_2 of 0.3, and that resulting from K_2 of 0.0 is 39.3~ 51.8% smaller than the reference value from K_2 of 0.3.

5.7 Effects of the Plastic Hinge Length

In order to evaluate the effects of the plastic hinge length on the seismic response of bridge, in this study the plastic hinge length L_p was varied by a factor of 1.1 to 1.5 times its nominal value which was 1 m for Bridge #1, 0.72 m for Bridge #2 according to CHBDC

(2006). The nominal value of L_p was considered as a reference value for the purpose of comparing the results.

The results of the response parameters corresponding to different plastic hinge length showed that the change of the L_p did not affect the deck displacement (Fig. 5.43), displacements of the fixed bearing and expansion bearing (Figs. 5.45 and 5.46, respectively), and displacements of the column at pier 1 (Fig. 5.47) and pier 2 (Fig. 5.48), i.e., all the values of L_p provided the same response. This is because the lateral stiffness of the bridge substructure only depends on the plan dimensions of the bearing pad and cross-sectional dimensions of the column, it is not related to the plastic hinge length. On the contrary, the plastic hinge length has significant effects on the bending moment at the base of the column and the column curvature ductility as discussed below.

The results of the bending moment at the base of the column resulting from different values of L_p are presented in Fig. 5.44. It can be clearly seen in the figure that larger L_p provides relatively small moment. It was found in this study that increasing every 10% of L_p would reduce the corresponding moment by 3%. For example, for Bridge #1, the bending moment at the base of the column based on reference L_p of 1.0 m, on average, is about 15% greater than the moment while that using L_p of 1.5 m (i.e., 50% larger than the reference L_p) as listed in Table 5.7. Similar observations were obtained from the results of the column curvature ductility, i.e., larger plastic hinge length led to smaller ductility. Furthermore, it was noticed that the change of the plastic hinge length by 10% would create around 2% difference in the response. For example, the L_p of 1.5 m for Bridge #1, 1.08 m for Bridge #2 which was 50% larger than the nominal value, gave the curvature ductility about 7 ~ 9% less than the reference ductility, as shown in Table 5.7.

5.8 Effects of Damping

In addition to the modeling parameters mentioned above, damping was another parameter used to assess the seismic response of bridge in this study. In the modeling of the two bridges, Rayleigh damping was considered in order to take into account the stiffness degradation of the bridge during nonlinear response, and a nominal value of the damping of 5% was applied to all the 12 vibration modes. For the purpose of the investigation, the variation of damping ranged from 2% to 8%, in which the 5% damping was considered as a reference to compare the analysis results.

The results of the deck displacement, moment at the base of the column, displacement of the fixed bearing, displacement of the expansion bearing, displacement of the column at pier 1, displacement of the column at pier 2, curvature ductility of the column at pier 1 where the fixed bearings were used, curvature ductility of the column at pier 2 on which expansion bearings were used are presented in Figs. 5.51 to 5.58, respectively. As expected, smaller damping provides larger response while larger damping creates smaller response. Detailed calculations showed that change of the damping by 1% would create variation on average about 3% in all the response parameters considered. Unlike Bridge #2 in which the variations in the response were almost the same for all the excitation levels (Table 5.8), for Bridge #1, the difference between the response using damping less than 5% and the reference response (using 5% damping) was extremely high at the lower excitation level for some of the response parameters. For example, as seen in Table 5.8, at the intensity level of $1.0Sa_{ref}$, both the column displacement and the curvature ductility of the column at pier 2 resulting from 2% damping is about 17% larger than the reference value (Table 5.8). However, at the excitation level of $5.0Sa_{ref}$, it is only 9% larger than the reference ductility. Such results indicate that damping

might have significant effects on a certain type of bridge (e.g., Bridge #1 in this study) during elastic analysis for a relatively low excitation level. Based on the results of the two bridges listed in Table 5.8, it was found that the response based on damping of 2% on average was about 10% larger than the reference response, while that based on damping of 8% was around 8% smaller than the reference.

Table 5.1 List of nominal value and variations of uncertainties considered.

Modeling parameter	Nominal value	Variation
Superstructure mass	100% superstructure mass	70% ~ 130% superstructure mass
Concrete compressive strength (f_c')	30 MPa	20 MPa ~ 40 MPa
Yield strength of the reinforcing steel (f_y)	400 MPa	300 MPa ~ 550 MPa
Yield displacement of the bearing (D_y)	Bridge #1: 8 mm	8 mm ~ 28 mm
	Bridge #2: 5 mm	5 mm ~ 18 mm
Post-yield stiffness of the bearing (K_2)	$0.3K_1$	$0 \sim 0.7K_1$
Plastic hinge length (L_p)	Bridge #1: 1000 mm	1000 mm ~ 1500 mm
	Bridge #2: 720 mm	720 mm ~ 1080 mm
Damping	5%	2% ~ 8%
Seismic excitation	$Sa_{ref} = Sa(T_1)$ *	$0.2Sa_{ref} \sim 5.0Sa_{ref}$
	Bridge #1: $Sa(T_1) = 0.24$ g; $T_1 = 0.99$ s.	
	Bridge #2: $Sa(T_1) = 0.26$ g; $T_1 = 0.89$ s.	

* $Sa(T_1)$ is determined based on the design spectrum.

Table 5.2 Maximum differences (in %) resulting from the variation of the superstructure mass at typical intensity levels.

Modeling parameter	Response parameter	Bridge No.	Reference response @ Sa_{ref}	$1.0Sa_{ref}$	$2.0Sa_{ref}$	$3.0Sa_{ref}$	$4.0Sa_{ref}$	$5.0Sa_{ref}$
Superstructure mass	Deck displacement	#1	54.1 mm	3.3 ~ 6.6	4.1 ~ 4.1	5.0 ~ 8.7	7.6 ~ 9.2	9.0 ~ 9.4
		#2	47.9 mm	3.2 ~ 8.0	5.2 ~ 7.2	5.0 ~ 8.4	5.9 ~ 7.9	6.4 ~ 8.2
	Maximum base moment	#1	1391 kN·m	5.5 ~ 8.9	4.6 ~ 6.1	6.6 ~ 8.6	8.9 ~ 9.0	9.3 ~ 10.1
		#2	3295 kN·m	6.4 ~ 11.1	8.4 ~ 10.5	8.2 ~ 11.6	9.2 ~ 11.1	9.7 ~ 11.4
	Fixed bearing displacement	#1	0.7 mm	7.1 ~ 13.0	19.6 ~ 36.3	28.7 ~ 63.0	40.3 ~ 68.7	46.4 ~ 67.2
		#2	1.4 mm	6.7 ~ 11.5	8.6 ~ 10.8	8.5 ~ 11.9	9.4 ~ 11.4	10.0 ~ 11.8
	Expansion bearing displacement	#1	51.2 mm	0.4 ~ 6.2	1.4 ~ 5.9	3.5 ~ 5.6	5.4 ~ 7.2	5.2 ~ 9.5
		#2	41.8 mm	4.0 ~ 8.5	5.5 ~ 7.8	5.1 ~ 9.1	5.8 ~ 8.5	6.3 ~ 8.5
	Column top displacement @ pier 1	#1	34.4 mm	2.8 ~ 6.7	2.9 ~ 3.5	4.1 ~ 7.1	6.6 ~ 7.5	7.7 ~ 7.9
		#2	46.0 mm	3.1 ~ 7.8	5.0 ~ 7.1	4.9 ~ 8.2	5.8 ~ 7.7	6.3 ~ 8.1
	Column top displacement @ pier 2	#1	14.6 mm	0.9 ~ 2.5	0.3 ~ 1.5	0.0 ~ 3.5	0.0 ~ 4.0	1.2 ~ 4.3
		#2	6.9 mm	0.0 ~ 4.3	0.0 ~ 3.5	0.3 ~ 2.8	1.7 ~ 1.7	1.4 ~ 2.8
	Column curvature ductility @ pier 1	#1	1.0	2.0 ~ 5.6	0.3 ~ 3.0	3.7 ~ 4.1	4.0 ~ 6.1	4.3 ~ 7.1
		#2	1.3	1.3 ~ 6.3	3.2 ~ 5.6	3.1 ~ 6.7	3.9 ~ 6.2	4.5 ~ 6.5
	Column curvature ductility @ pier 2	#1	0.4	0.0 ~ 2.7	0.0 ~ 1.4	0.0 ~ 4.1	1.3 ~ 5.2	2.8 ~ 5.5
		#2	0.2	0.3 ~ 5.0	0.1 ~ 4.1	1.2 ~ 5.6	1.4 ~ 6.0	1.8 ~ 6.8

Reference response is calculated using the nominal value (see Table 5.1) for the given modeling parameter.

Table 5.3 Maximum differences (in %) resulting from the variation of the concrete compressive strength at typical intensity levels.

Modeling parameter	Response parameter	Bridge No.	Reference response @ Sa_{ref}	$1.0Sa_{ref}$	$2.0Sa_{ref}$	$3.0Sa_{ref}$	$4.0Sa_{ref}$	$5.0Sa_{ref}$
Concrete compressive strength	Deck displacement	#1	54.1 mm	0.3 ~ 1.5	0.9 ~ 1.7	1.0 ~ 2.4	1.8 ~ 3.4	2.0 ~ 3.7
		#2	47.9 mm	0.9 ~ 1.0	0.9 ~ 1.7	1.1 ~ 1.7	1.2 ~ 2.0	1.4 ~ 1.8
	Maximum base moment	#1	1391 kN·m	5.1 ~ 7.9	4.2 ~ 7.4	4.0 ~ 6.5	3.2 ~ 5.6	3.0 ~ 5.3
		#2	3295 kN·m	5.8 ~ 8.7	5.7 ~ 8.1	5.6 ~ 8.1	5.5 ~ 7.8	5.2 ~ 8.0
	Fixed bearing displacement	#1	0.7 mm	4.2 ~ 7.8	8.2 ~ 13.8	12.1 ~ 19.6	12.1 ~ 23.7	11.3 ~ 23.7
		#2	1.4 mm	5.8 ~ 8.7	5.7 ~ 8.1	5.6 ~ 8.1	5.5 ~ 7.8	5.2 ~ 8.0
	Expansion bearing displacement	#1	51.2 mm	0.2 ~ 1.6	0.8 ~ 1.2	0.1 ~ 0.5	0.3 ~ 0.5	0.3 ~ 1.5
		#2	41.8 mm	0.1 ~ 0.3	0.1 ~1.1	0.3 ~ 0.6	0.3 ~ 0.8	0.5 ~0.6
	Column top displacement @ pier 1	#1	34.4 mm	0.4 ~ 1.7	1.2 ~ 2.0	1.4 ~ 3.0	2.1 ~ 4.0	2.3 ~ 4.3
		#2	46.0 mm	1.1 ~ 1.4	1.2 ~ 2.1	1.4 ~ 2.1	1.4 ~ 2.4	1.7 ~ 2.2
	Column top displacement @ pier 2	#1	14.6 mm	3.3 ~ 6.1	2.5 ~ 4.5	1.7 ~ 3.7	2.4 ~ 5.0	2.7 ~ 5.5
		#2	6.9 mm	6.6 ~ 12.2	5.6 ~ 12.7	6.1 ~ 11.1	6.5 ~ 10.6	6.6 ~ 12.1
	Column curvature ductility @ pier 1	#1	1.0	1.9 ~ 3.7	0.9 ~ 3.0	0.6 ~ 1.9	0.0 ~ 0.7	0.0 ~ 0.4
		#2	1.3	2.1 ~ 3.9	2.0 ~ 3.2	1.8 ~ 3.2	1.8 ~ 2.9	1.5 ~ 3.1
	Column curvature ductility @ pier 2	#1	0.4	0.4 ~ 1.5	0.0 ~ 1.1	0.8 ~ 1.9	0.1 ~ 0.8	0.0 ~ 0.5
		#2	0.2	3.7 ~ 6.5	2.4 ~ 7.1	2.7 ~ 5.0	3.1 ~ 4.0	2.5 ~ 5.1

Reference response is calculated using the nominal value (see Table 5.1) for the given modeling parameter.

Table 5.4 Maximum differences (in %) resulting from the variation of the yield strength of the reinforcing steel at typical intensity levels.

Modeling parameter	Response parameter	Bridge No.	Reference response @ Sa_{ref}	$1.0Sa_{ref}$	$2.0Sa_{ref}$	$3.0Sa_{ref}$	$4.0Sa_{ref}$	$5.0Sa_{ref}$
Yield strength of the reinforcing steel	Deck displacement	#1	54.1 mm	1.1 ~ 1.3	2.1 ~ 3.3	0.6 ~ 2.2	0.0 ~ 0.2	0.1 ~ 0.6
		#2	47.9 mm	1.7 ~ 2.5	1.6 ~ 3.7	0.8 ~ 1.0	0.2 ~ 0.5	0.0 ~ 0.1
	Maximum base moment	#1	1391 kN·m	3.6 ~ 4.0	2.2 ~ 2.4	3.1 ~ 3.4	3.8 ~ 4.6	4.4 ~ 4.5
		#2	3295 kN·m	3.5 ~ 3.8	2.0 ~ 4.5	4.6 ~ 5.3	5.0 ~ 6.0	5.5 ~ 6.2
	Fixed bearing displacement	#1	0.7 mm	0.0 ~ 7.7	3.5 ~ 9.5	0.5 ~ 7.4	9.8 ~ 12.7	14.2 ~ 15.5
		#2	1.4 mm	3.5 ~ 3.8	2.0 ~ 4.5	4.6 ~ 5.3	5.0 ~ 6.0	5.5 ~ 6.2
	Expansion bearing displacement	#1	51.2 mm	0.7 ~ 1.0	2.2 ~ 3.3	4.1 ~ 4.8	3.0 ~ 4.3	1.0 ~ 3.8
		#2	41.8 mm	1.0 ~ 2.0	0.9 ~ 3.0	0.1 ~ 0.2	0.1 ~ 0.4	0.5 ~ 0.5
	Column top displacement @ pier 1	#1	34.4 mm	0.8 ~ 1.1	2.0 ~ 2.9	0.8 ~ 2.1	0.3 ~ 0.4	0.0 ~ 0.4
		#2	46.0 mm	1.9 ~ 2.7	1.8 ~ 3.9	1.0 ~ 1.2	0.4 ~ 0.7	0.2 ~ 0.2
	Column top displacement @ pier 2	#1	14.6 mm	3.2 ~ 3.6	3.7 ~ 4.1	2.0 ~ 6.7	0.0 ~ 1.8	0.4 ~ 1.8
		#2	6.9 mm	7.4 ~ 7.9	6.4 ~ 7.8	5.4 ~ 6.4	5.2 ~ 5.3	4.2 ~ 4.7
	Column curvature ductility @ pier 1	#1	1.0	24.0 ~ 28.0	23.0 ~ 25.8	23.3 ~ 26.9	24.3 ~ 27.3	24.1 ~ 28.0
		#2	1.3	22.2 ~ 23.6	20.7 ~ 24.8	22.8 ~ 25.7	23.1 ~ 26.5	23.5 ~ 26.8
	Column curvature ductility @ pier 2	#1	0.4	22.4 ~ 23.2	22.0 ~ 23.2	20.0 ~ 25.5	23.1 ~ 29.0	25.0 ~ 30.3
		#2	0.2	17.0 ~ 18.1	17.4 ~ 18.8	18.9 ~ 19.9	19.4 ~ 20.1	19.8 ~ 22.8

Reference response is calculated using the nominal value (see Table 5.1) for the given modeling parameter.

Table 5.5 Maximum differences (in %) resulting from the variation of the yield displacement of the bearing at typical intensity levels.

Modeling parameter	Response parameter	Bridge No.	Reference response @ Sa_{ref}	$1.0Sa_{ref}$	$2.0Sa_{ref}$	$3.0Sa_{ref}$	$4.0Sa_{ref}$	$5.0Sa_{ref}$
Yield displacement of the bearing	Deck displacement	#1	54.1 mm	0.0 ~ 7.0	0.0 ~ 0.9	0.0 ~ 1.3	0.0 ~ 1.2	0.1 ~ 0.7
		#2	47.9 mm	0.0 ~ 1.9	0.0 ~ 1.8	0.0 ~ 1.5	0.0 ~ 1.0	0.0 ~ 0.7
	Maximum base moment	#1	1391 kN·m	0.0 ~ 7.3	0.0 ~ 0.9	0.0 ~ 1.3	0.0 ~ 1.2	0.1 ~ 0.8
		#2	3295 kN·m	0.0 ~ 2.0	0.0 ~ 1.8	0.0 ~ 1.5	0.0 ~ 1.0	0.0 ~ 0.7
	Fixed bearing displacement	#1	0.7 mm	0.0 ~ 3.8	0.0 ~ 0.4	0.0 ~ 0.8	0.0 ~ 1.6	0.2 ~ 0.5
		#2	1.4 mm	0.0 ~ 2.0	0.0 ~ 1.8	0.0 ~ 1.5	0.0 ~ 1.0	0.0 ~ 0.7
	Expansion bearing displacement	#1	51.2 mm	0.0 ~ 8.9	0.0 ~ 8.4	0.0 ~ 4.2	0.0 ~ 2.1	0.0 ~ 2.0
		#2	41.8 mm	0.0 ~ 4.4	0.0 ~ 1.9	0.0 ~ 1.1	0.0 ~ 0.7	0.0 ~ 0.9
	Column top displacement @ pier 1	#1	34.4 mm	0.0 ~ 7.3	0.0 ~ 0.9	0.0 ~ 1.3	0.0 ~ 1.2	0.1 ~ 0.8
		#2	46.0 mm	0.0 ~ 2.0	0.0 ~ 1.8	0.0 ~ 1.5	0.0 ~ 1.0	0.0 ~ 0.7
	Column top displacement @ pier 2	#1	14.6 mm	0.0 ~ 15.8	1.4 ~ 3.6	1.6 ~ 2.7	0.0 ~ 2.4	0.0 ~ 2.1
		#2	6.9 mm	0.0 ~ 38.3	0.0 ~ 24.8	0.0 ~ 16.6	0.0 ~ 12.7	0.0 ~ 10.1
	Column curvature ductility @ pier 1	#1	1.0	0.0 ~ 7.5	0.0 ~ 1.0	0.0 ~ 1.3	0.0 ~ 1.2	0.1 ~ 0.8
		#2	1.3	0.0 ~ 2.0	0.0 ~ 1.8	0.0 ~ 1.5	0.0 ~ 1.0	0.0 ~ 0.7
	Column curvature ductility @ pier 2	#1	0.4	0.0 ~ 14.2	2.0 ~ 3.0	1.7 ~ 2.1	0.0 ~ 2.7	0.0 ~ 2.5
		#2	0.2	0.0 ~ 43.1	0.0 ~ 26.7	0.0 ~ 15.3	0.0 ~ 10.5	0.0 ~ 8.1

Reference response is calculated using the nominal value (see Table 5.1) for the given modeling parameter.

Table 5.6 Maximum differences (in %) resulting from the variation of the post-yield stiffness of the bearing at typical intensity levels.

Modeling parameter	Response parameter	Bridge No.	Reference response @ Sa_{ref}	$1.0Sa_{ref}$	$2.0Sa_{ref}$	$3.0Sa_{ref}$	$4.0Sa_{ref}$	$5.0Sa_{ref}$
Post-yield stiffness of the bearing	Deck displacement	#1	54.1 mm	0.1 ~ 1.9	0.2 ~ 1.1	1.8 ~ 3.7	3.5 ~ 5.6	4.2 ~ 6.3
		#2	47.9 mm	0.5 ~ 1.7	1.6 ~ 2.7	2.6 ~ 5.1	2.4 ~ 6.2	3.0 ~ 7.3
	Maximum base moment	#1	1391 kN·m	0.0 ~ 1.9	0.2 ~ 1.1	1.9 ~ 3.7	3.5 ~ 5.5	4.2 ~ 6.2
		#2	3295 kN·m	0.5 ~ 1.6	1.6 ~ 2.7	2.5 ~ 5.1	2.4 ~ 6.2	3.0 ~ 7.2
	Fixed bearing displacement	#1	0.7 mm	0.4 ~ 2.4	0.4 ~ 1.0	1.4 ~ 3.0	3.6 ~ 6.0	3.8 ~ 6.6
		#2	1.4 mm	0.6 ~ 1.6	1.5 ~ 2.7	2.5 ~ 5.0	2.4 ~ 6.1	3.0 ~ 7.2
	Expansion bearing displacement	#1	51.2 mm	15.6 ~ 17.1	17.0 ~ 20.6	16.9 ~ 22.9	18.9 ~ 29.9	20.4 ~ 36.7
		#2	41.8 mm	11.1 ~ 12.0	11.5 ~ 15.2	12.8 ~ 17.5	12.9 ~ 18.9	15.2 ~ 20.4
	Column top displacement @ pier 1	#1	34.4 mm	0.0 ~ 1.9	0.2 ~ 1.1	1.8 ~ 3.7	3.5 ~ 5.5	4.2 ~ 6.2
		#2	46.0 mm	0.5 ~ 1.6	1.6 ~ 2.7	2.5 ~ 5.1	2.4 ~ 6.2	3.0 ~ 7.2
	Column top displacement @ pier 2	#1	14.6 mm	4.9 ~ 11.9	3.0 ~ 23.0	2.8 ~ 30.6	1.6 ~ 36.1	1.0 ~ 35.6
		#2	6.9 mm	48.2 ~ 59.0	52.5 ~ 63.5	57.4 ~ 65.2	59.4 ~ 69.7	60.4 ~ 83.0
	Column curvature ductility @ pier 1	#1	1.0	0.1 ~ 1.9	0.2 ~ 1.1	1.9 ~ 3.7	3.5 ~ 5.4	4.1 ~ 6.2
		#2	1.3	0.5 ~ 1.6	1.6 ~ 2.7	2.5 ~ 5.1	2.4 ~ 6.2	3.0 ~ 7.2
	Column curvature ductility @ pier 2	#1	0.4	6.4 ~ 13.3	4.4 ~ 25.9	4.0 ~ 34.2	2.6 ~ 40.4	1.8 ~ 39.8
		#2	0.2	39.3 ~ 66.9	43.3 ~ 71.5	48.0 ~ 69.7	50.7 ~ 73.3	51.8 ~ 89.3

Reference response is calculated using the nominal value (see Table 5.1) for the given modeling parameter.

Table 5.7 Maximum differences (in %) resulting from the variation of the plastic hinge length at typical intensity levels.

Modeling parameter	Response parameter	Bridge No.	Reference response @ Sa_{ref}	$1.0Sa_{ref}$	$2.0Sa_{ref}$	$3.0Sa_{ref}$	$4.0Sa_{ref}$	$5.0Sa_{ref}$
Plastic hinge length	Deck displacement	#1	54.1 mm	0.0 ~ 0.6	0.0 ~ 0.8	0.1 ~ 0.3	0.0 ~ 2.3	0.0 ~ 2.8
		#2	47.9 mm	0.0 ~ 0.6	0.0 ~ 0.5	0.0 ~ 2.3	0.0 ~ 3.2	0.0 ~ 3.5
	Maximum base moment	#1	1391 kN·m	0.0 ~ 13.5	0.0 ~ 15.2	0.0 ~ 16.7	0.0 ~ 18.5	0.0 ~ 18.8
		#2	3295 kN·m	0.0 ~ 9.8	0.0 ~ 10.6	0.0 ~ 12.4	0.0 ~ 13.1	0.0 ~ 13.4
	Fixed bearing displacement	#1	0.7 mm	0.0 ~ 0.5	0.0 ~ 4.2	0.0 ~ 6.3	2.3 ~ 4.4	3.0 ~ 7.2
		#2	1.4 mm	0.0 ~ 0.3	0.0 ~ 1.2	0.0 ~ 3.1	0.0 ~ 3.9	0.0 ~ 4.2
	Expansion bearing displacement	#1	51.2 mm	0.0 ~ 0.6	0.0 ~ 1.0	0.0 ~ 0.2	0.0 ~ 4.2	0.0 ~ 3.8
		#2	41.8 mm	0.0 ~ 0.1	0.0 ~ 0.5	0.0 ~ 2.7	0.0 ~ 3.4	0.0 ~ 3.9
	Column top displacement @ pier 1	#1	34.4 mm	0.0 ~ 1.8	0.0 ~ 2.3	0.0 ~ 1.2	0.0 ~ 1.1	0.1 ~ 1.8
		#2	46.0 mm	0.0 ~ 0.6	0.0 ~ 0.4	0.0 ~ 2.3	0.0 ~ 3.1	0.0 ~ 3.4
	Column top displacement @ pier 2	#1	14.6 mm	0.0 ~ 3.4	0.0 ~ 3.2	0.0 ~ 2.9	0.0 ~ 2.4	0.0 ~ 1.8
		#2	6.9 mm	0.0 ~ 2.3	0.0 ~ 0.4	0.0 ~ 1.5	0.0 ~ 2.6	0.0 ~ 2.9
	Column curvature ductility @ pier 1	#1	1.0	0.0 ~ 7.2	0.0 ~ 7.4	0.0 ~ 8.8	0.0 ~ 11.0	0.0 ~ 11.8
		#2	1.3	0.0 ~ 4.7	0.0 ~ 5.5	0.0 ~ 7.4	0.0 ~ 8.2	0.0 ~ 8.5
	Column curvature ductility @ pier 2	#1	0.4	0.0 ~ 7.4	0.0 ~ 7.7	0.0 ~ 7.9	0.0 ~ 8.4	0.0 ~ 9.0
		#2	0.2	0.0 ~ 4.0	0.0 ~ 6.1	0.0 ~ 8.0	0.0 ~ 8.9	0.0 ~ 9.9

Reference response is calculated using the nominal value (see Table 5.1) for the given modeling parameter.

Table 5.8 Maximum differences (in %) resulting from the variation of the damping at typical intensity levels.

Modeling parameter	Response parameter	Bridge No.	Reference response @ Sa_{ref}	$1.0Sa_{ref}$	$2.0Sa_{ref}$	$3.0Sa_{ref}$	$4.0Sa_{ref}$	$5.0Sa_{ref}$
Damping	Deck displacement	#1	54.1 mm	7.6 ~ 11.7	6.1 ~ 7.3	6.3 ~ 9.3	8.2 ~ 10.5	8.6 ~ 10.9
		#2	47.9 mm	8.0 ~ 10.6	6.7 ~ 9.6	7.7 ~ 9.7	7.7 ~ 10.5	8.4 ~ 10.2
	Maximum base moment	#1	1391 kN·m	7.7 ~ 12.2	6.2 ~ 7.5	6.4 ~ 9.4	8.2 ~ 10.4	8.6 ~ 10.9
		#2	3295 kN·m	8.0 ~ 10.6	6.7 ~ 9.7	7.7 ~ 9.7	7.7 ~ 10.5	8.4 ~ 10.2
	Fixed bearing displacement	#1	0.7 mm	6.6 ~ 7.0	3.8 ~ 4.8	4.8 ~ 8.3	7.9 ~ 11.8	8.8 ~ 11.6
		#2	1.4 mm	8.0 ~ 10.5	6.7 ~ 9.7	7.7 ~ 9.7	7.7 ~ 10.5	8.4 ~ 10.2
	Expansion bearing displacement	#1	51.2 mm	9.1 ~ 14.0	8.4 ~ 9.5	8.0 ~ 8.9	8.7 ~ 11.4	8.7 ~ 12.8
		#2	41.8 mm	8.3 ~ 11.0	6.8 ~ 9.9	7.6 ~ 10.1	7.7 ~ 10.6	8.2 ~ 10.3
	Column top displacement @ pier 1	#1	34.4 mm	7.7 ~ 12.1	6.2 ~ 7.5	6.3 ~ 9.4	8.2 ~ 10.4	8.6 ~ 10.9
		#2	46.0 mm	8.0 ~ 10.6	6.7 ~ 9.7	7.7 ~ 9.7	7.7 ~ 10.5	8.4 ~ 10.2
	Column top displacement @ pier 2	#1	14.6 mm	11.4 ~ 17.0	8.6 ~ 13.3	7.3 ~ 11.3	6.9 ~ 9.3	6.9 ~ 9.5
		#2	6.9 mm	7.2 ~ 10.4	7.3 ~ 12.2	7.7 ~ 11.9	7.6 ~ 12.6	8.4 ~ 14.2
	Column curvature ductility @ pier 1	#1	1.0	7.7 ~ 12.5	6.3 ~ 7.7	6.5 ~ 9.4	8.2 ~ 10.4	8.6 ~ 10.9
		#2	1.3	8.0 ~ 10.6	6.7 ~ 9.7	7.7 ~ 9.7	7.7 ~ 10.5	8.4 ~ 10.2
	Column curvature ductility @ pier 2	#1	0.4	11.5 ~ 16.7	8.7 ~ 12.9	7.3 ~ 11.3	7.0 ~ 9.2	6.9 ~ 9.3
		#2	0.2	7.1 ~ 10.3	7.7 ~ 12.7	8.2 ~ 12.8	8.0 ~ 13.3	7.9 ~ 14.7

Reference response is calculated using the nominal value (see Table 5.1) for the given modeling parameter.

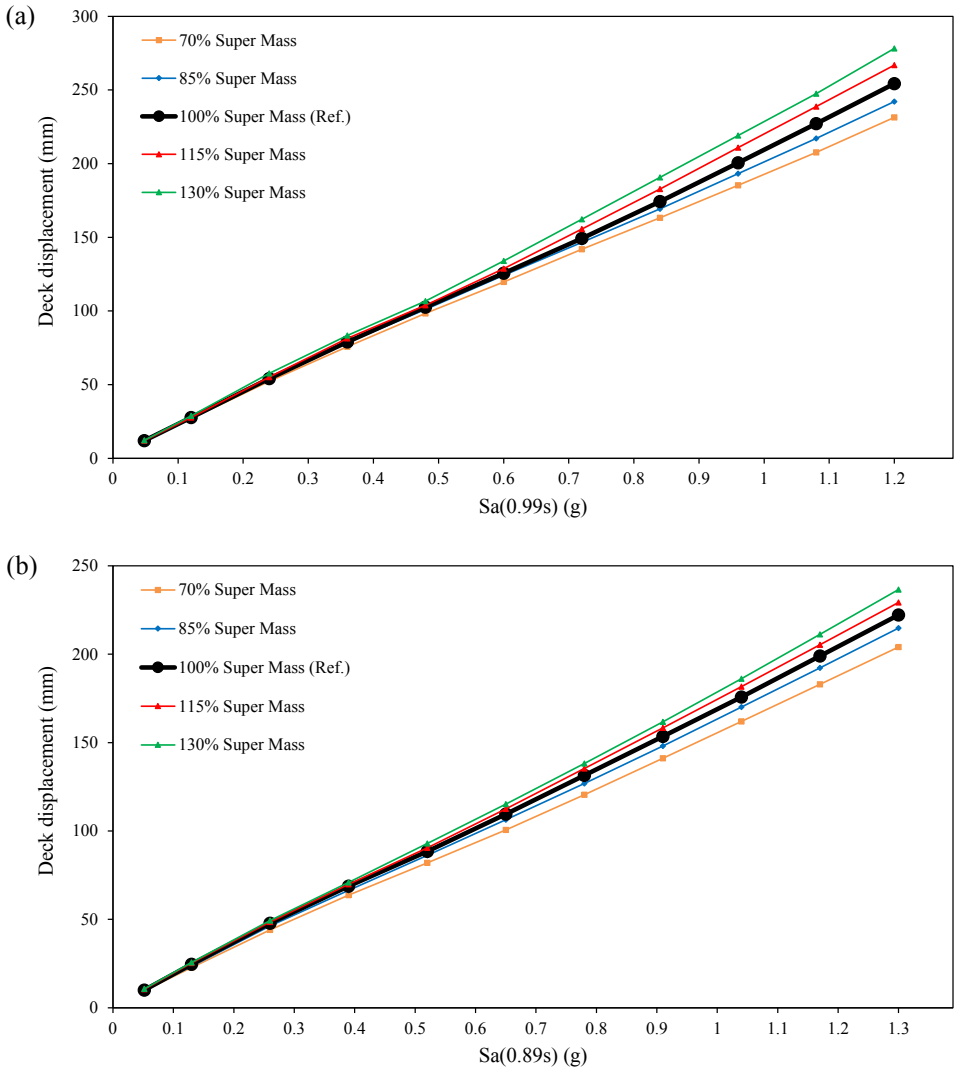

Figure 5.1 Maximum mean deck displacements according to different superstructure mass: (a) Bridge #1; (b) Bridge #2.

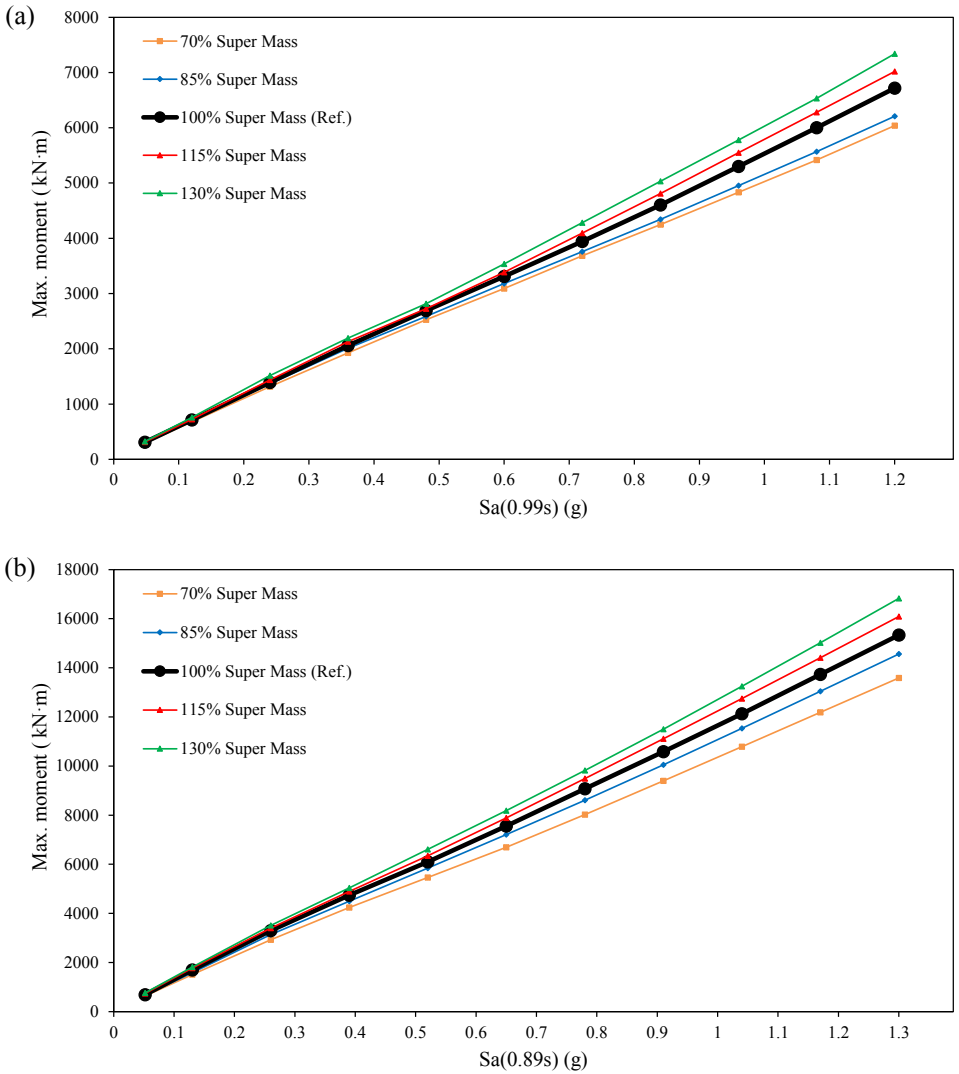

Figure 5.2 Maximum mean moments at the base of the column according to different superstructure mass: (a) Bridge #1; (b) Bridge #2.

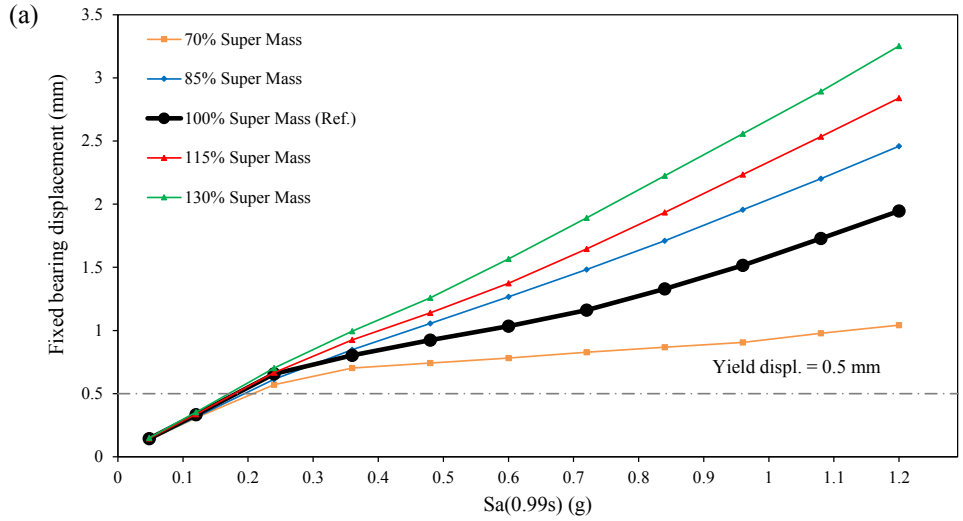

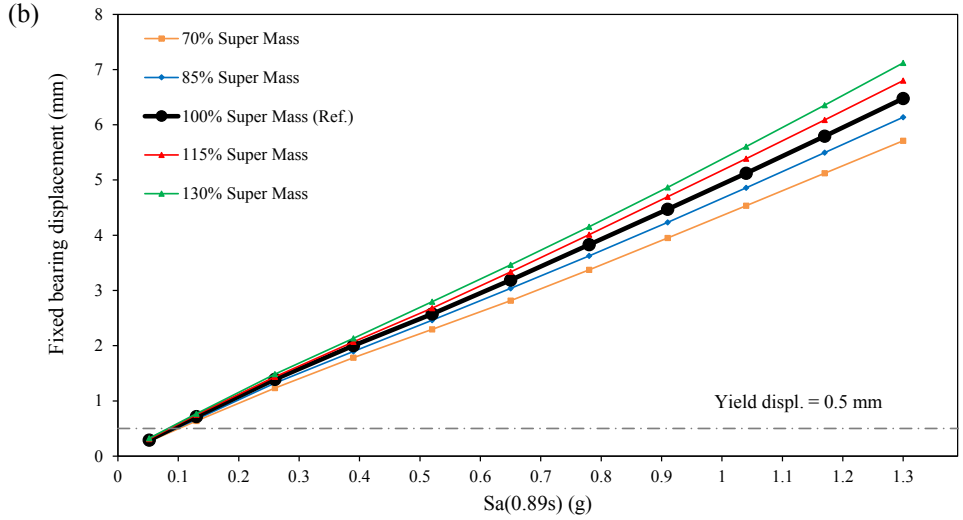

Figure 5.3 Maximum mean fixed bearing displacements according to different superstructure mass: (a) Bridge #1; (b) Bridge #2.

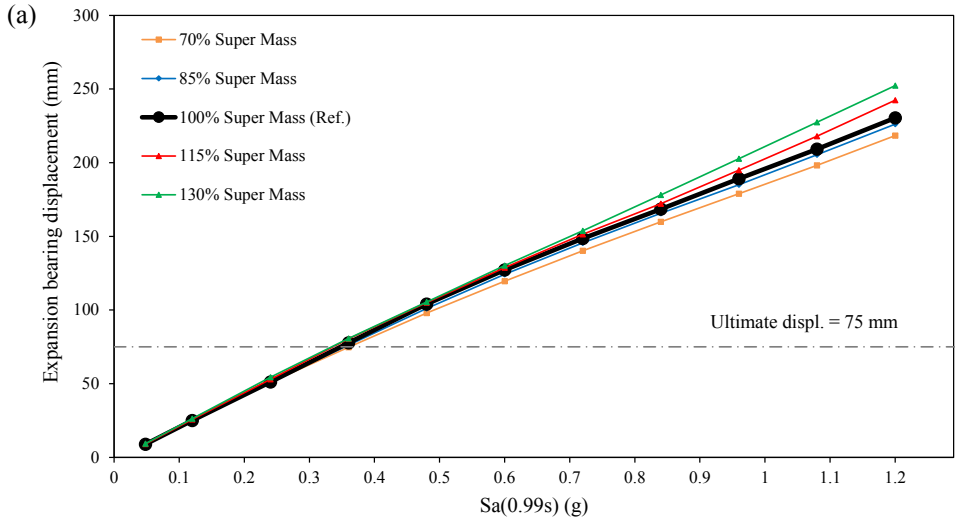

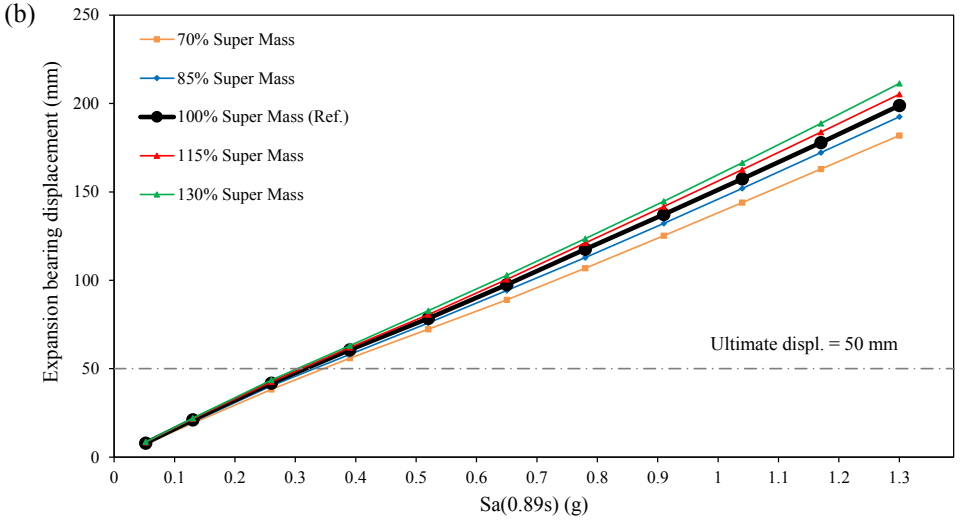

Figure 5.4 Maximum mean expansion bearing displacements according to different superstructure mass: (a) Bridge #1; (b) Bridge #2.

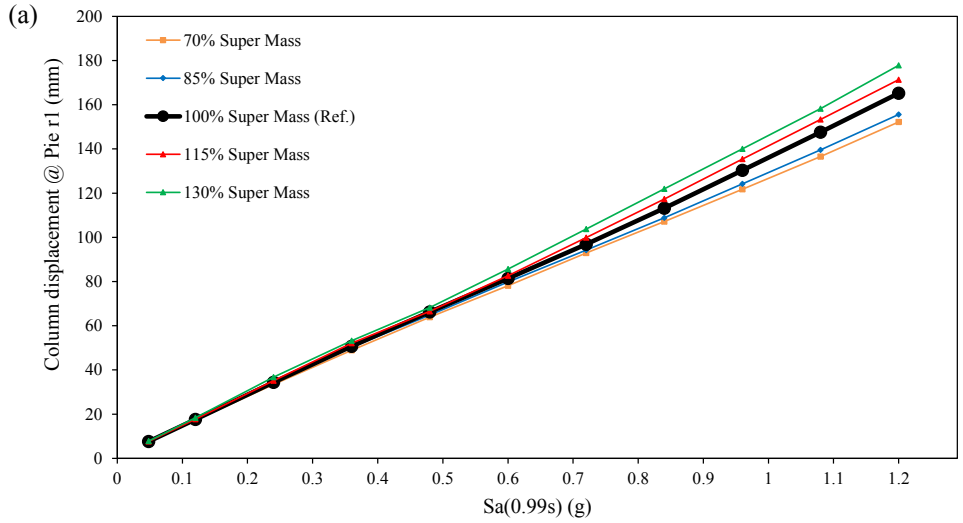

Figure 5.5 Maximum mean column displacements at pier 1 (fixed bearing) according to different superstructure mass: (a) Bridge #1; (b) Bridge #2.

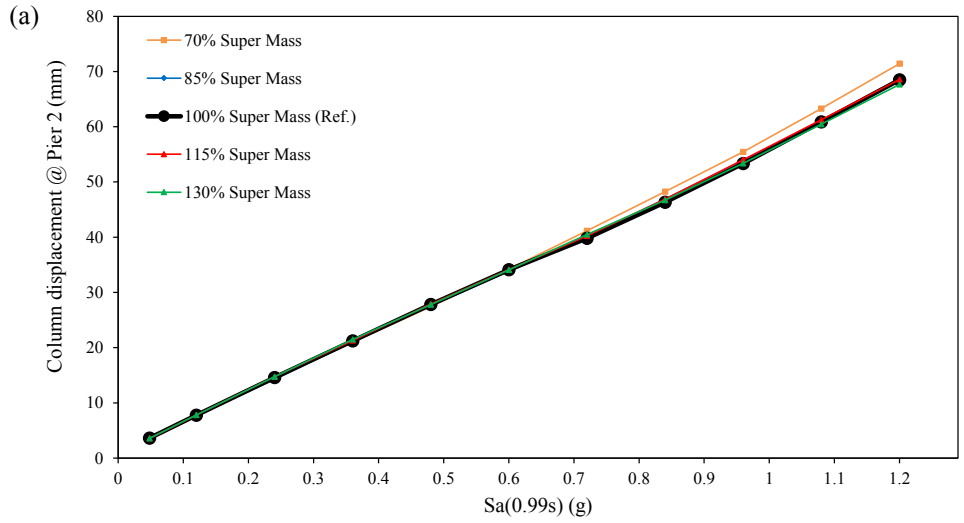

Figure 5.6 Maximum mean column displacements at pier 2 (expansion bearing) according to different superstructure mass: (a) Bridge #1; (b) Bridge #2.

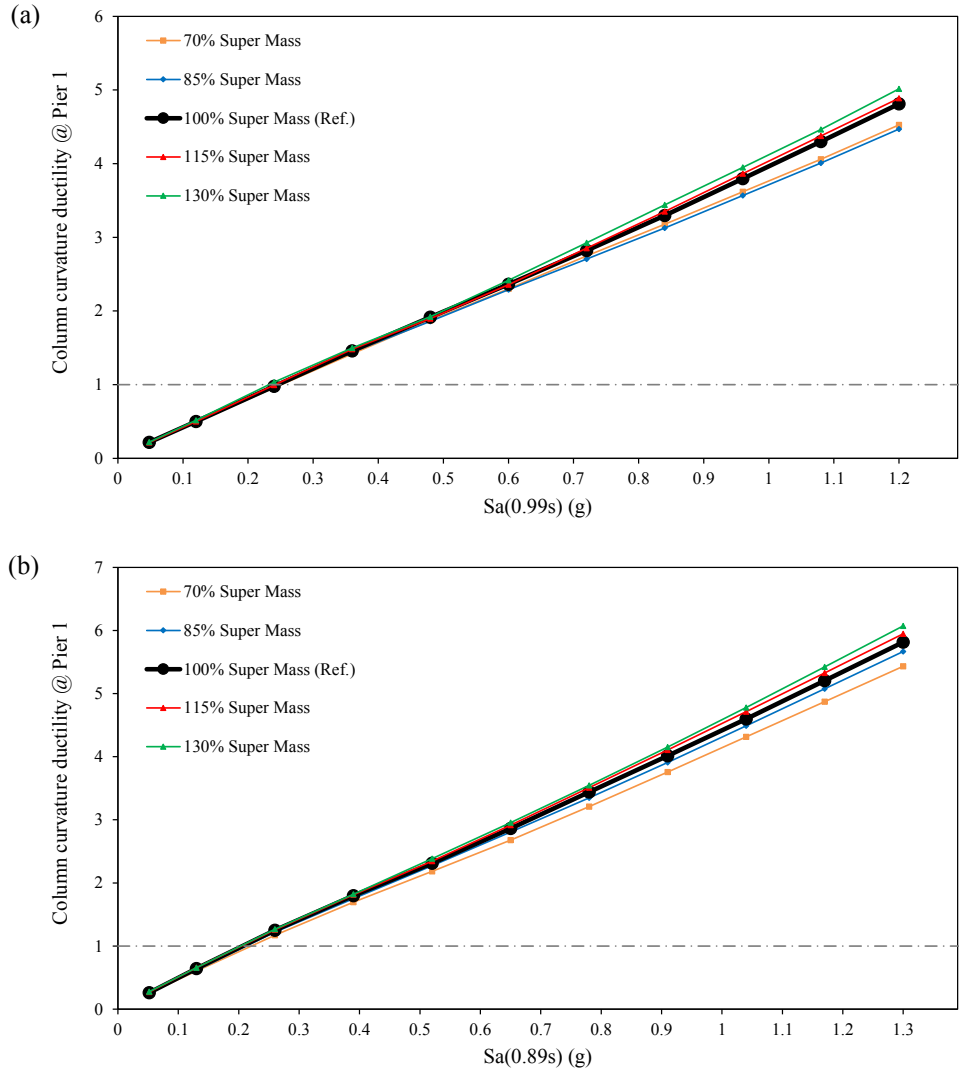

Figure 5.7 Maximum mean column curvature ductilities at pier 1 (fixed bearing) according to different superstructure mass: (a) Bridge #1; (b) Bridge #2.

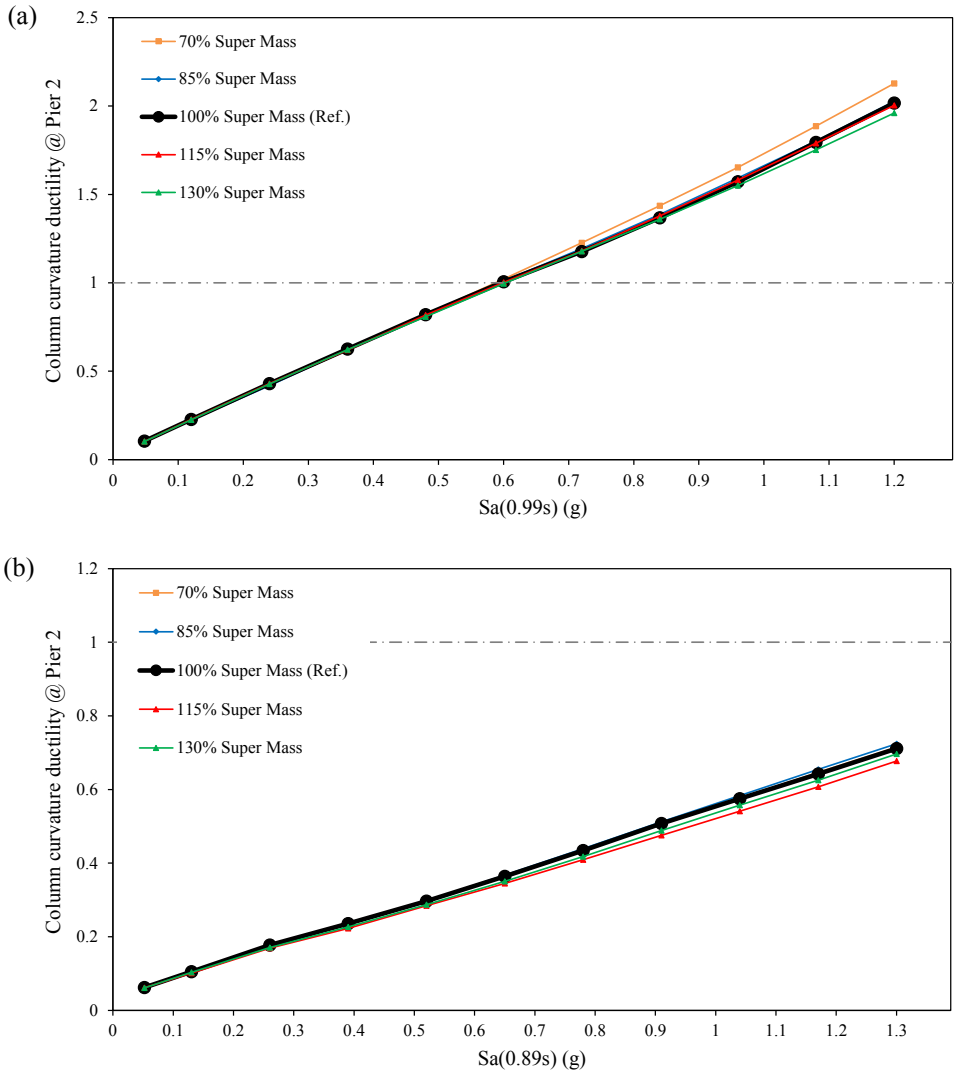

Figure 5.8 Maximum mean column curvature ductilities at pier 2 (expansion bearing) according to different superstructure mass: (a) Bridge #1; (b) Bridge #2.

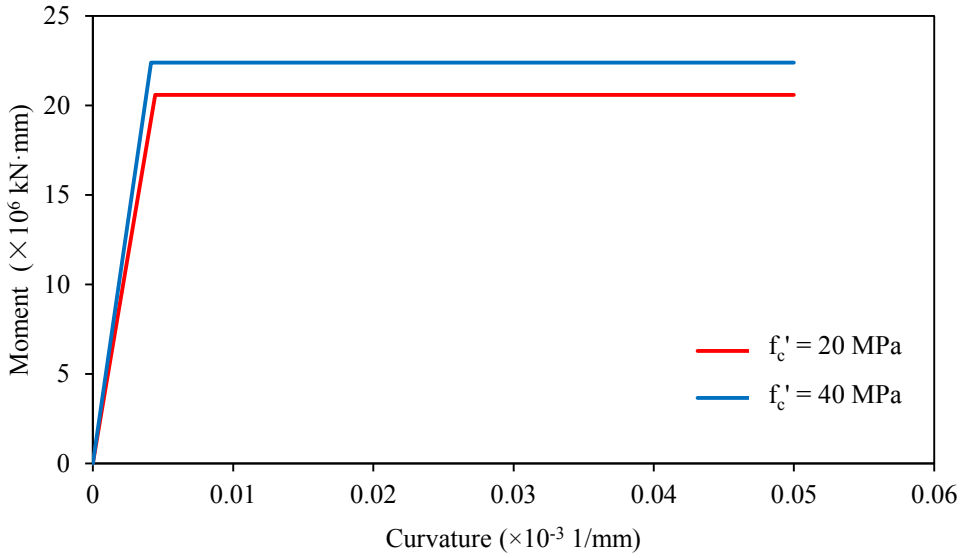

Figure 5.9 Moment – curvature relation of an end section of a column using f_c' = 20 MPa, and f_c' = 40 MPa.

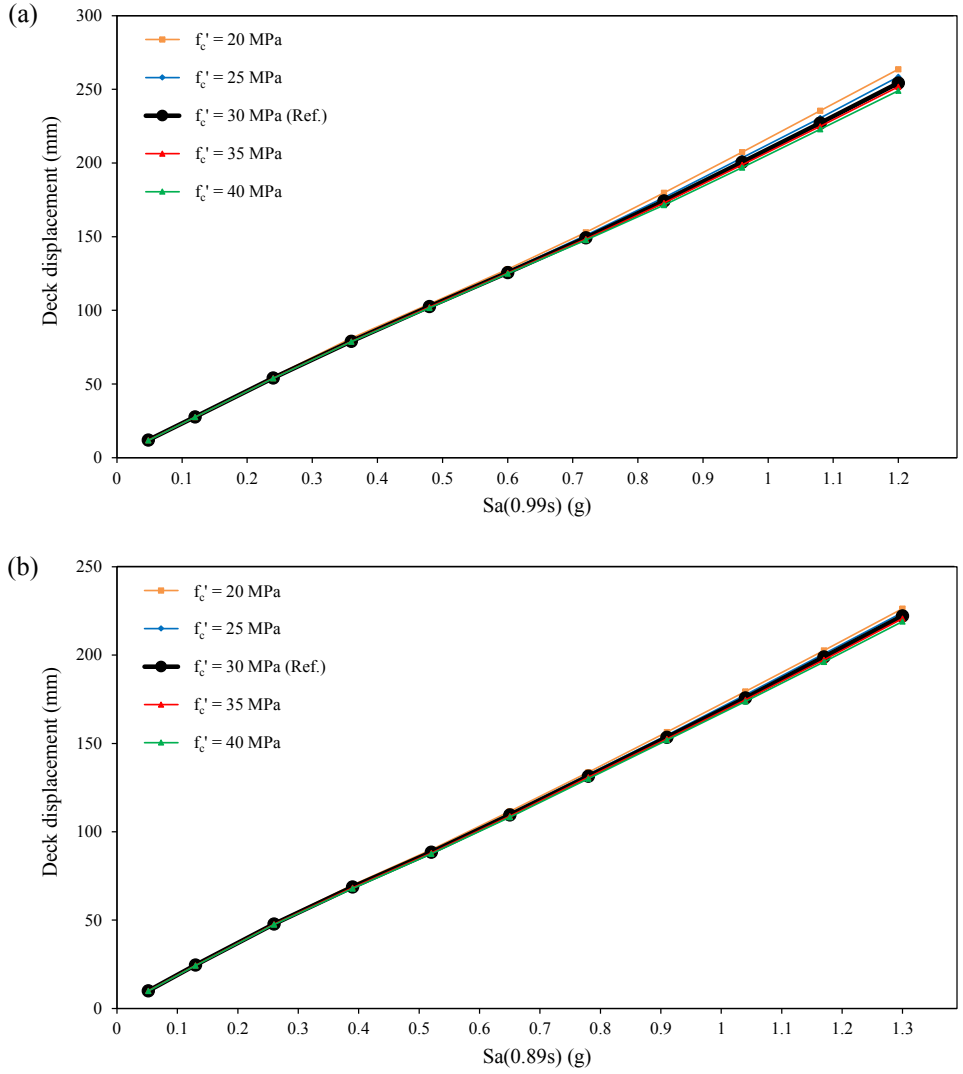

Figure 5.10 Maximum mean deck displacements according to different concrete compressive strength: (a) Bridge #1; (b) Bridge #2.

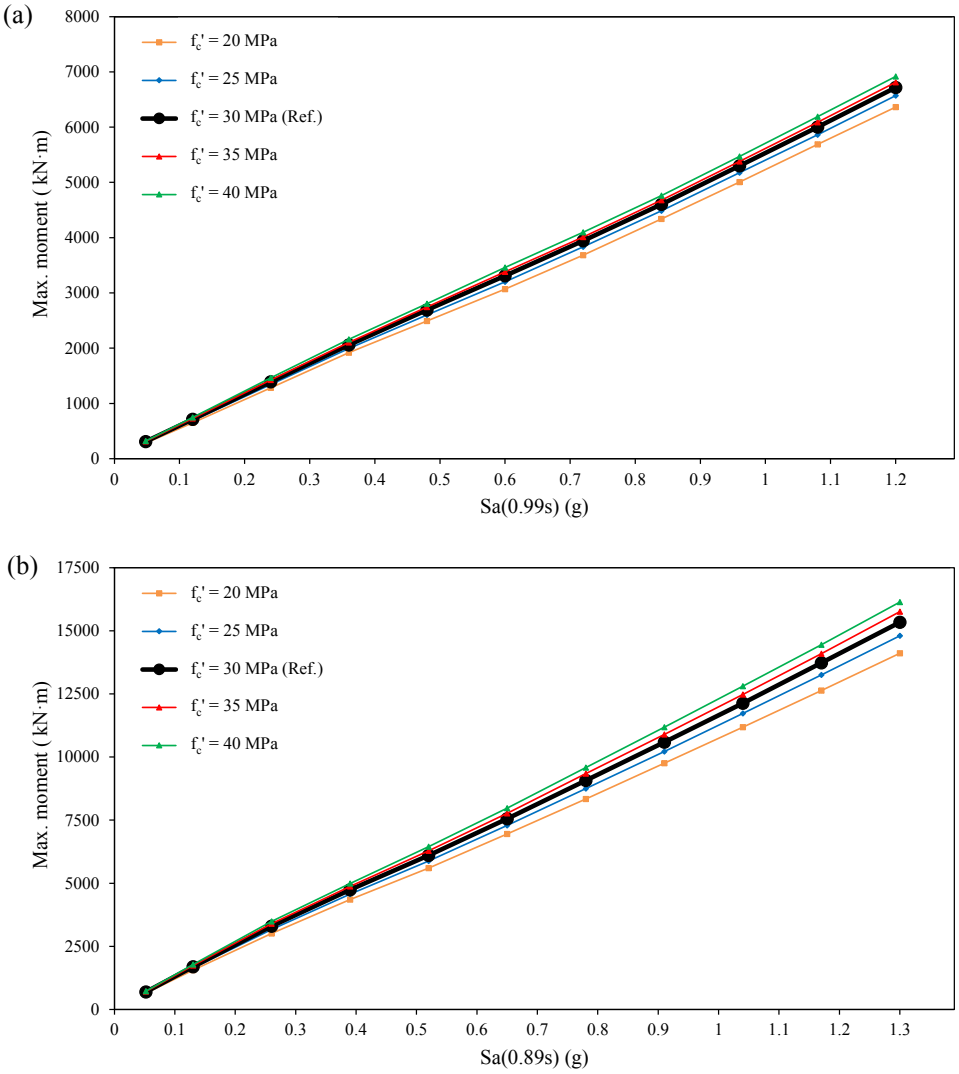

Figure 5.11 Maximum mean moments at the base of the column according to different concrete compressive strength: (a) Bridge #1; (b) Bridge #2.

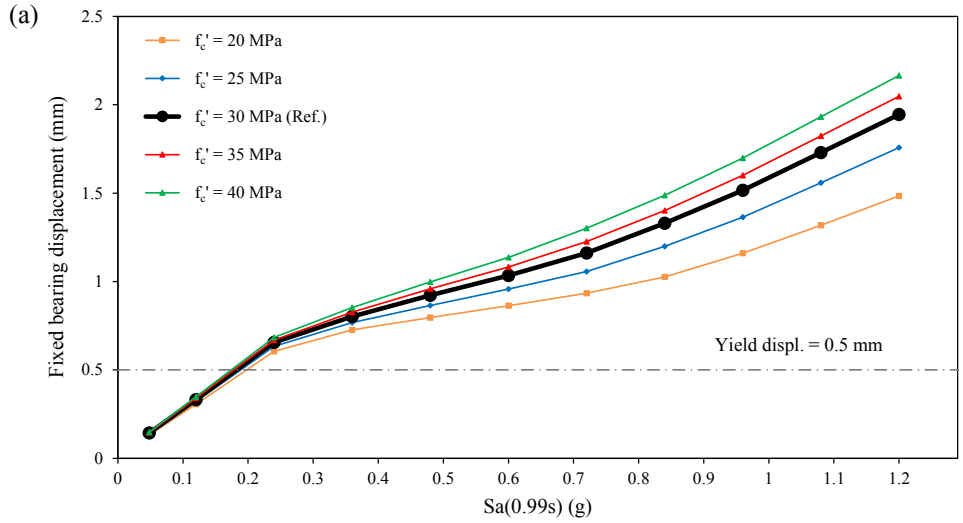

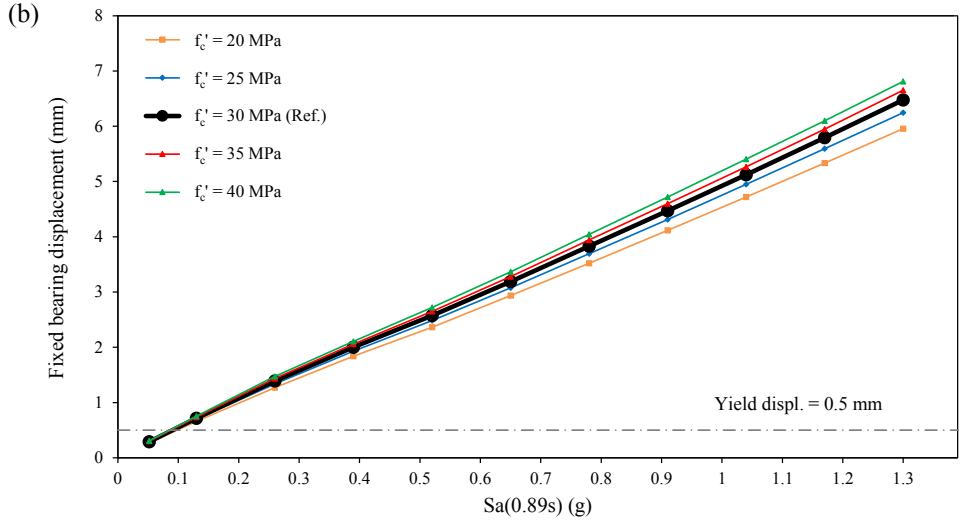

Figure 5.12 Maximum mean fixed bearing displacements according to different concrete compressive strength: (a) Bridge #1; (b) Bridge #2.

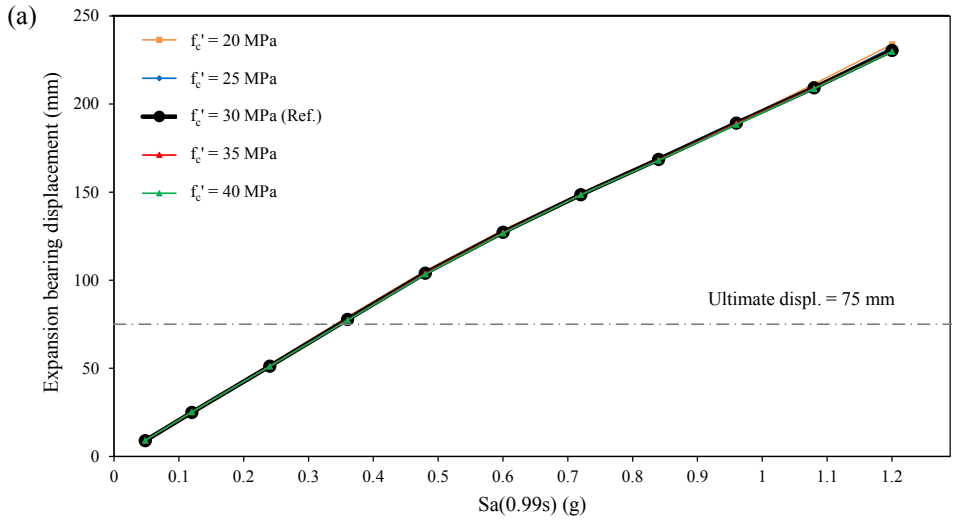

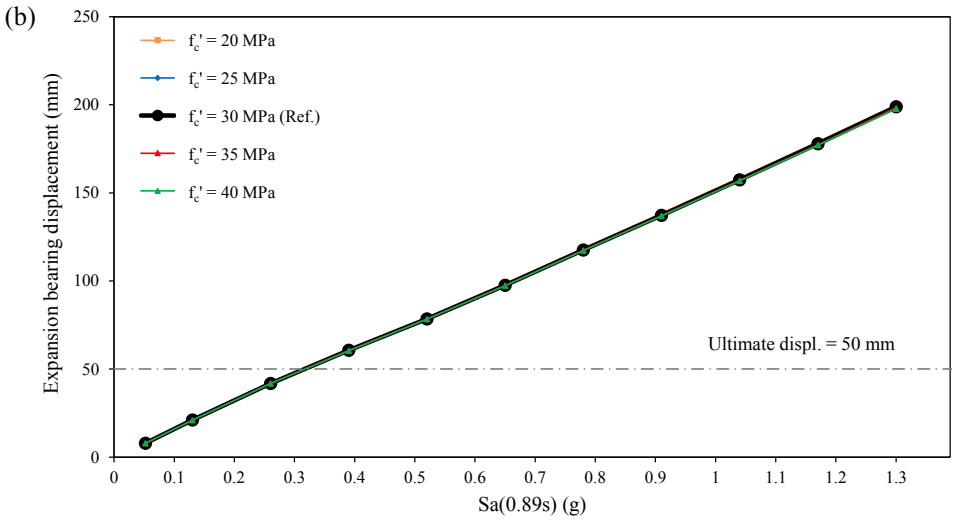

Figure 5.13 Maximum mean expansion bearing displacements according to different concrete compressive strength: (a) Bridge #1; (b) Bridge #2.

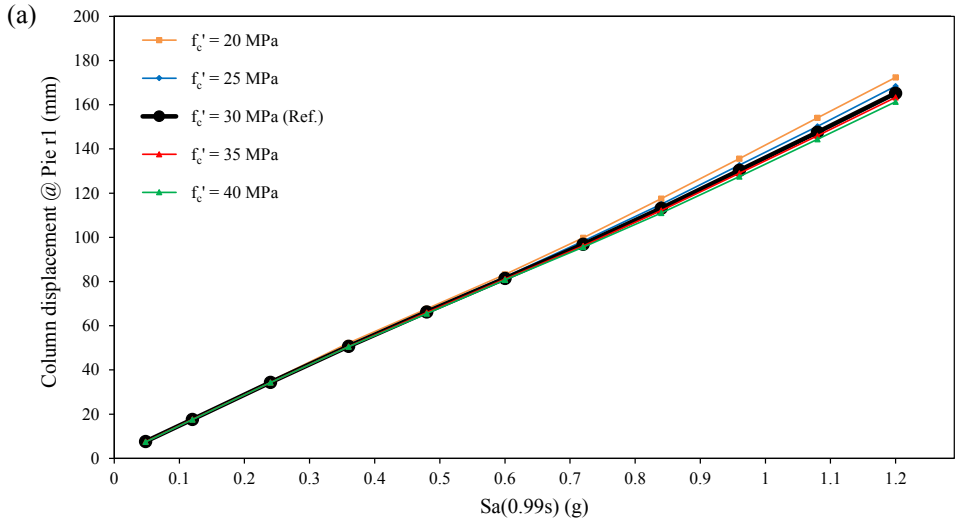

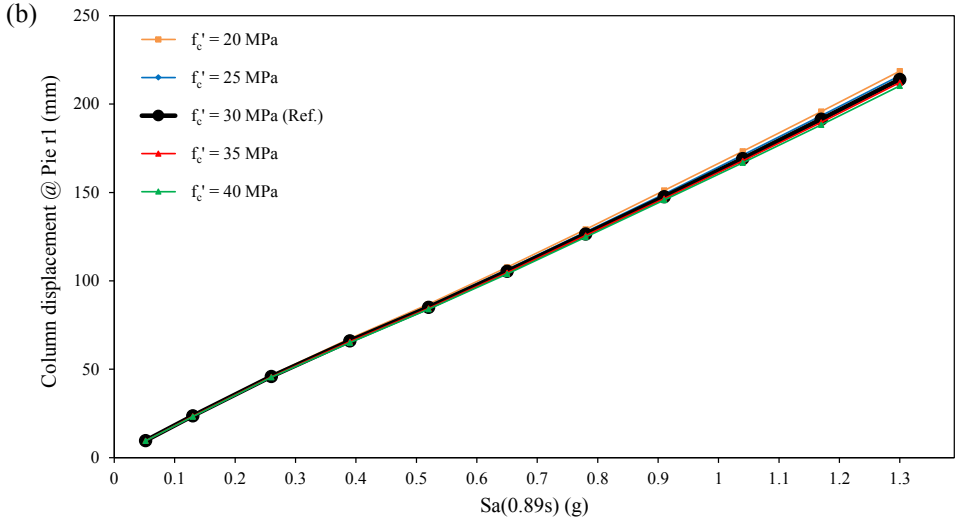

Figure 5.14 Maximum mean column displacements at pier 1 (fixed bearing) according to different concrete compressive strength: (a) Bridge #1; (b) Bridge #2.

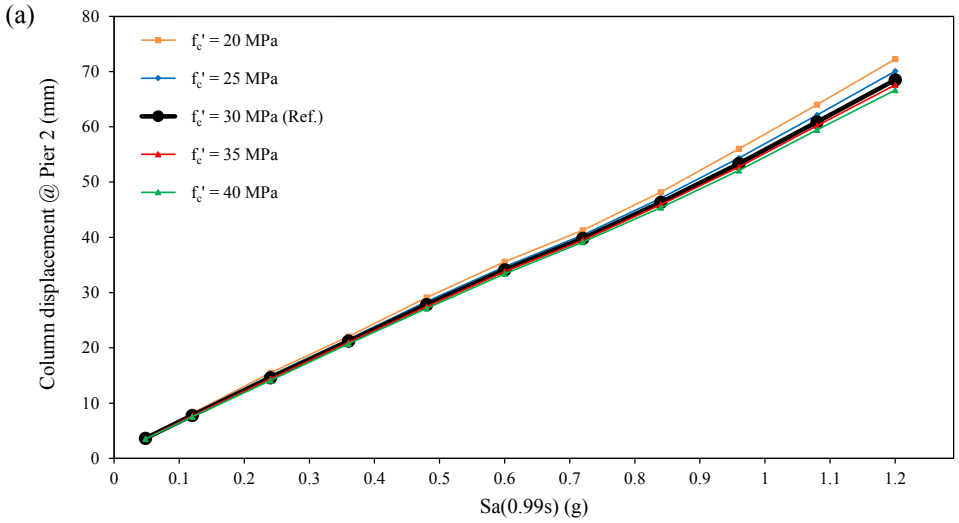

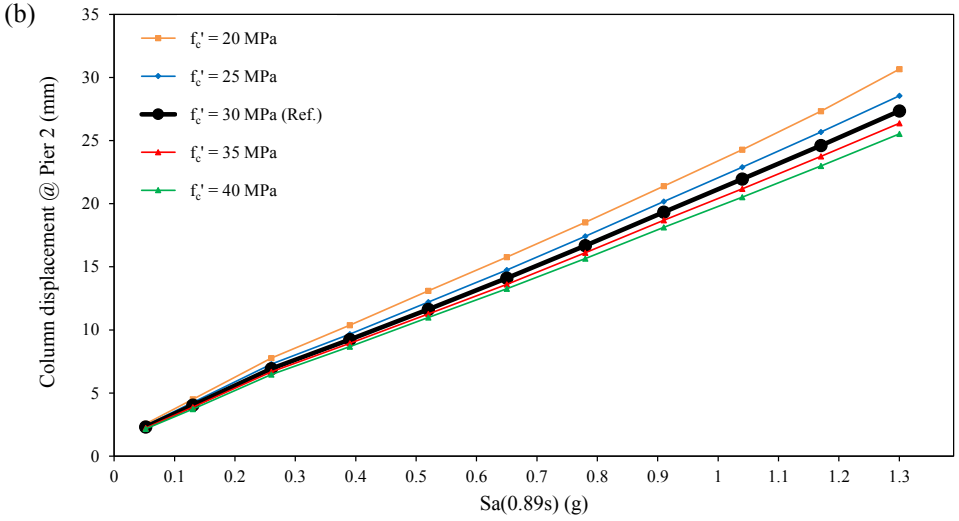

Figure 5.15 Maximum mean column displacements at pier 2 (expansion bearing) according to different concrete compressive strength: (a) Bridge #1; (b) Bridge #2.

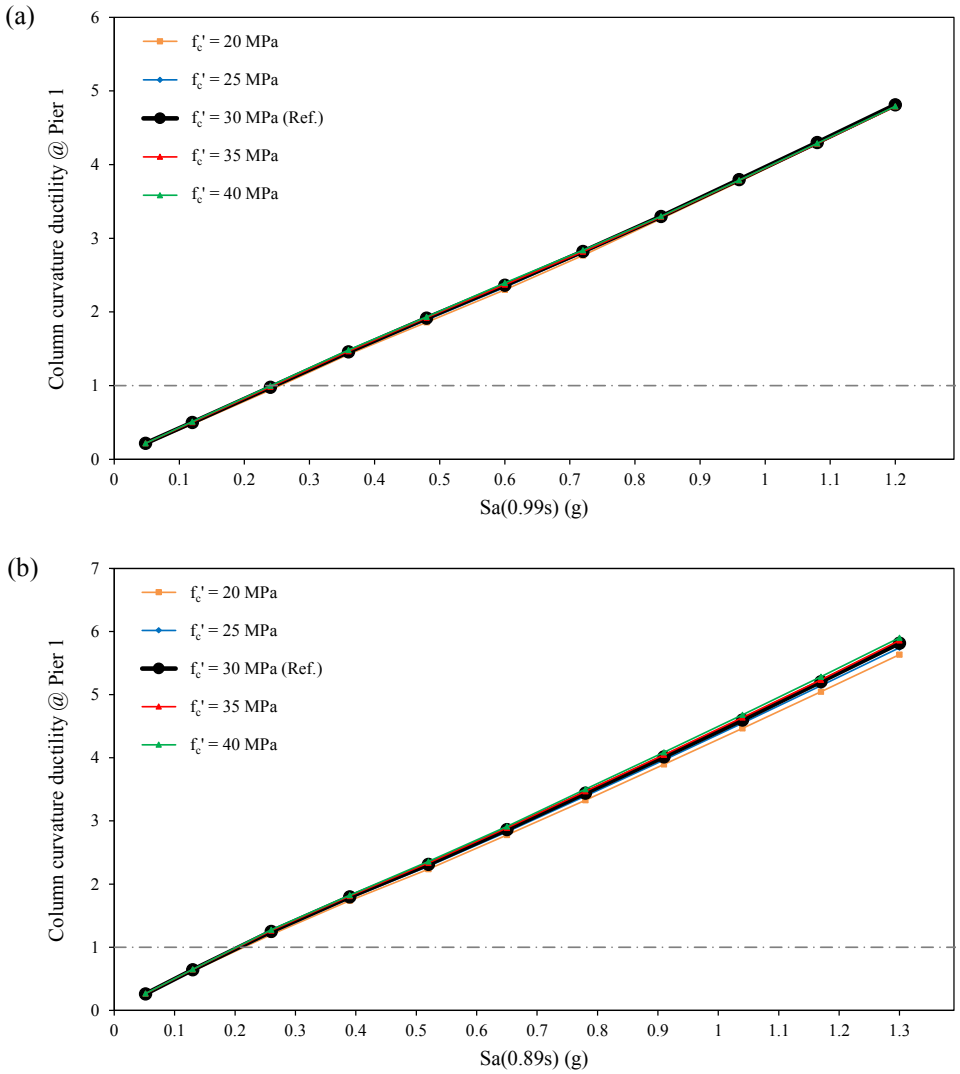

Figure 5.16 Maximum mean column curvature ductilities at pier 1 (fixed bearing) according to different concrete compressive strength: (a) Bridge #1; (b) Bridge #2.

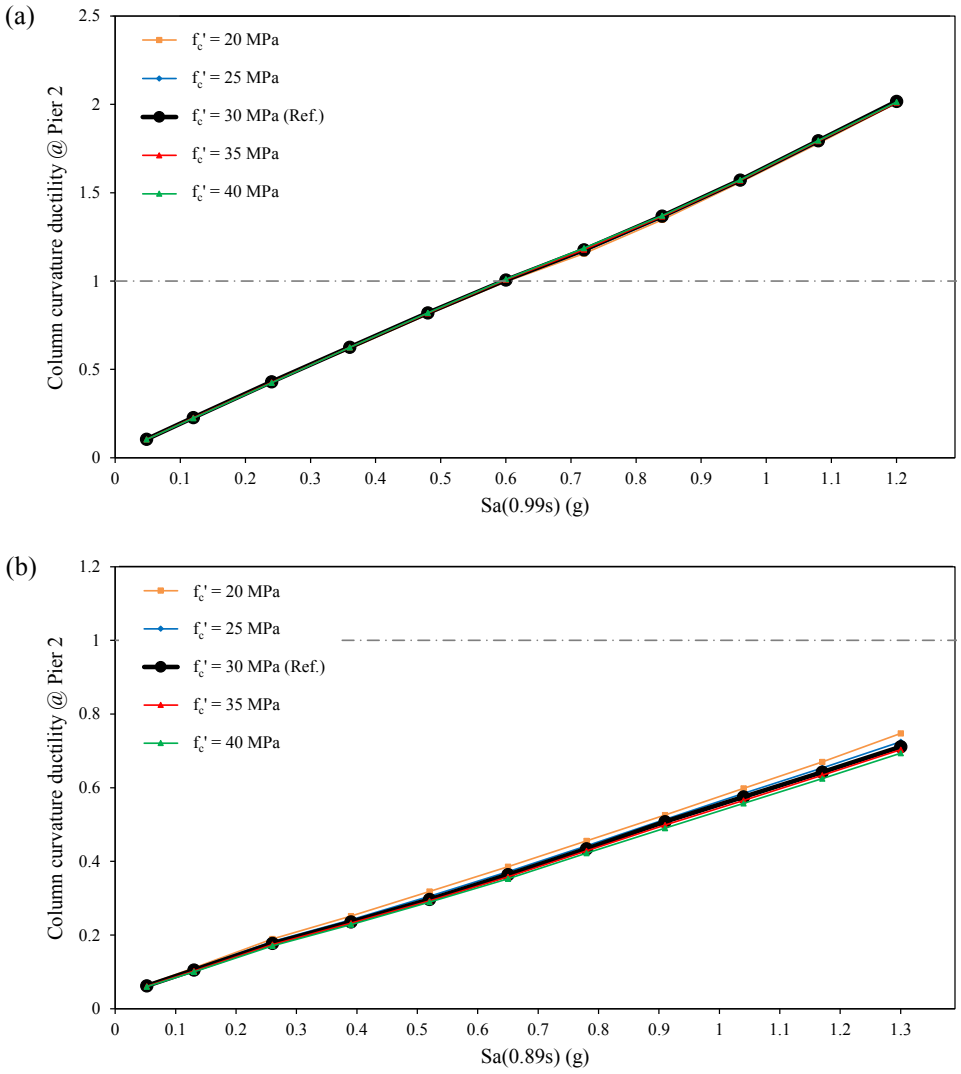

Figure 5.17 Maximum mean column curvature ductilities at pier 2 (expansion bearing) according to different concrete compressive strength: (a) Bridge #1; (b) Bridge #2.

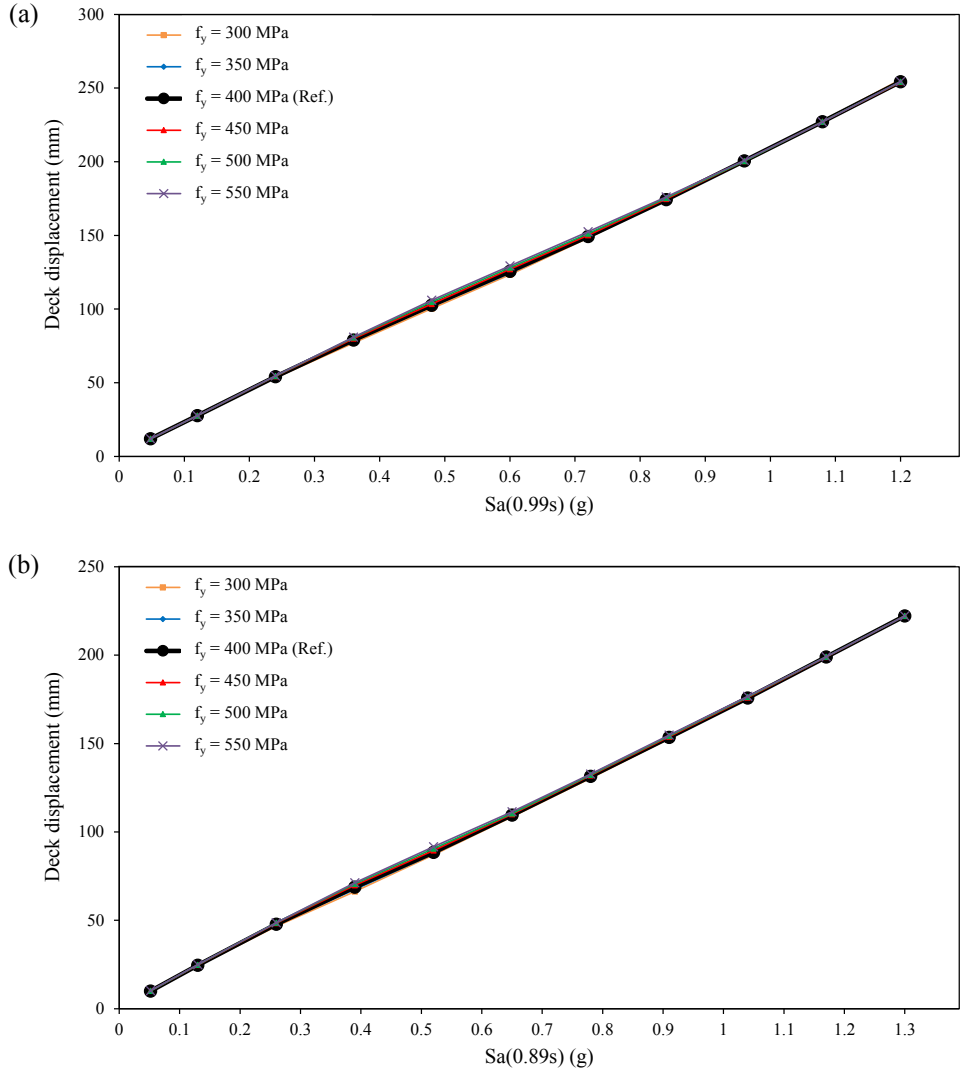

Figure 5.18 Maximum mean deck displacements according to different yield strength of the reinforcing steel: (a) Bridge #1; (b) Bridge #2.

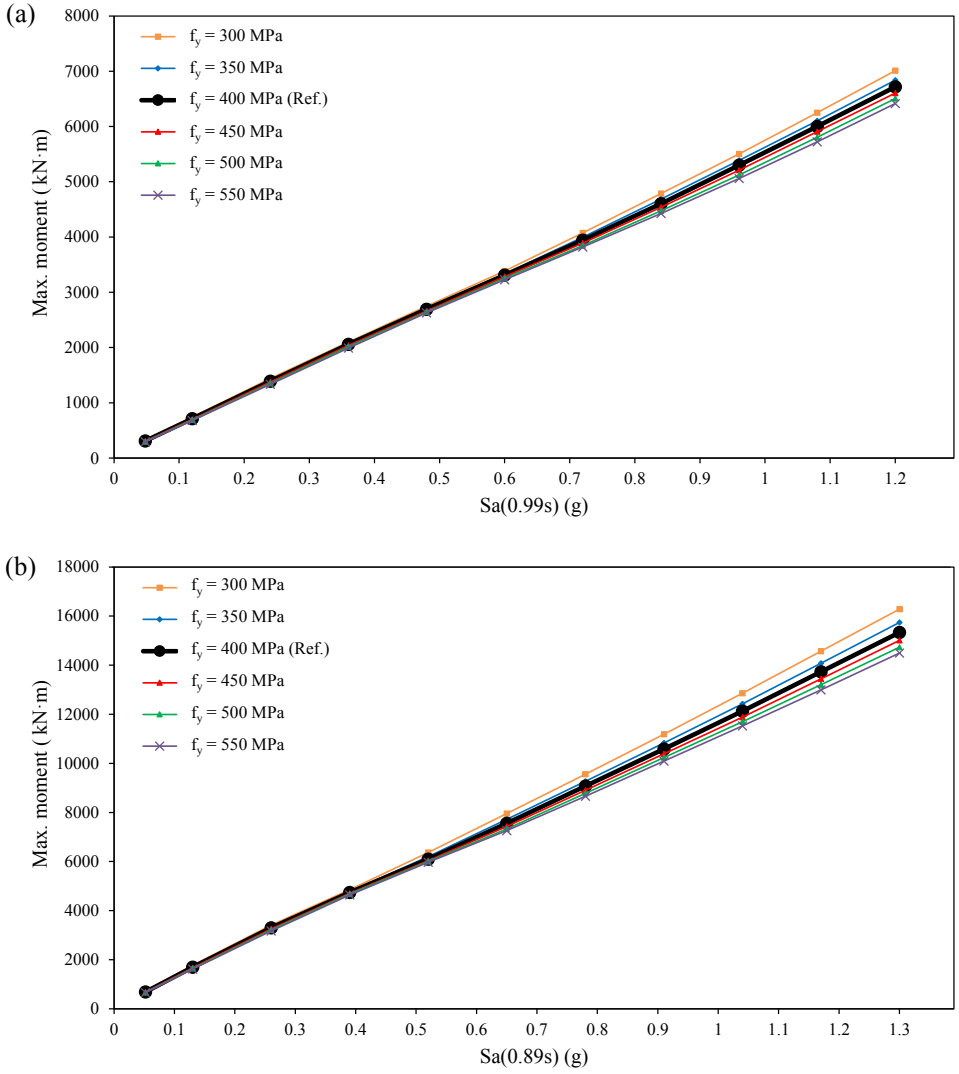

Figure 5.19 Maximum mean moments at the base of the column according to different yield strength of the reinforcing steel: (a) Bridge #1; (b) Bridge #2.

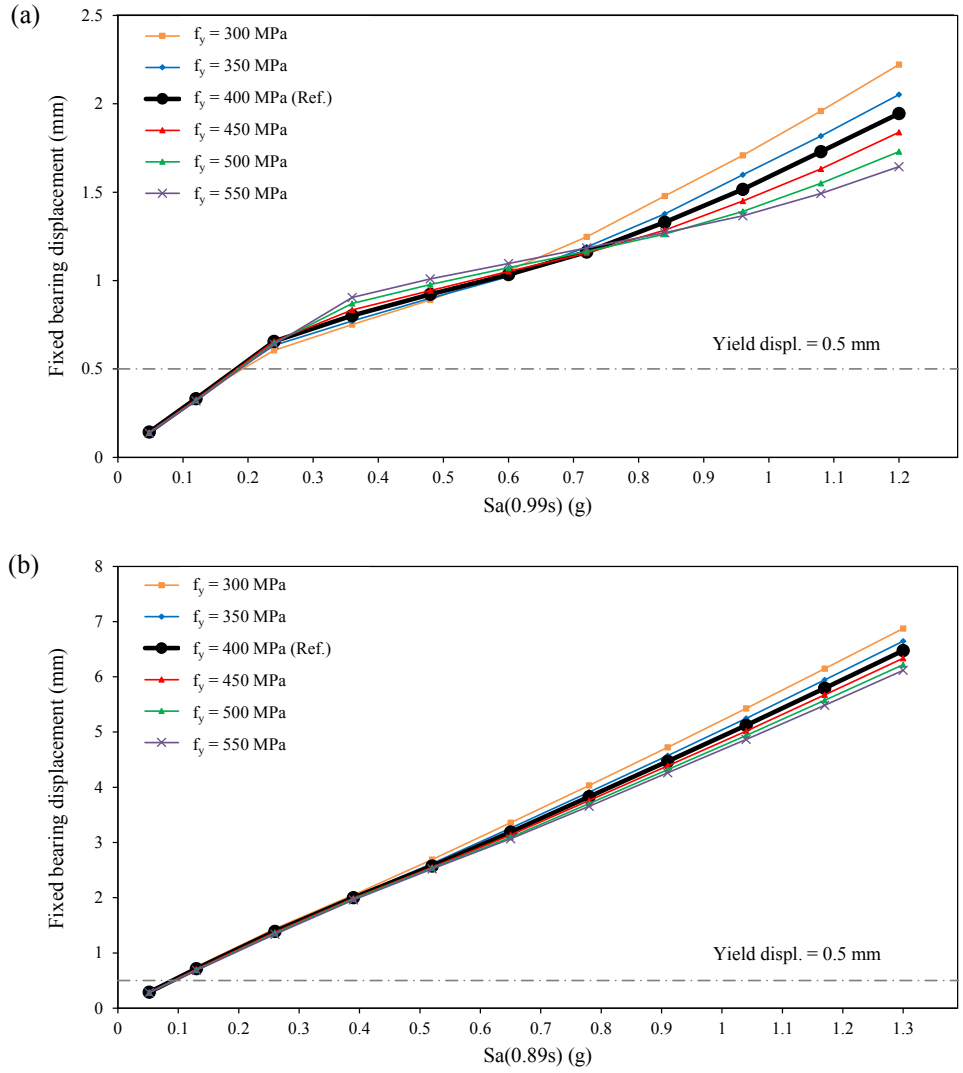

Figure 5.20 Maximum mean fixed bearing displacements according to different yield strength of the reinforcing steel: (a) Bridge #1; (b) Bridge #2.

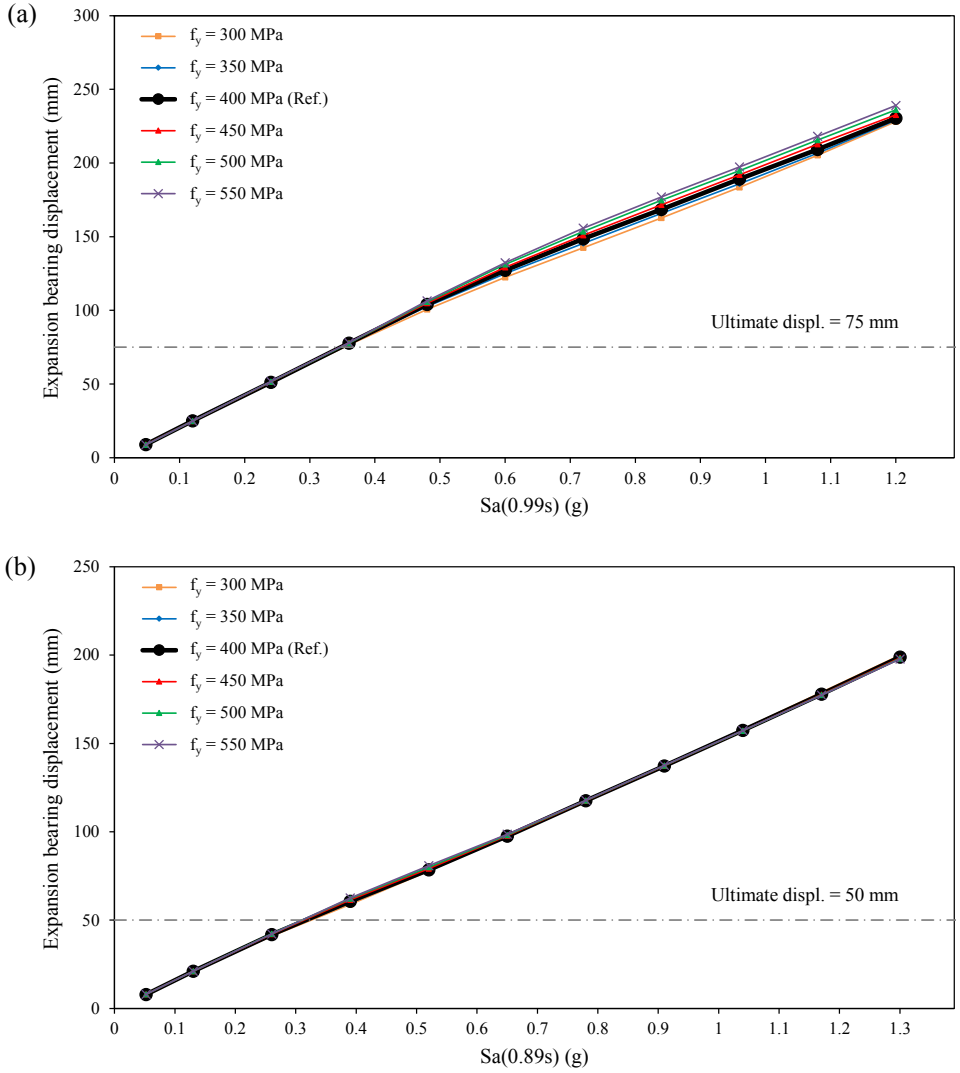

Figure 5.21 Maximum mean expansion bearing displacements according to different yield strength of the reinforcing steel: (a) Bridge #1; (b) Bridge #2.

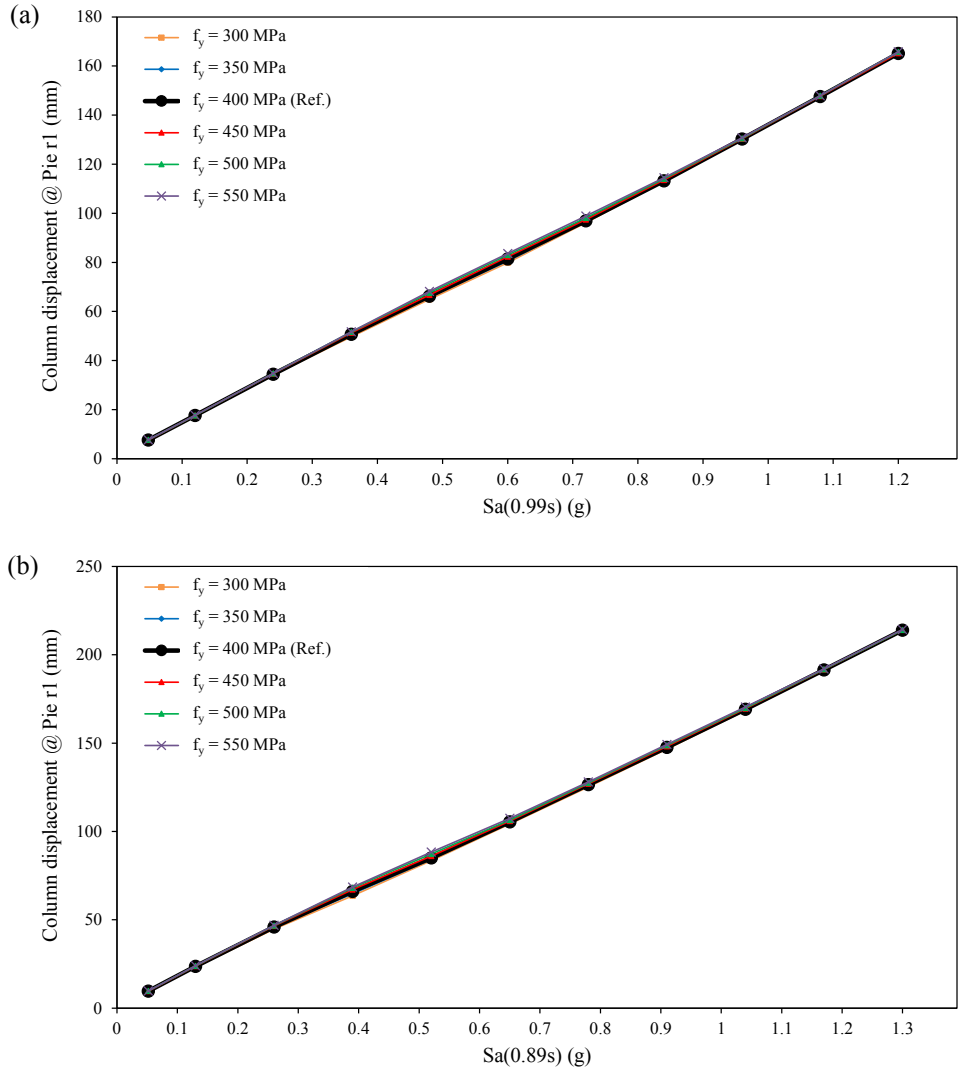

Figure 5.22 Maximum mean column displacements at pier 1 (fixed bearing) according to different yield strength of the reinforcing steel: (a) Bridge #1; (b) Bridge #2.

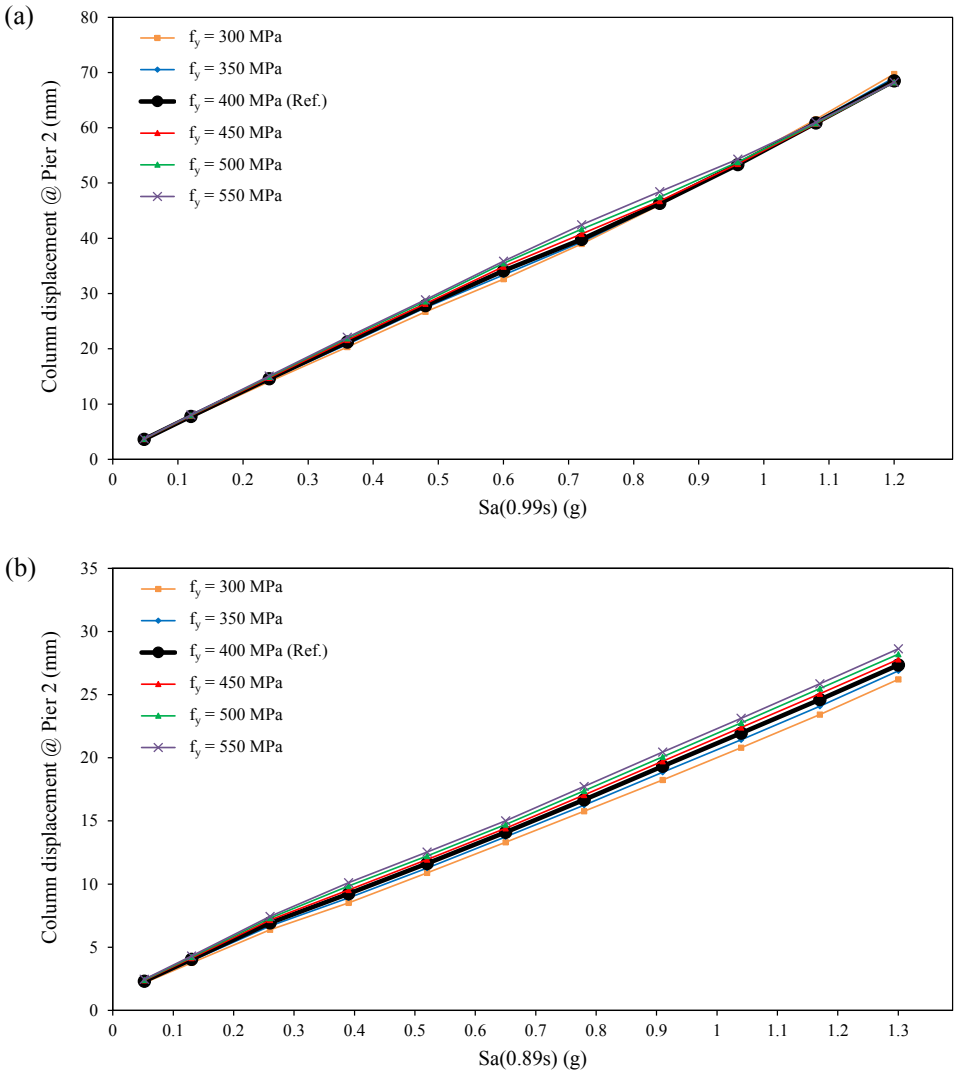

Figure 5.23 Maximum mean column displacements at pier 2 (expansion bearing) according to different yield strength of the reinforcing steel: (a) Bridge #1; (b) Bridge #2.

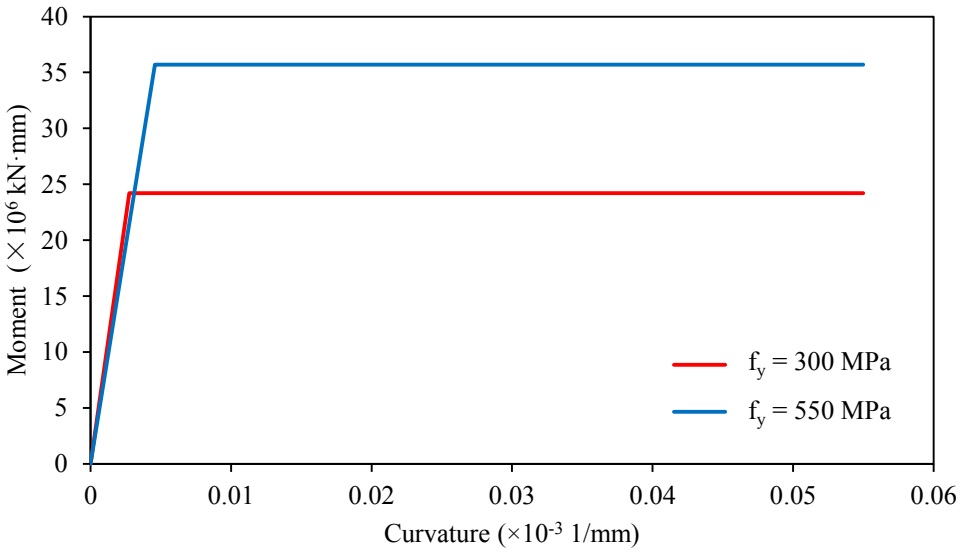

Figure 5.24 Moment – curvature relation of an end section of a column using f_y = 300 MPa, and f_y = 550 MPa.

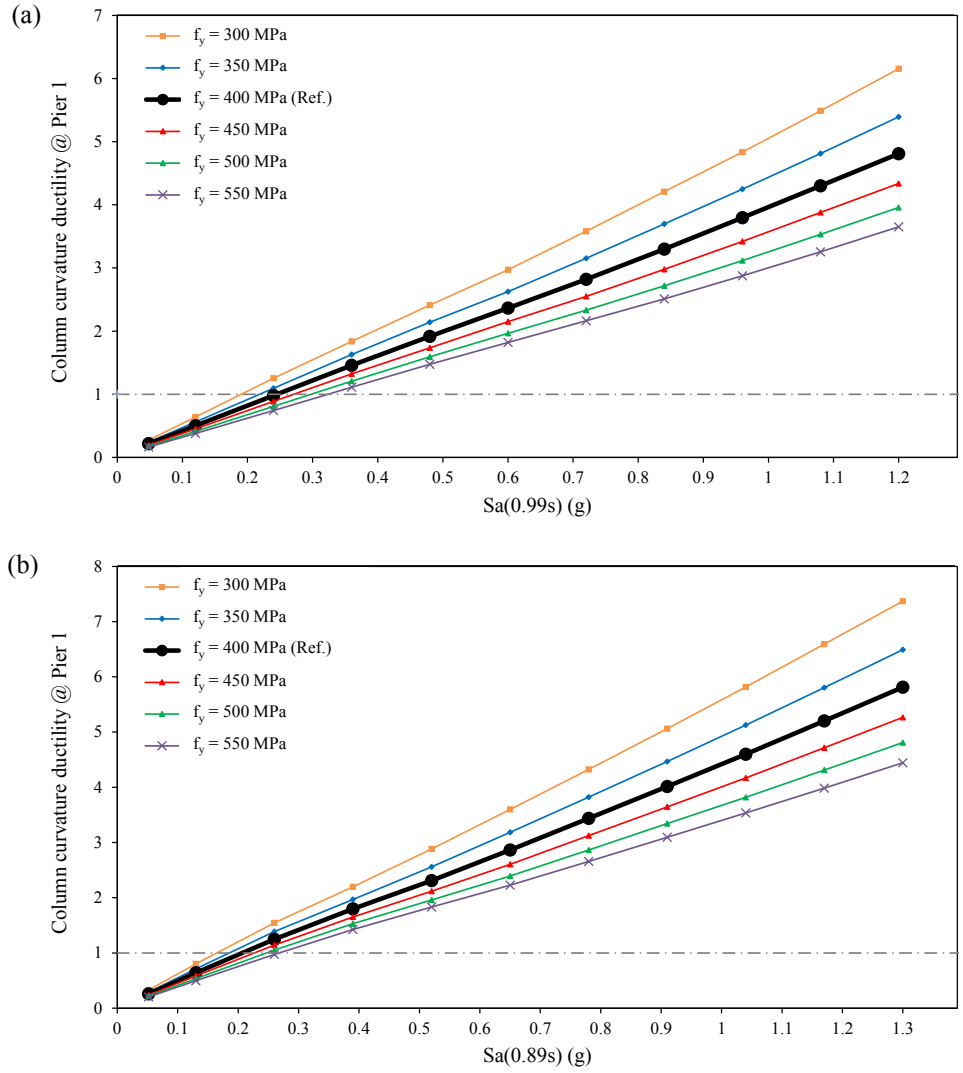

Figure 5.25 Maximum mean column curvature ductilities at pier 1 (fixed bearing) according to different yield strength of the reinforcing steel: (a) Bridge #1; (b) Bridge #2.

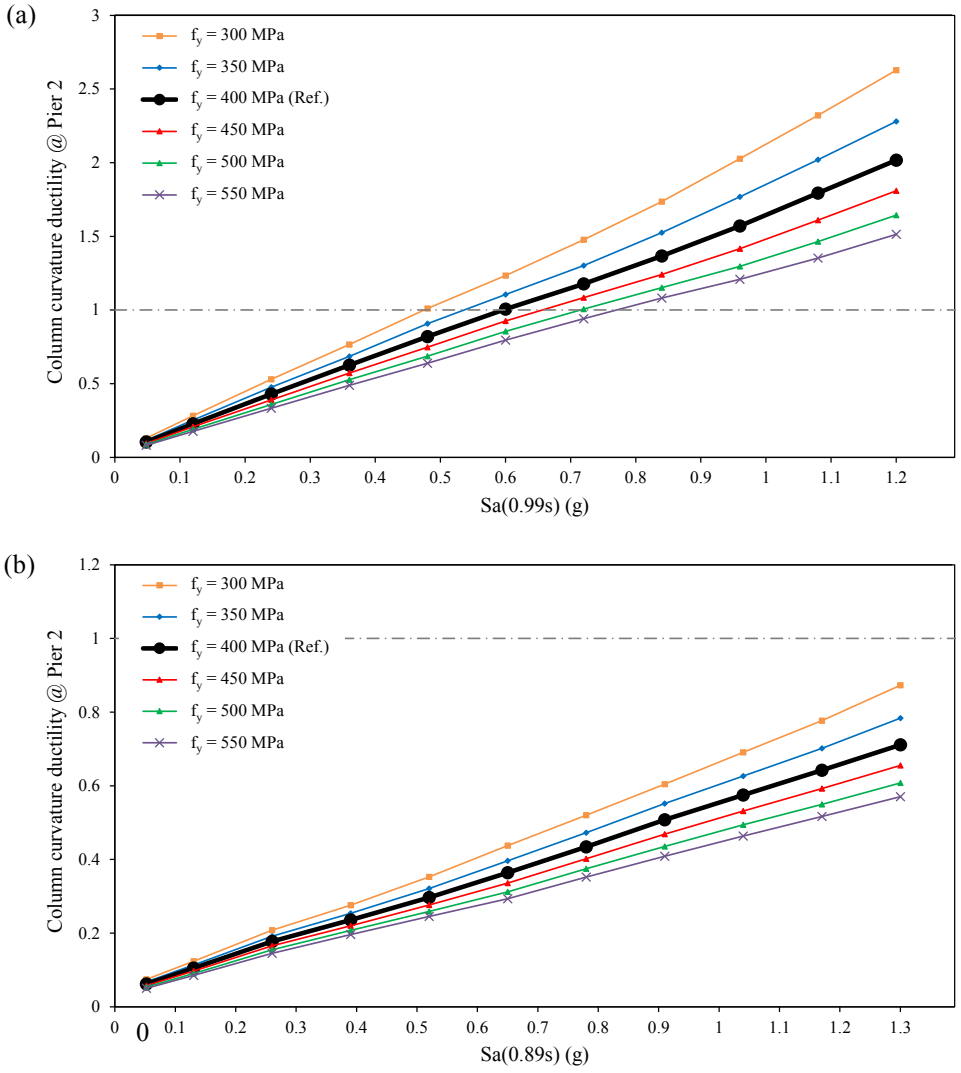

Figure 5.26 Maximum mean column curvature ductilities at pier 2 (expansion bearing) according to different yield strength of the reinforcing steel: (a) Bridge #1; (b) Bridge #2.

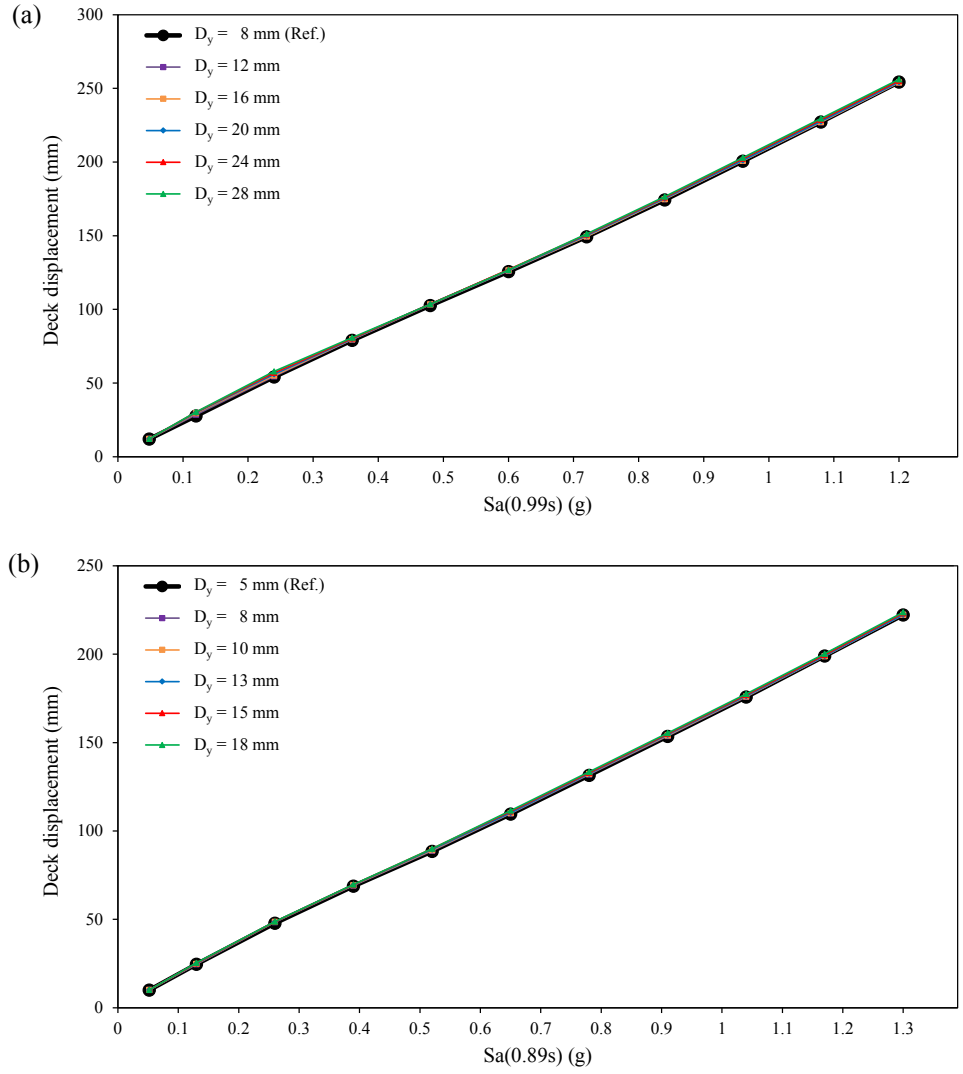

Figure 5.27 Maximum mean deck displacements according to different yield displacement of the bearing: (a) Bridge #1; (b) Bridge #2.

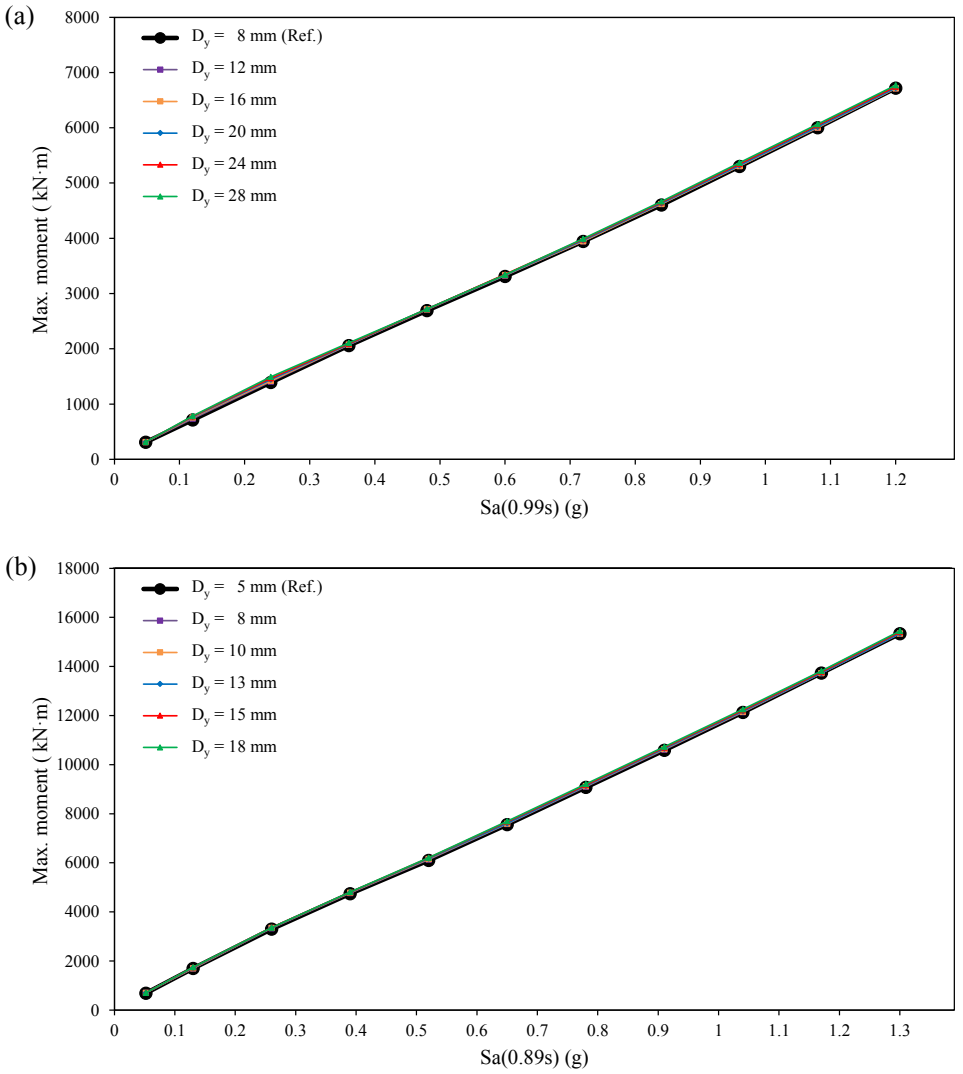

Figure 5.28 Maximum mean moments at the base of the column according to different yield displacement of the bearing: (a) Bridge #1; (b) Bridge #2.

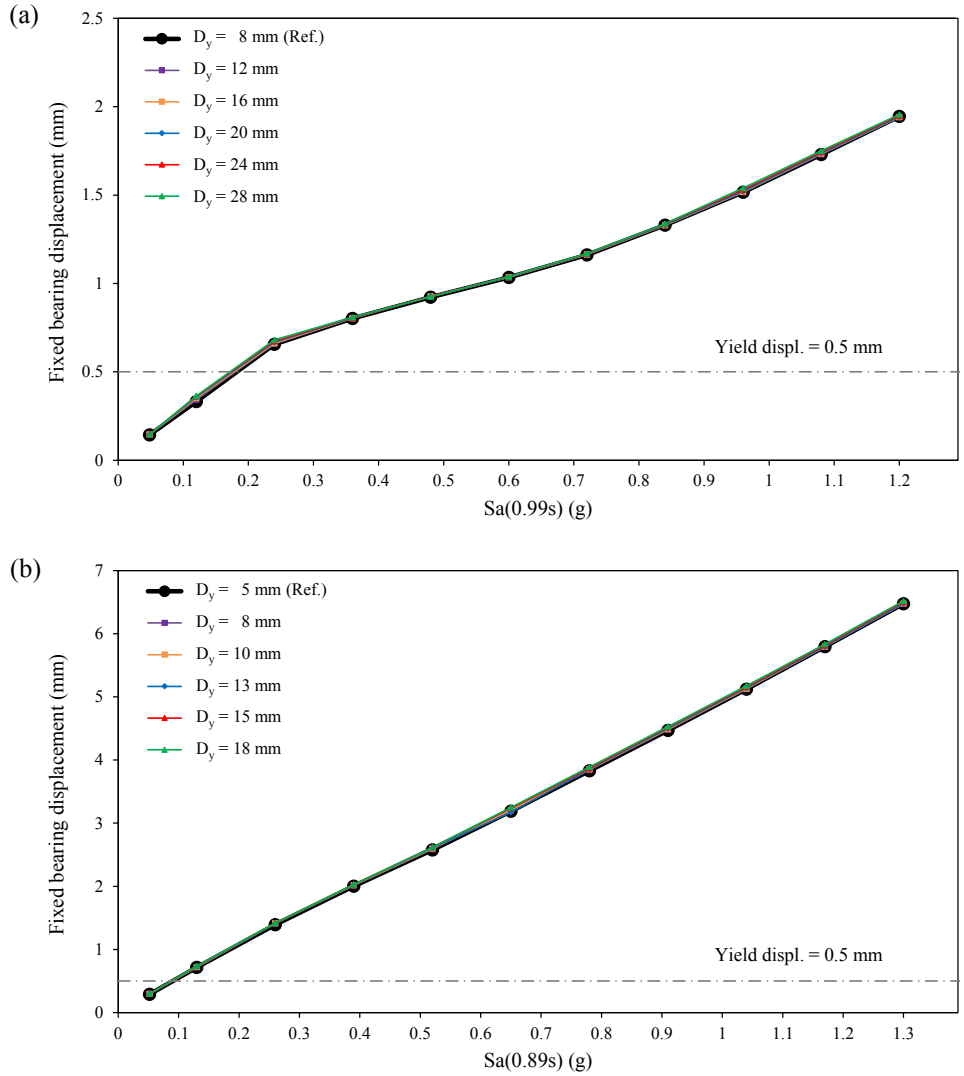

Figure 5.29 Maximum mean fixed bearing displacements according to different yield displacement of the bearing: (a) Bridge #1; (b) Bridge #2.

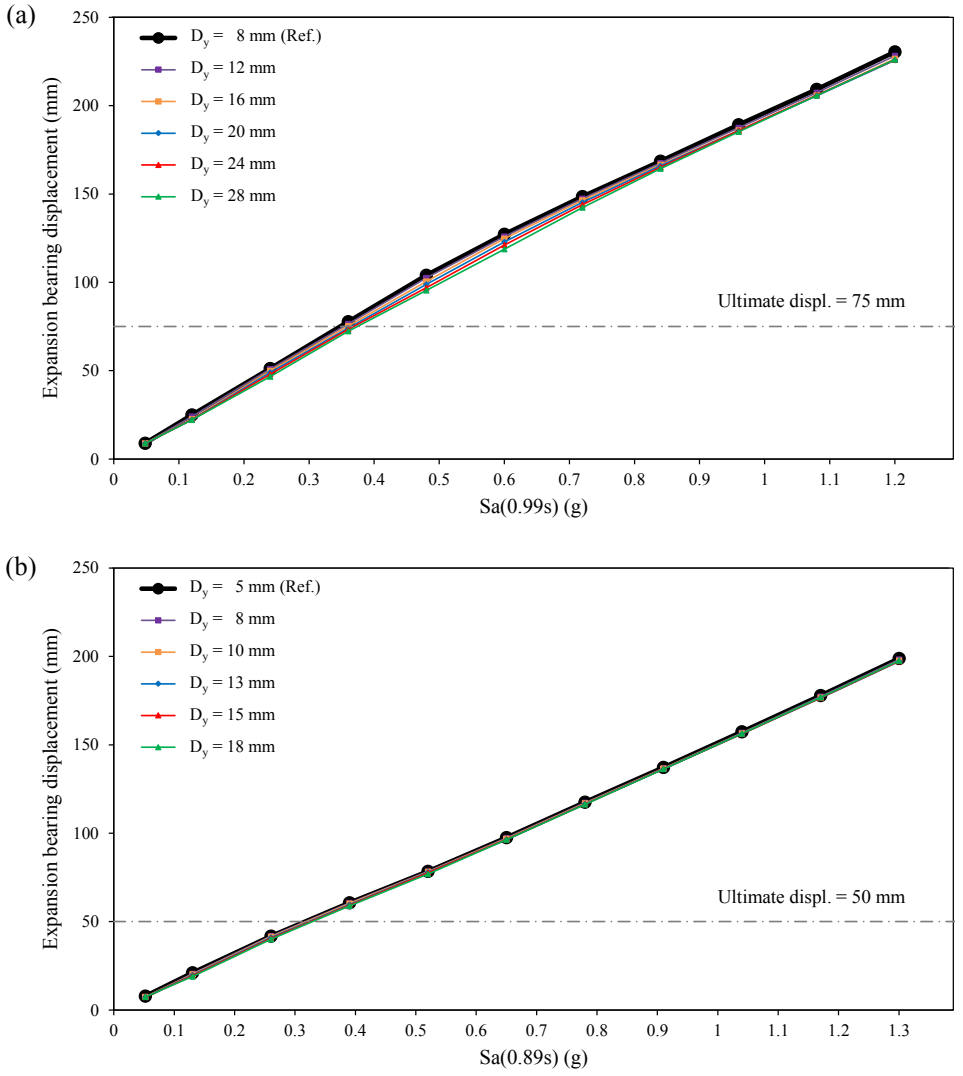

Figure 5.30 Maximum mean expansion bearing displacements to different yield displacement of the bearing: (a) Bridge #1; (b) Bridge #2.

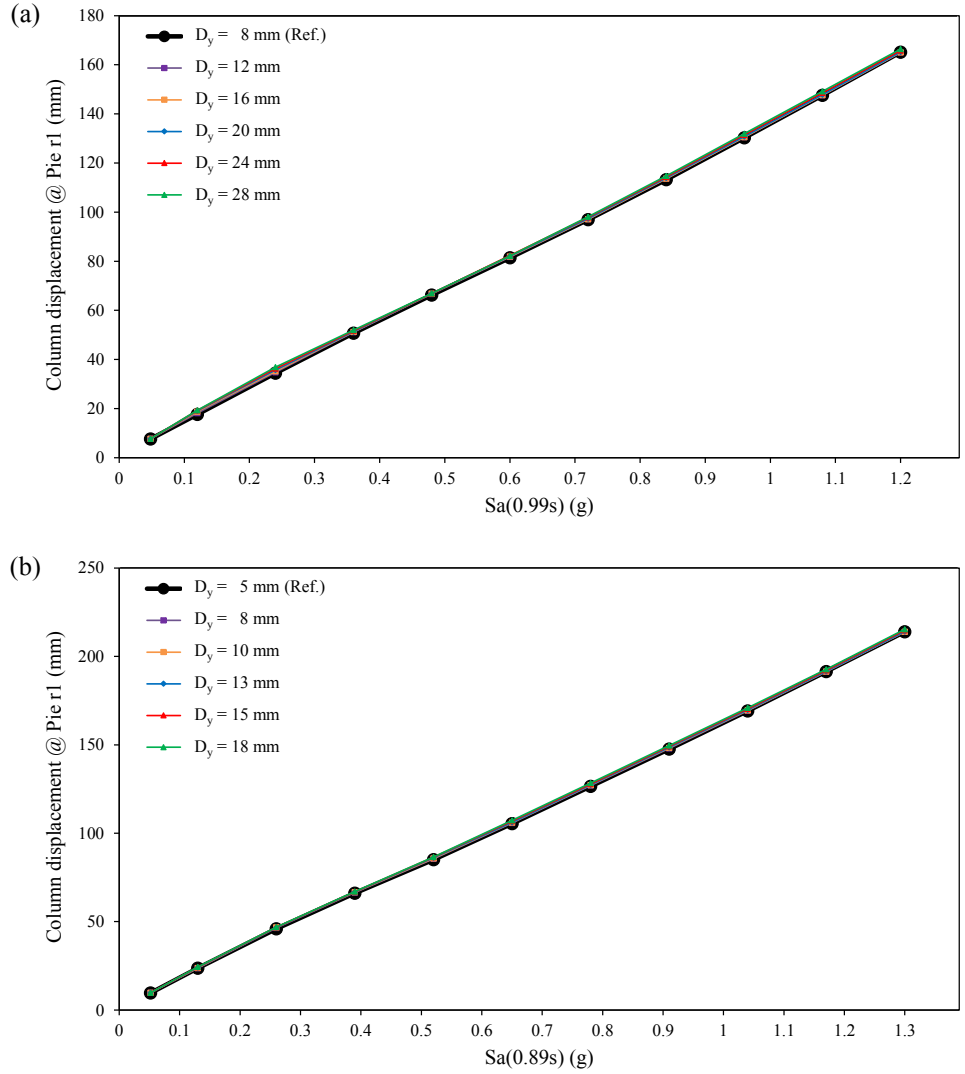

Figure 5.31 Maximum mean column displacements at pier 1 (fixed bearing) according to different yield displacement of the bearing: (a) Bridge #1; (b) Bridge #2.

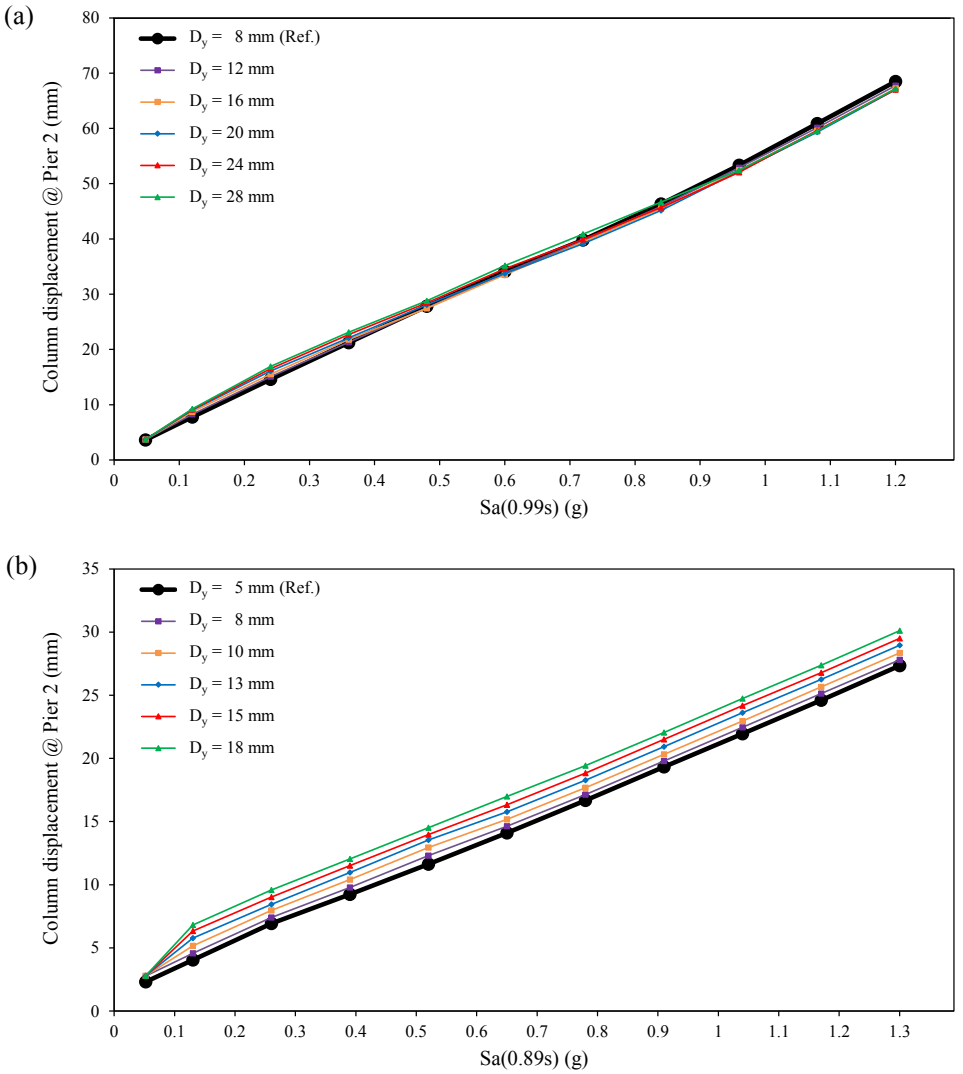

Figure 5.32 Maximum mean column displacements at pier 2 (expansion bearing) according to different yield displacement of the bearing: (a) Bridge #1; (b) Bridge #2.

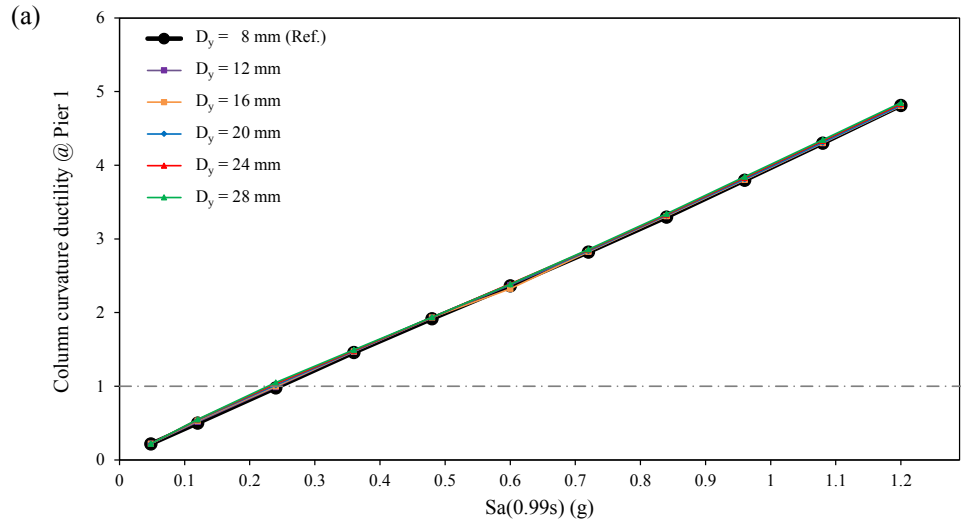

Figure 5.33 Maximum mean column curvature ductilities at pier 1 (fixed bearing) according to different yield displacement of the bearing: (a) Bridge #1; (b) Bridge #2.

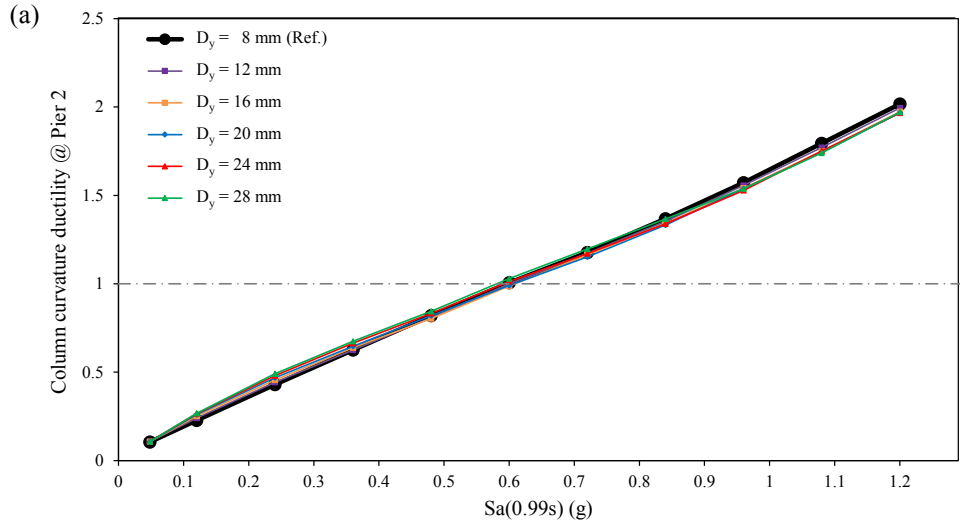

Figure 5.34 Maximum mean column curvature ductilities at pier 2 (expansion bearing) according to different yield displacement of the bearing: (a) Bridge #1; (b) Bridge #2.

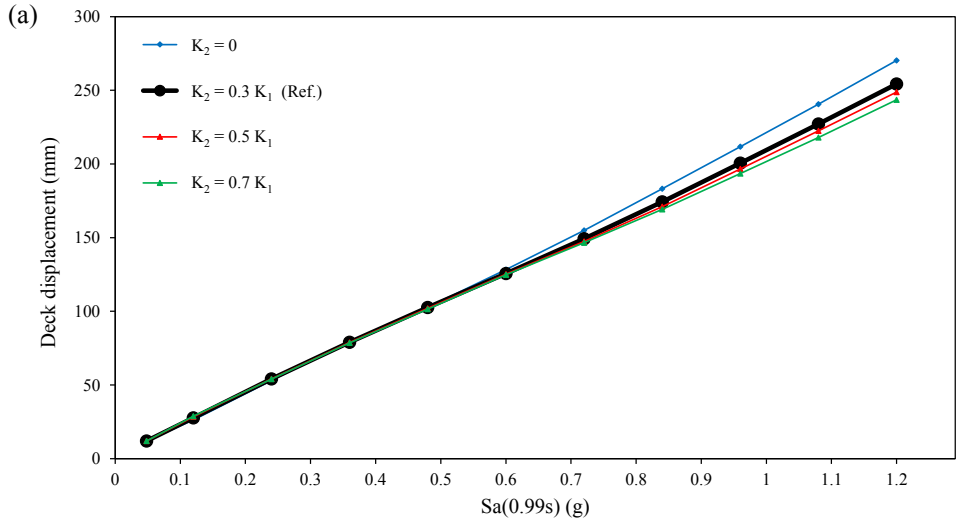

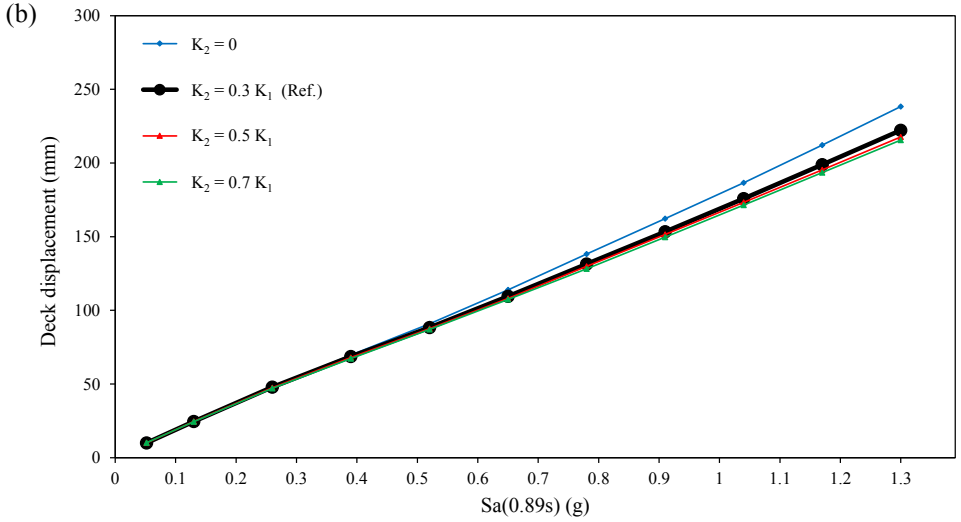

Figure 5.35 Maximum mean deck displacements according to different post-yield strength of the bearing: (a) Bridge #1; (b) Bridge #2.

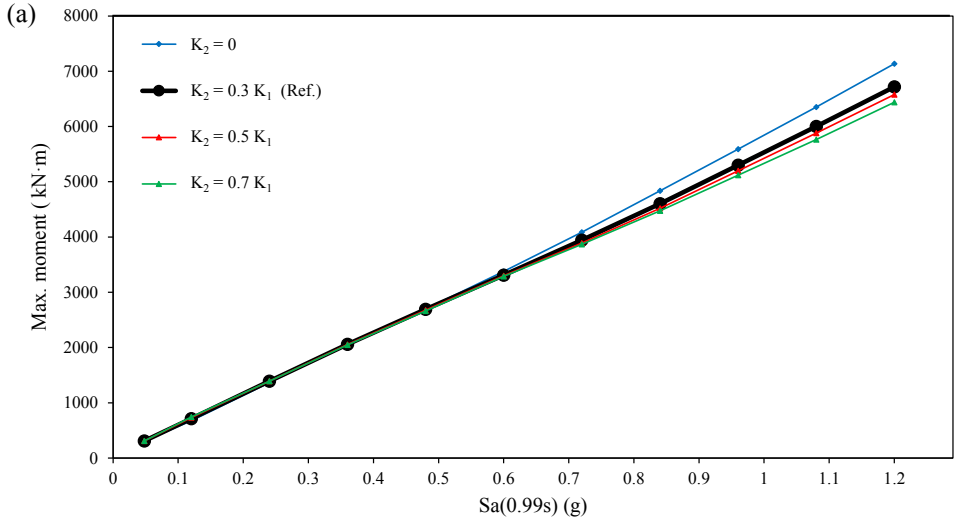

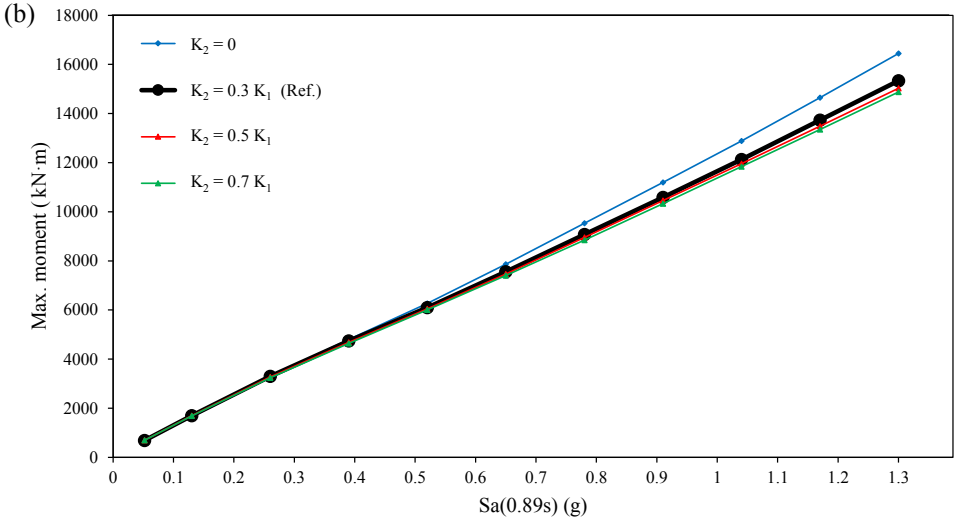

Figure 5.36 Maximum mean moments at the base of the column according to different post-yield strength of the bearing: (a) Bridge #1; (b) Bridge #2.

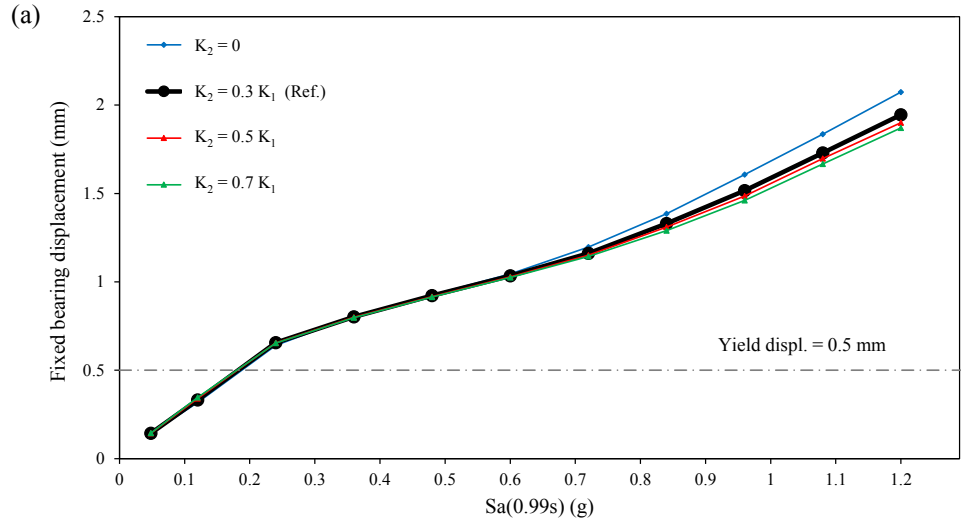

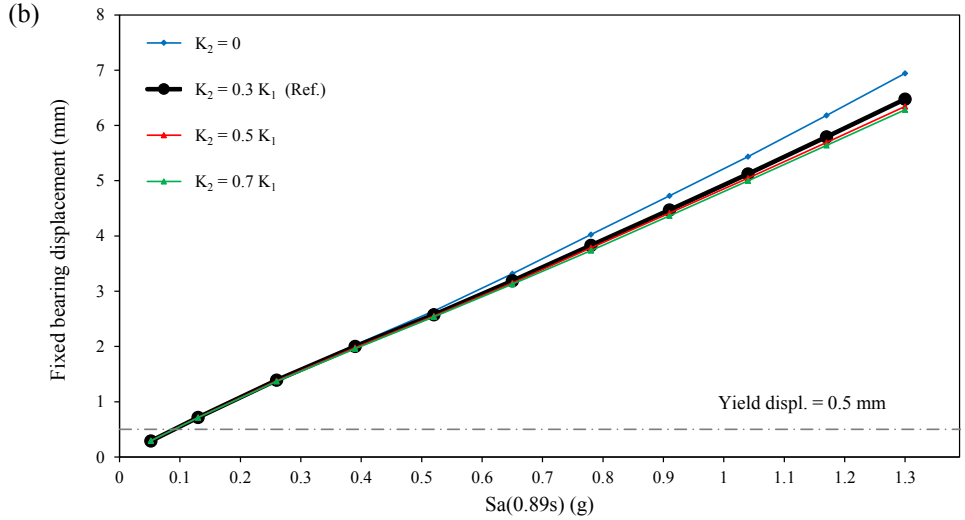

Figure 5.37 Maximum mean fixed bearing displacements according to different post-yield strength of the bearing: (a) Bridge #1; (b) Bridge #2.

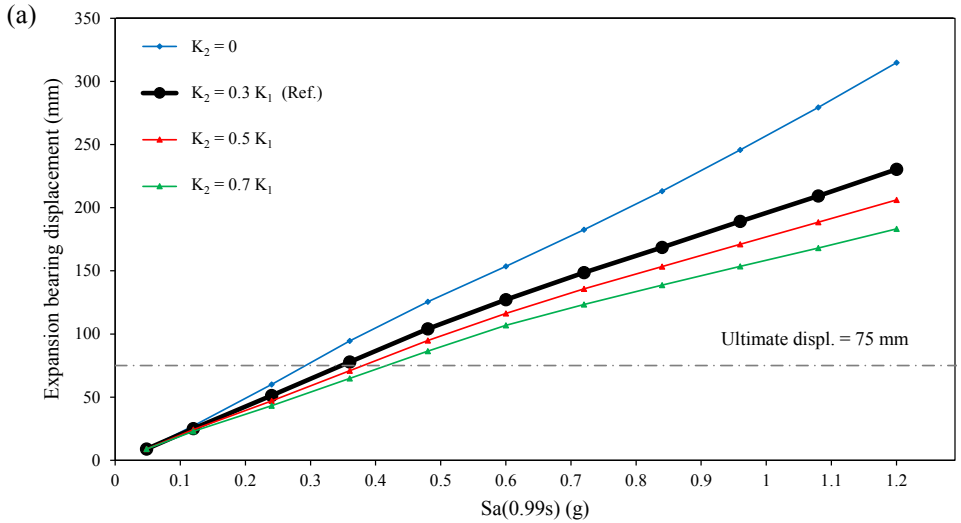

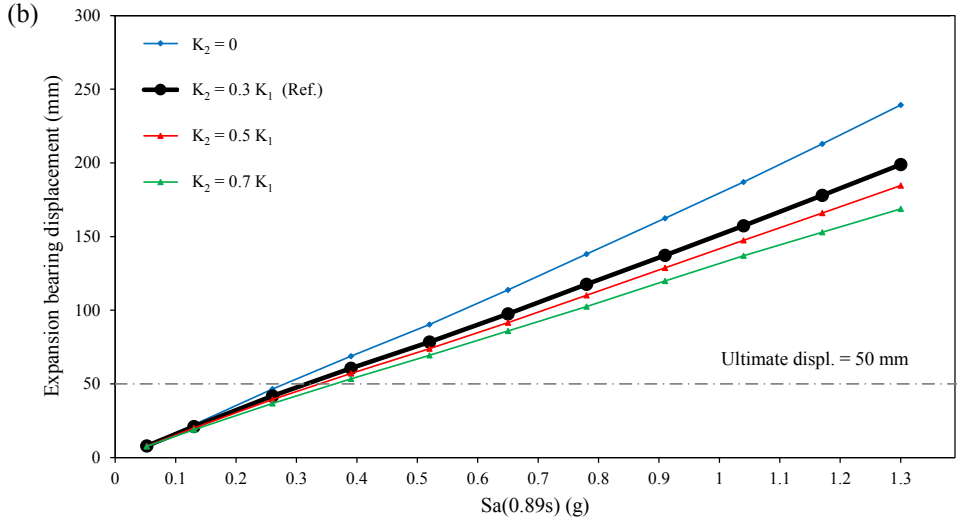

Figure 5.38 Maximum mean expansion bearing displacements according to different post-yield strength of the bearing: (a) Bridge #1; (b) Bridge #2.

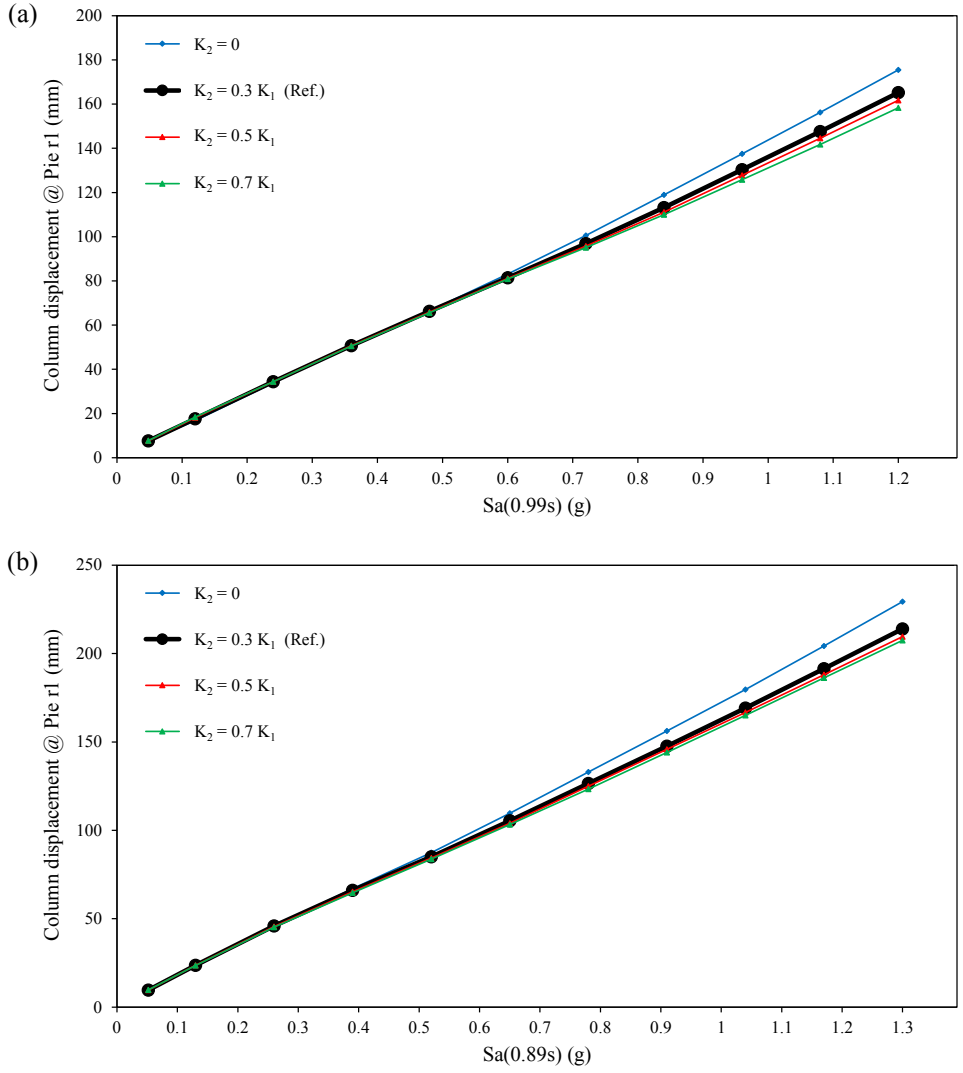

Figure 5.39 Maximum mean column displacements at pier 1 (fixed bearing) according to different post-yield strength of the bearing: (a) Bridge #1; (b) Bridge #2.

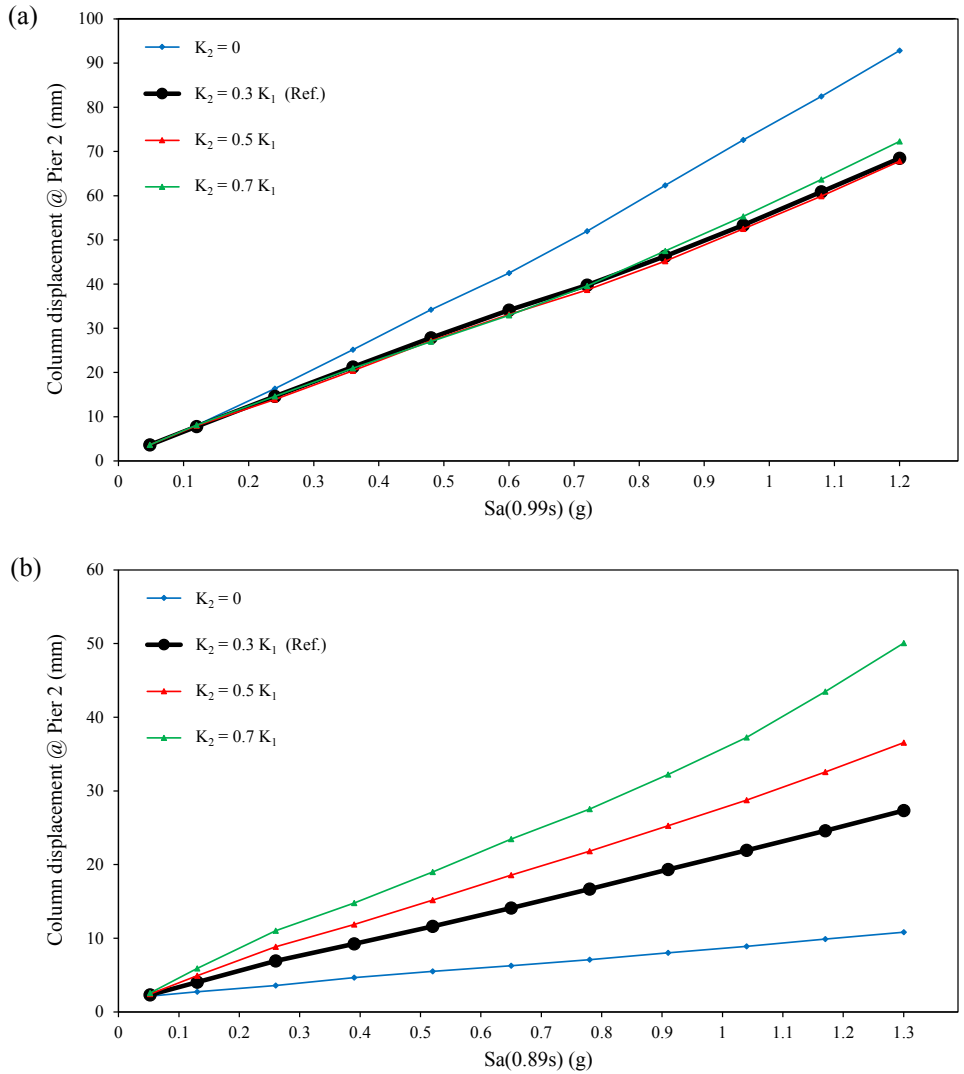

Figure 5.40 Maximum mean column displacements at pier 2 (expansion bearing) levels according to different post-yield strength of the bearing: (a) Bridge #1; (b) Bridge #2.

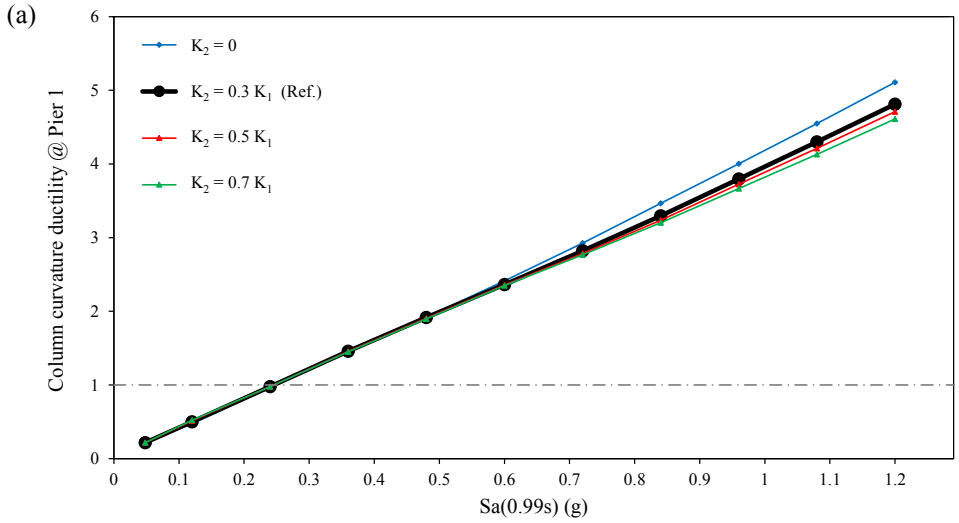

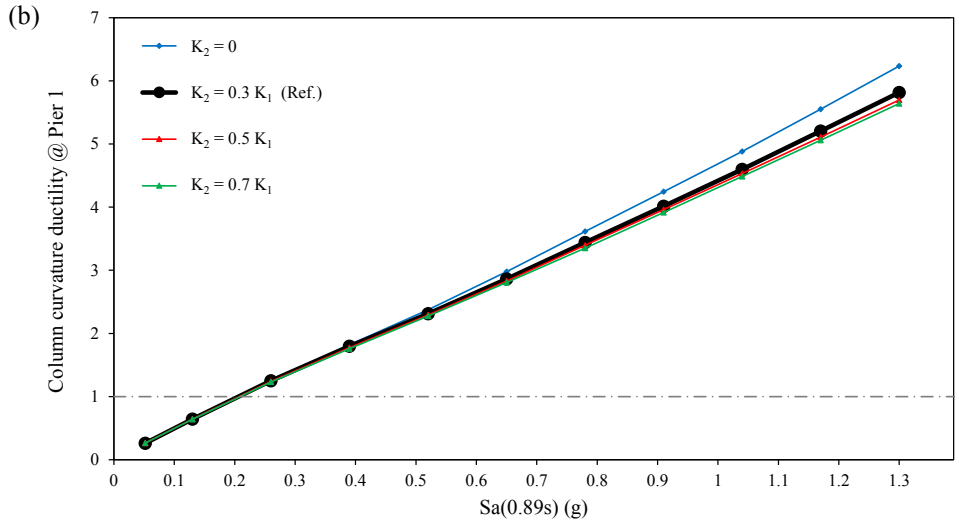

Figure 5.41 Maximum mean column curvature ductilities at pier 1 (fixed bearing) according to different post-yield strength of the bearing: (a) Bridge #1; (b) Bridge #2.

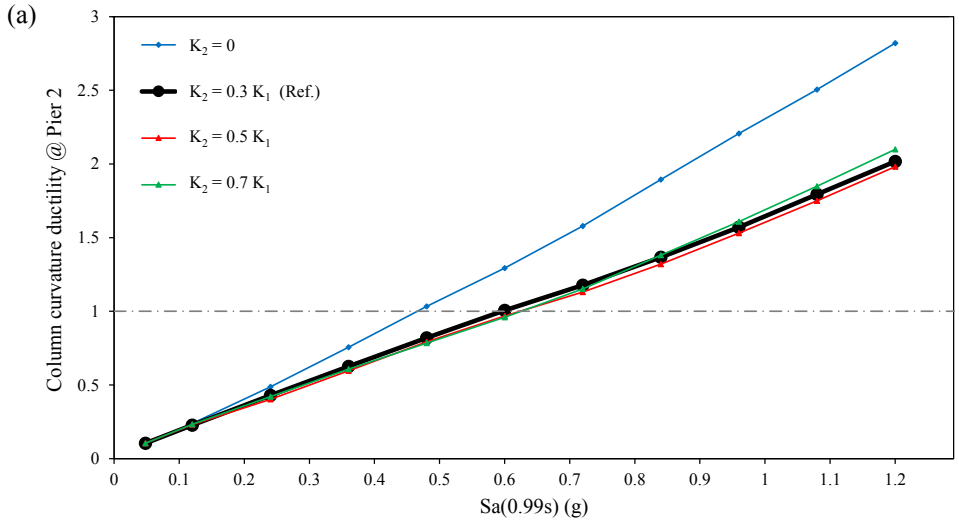

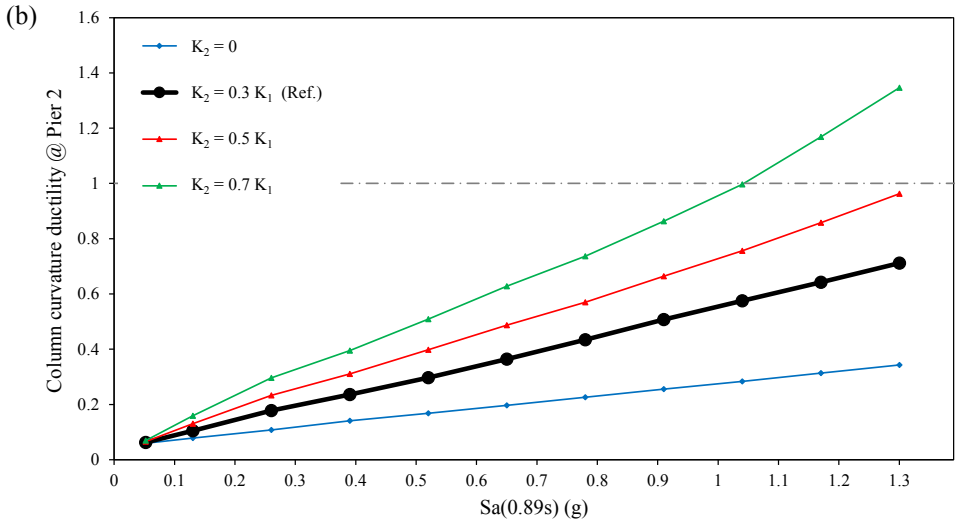

Figure 5.42 Maximum mean column curvature ductilities at pier 2 (expansion bearing) according to different post-yield strength of the bearing: (a) Bridge #1; (b) Bridge #2.

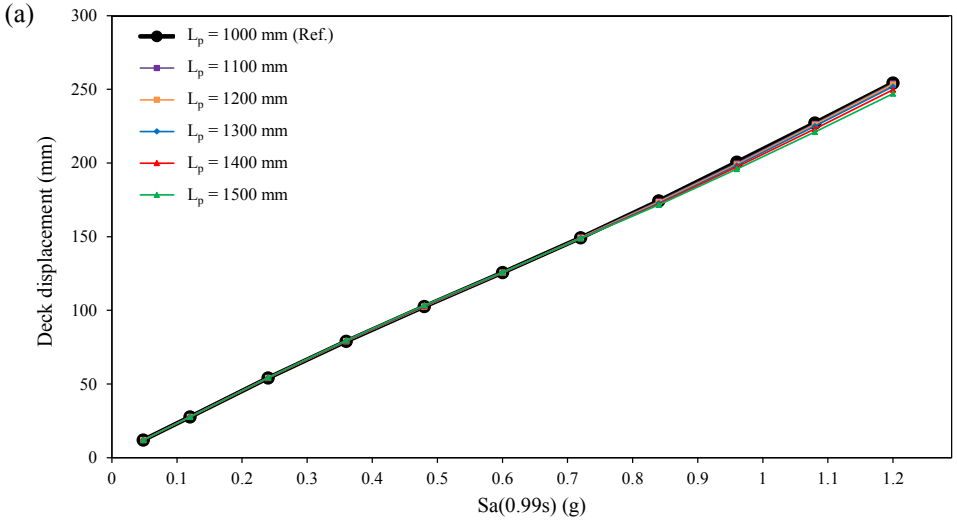

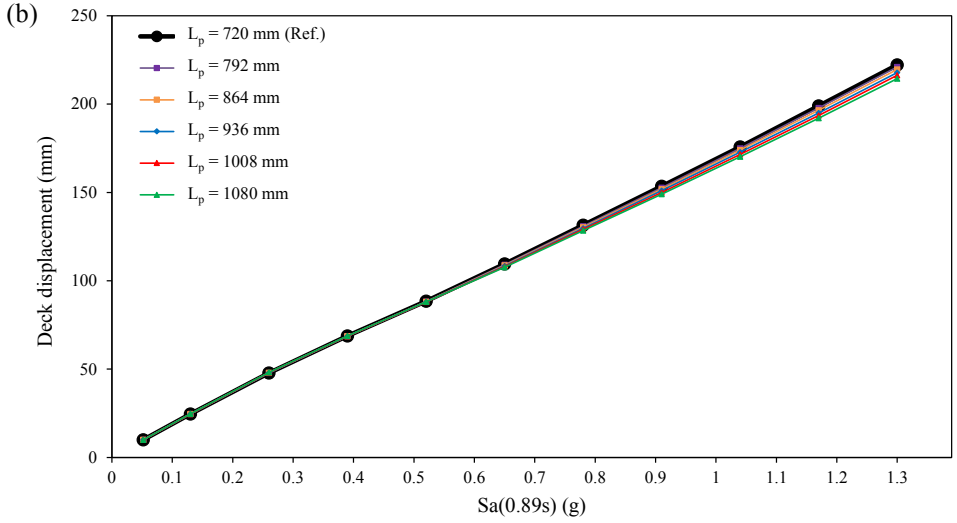

Figure 5.43 Maximum mean deck displacements according to different plastic hinge length: (a) Bridge #1; (b) Bridge #2.

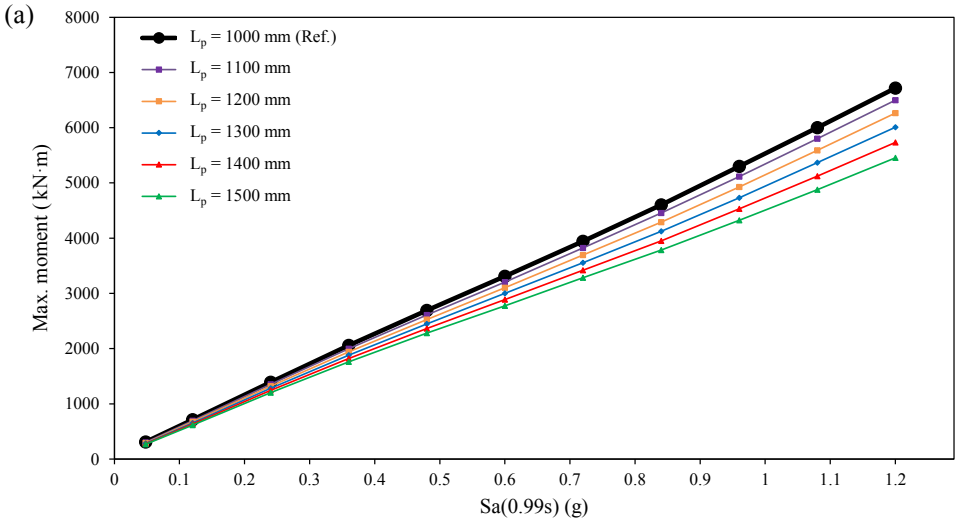

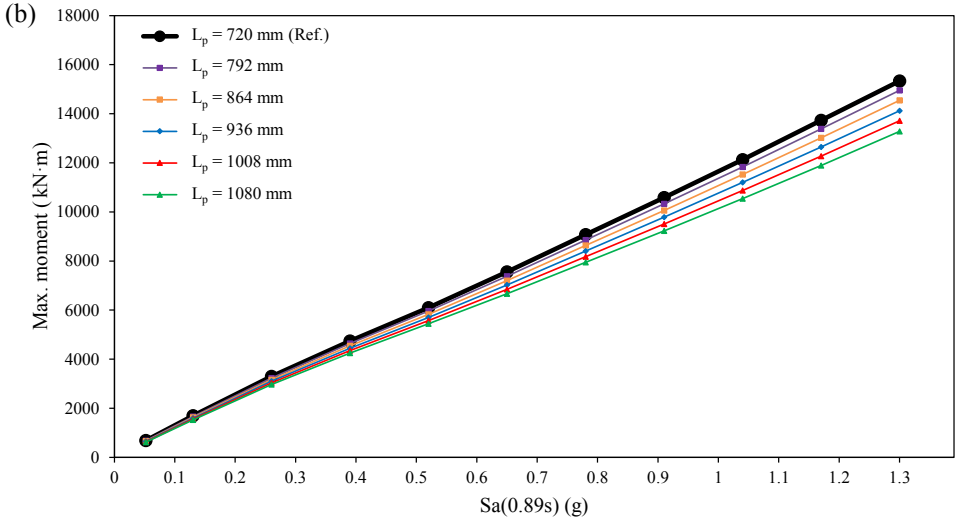

Figure 5.44 Maximum mean moments at the base of the column according to different plastic hinge length: (a) Bridge #1; (b) Bridge #2.

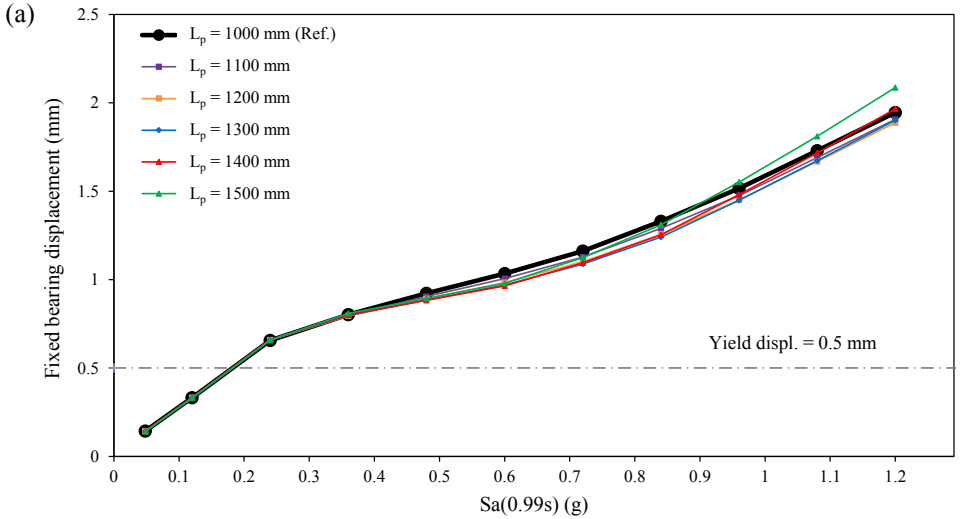

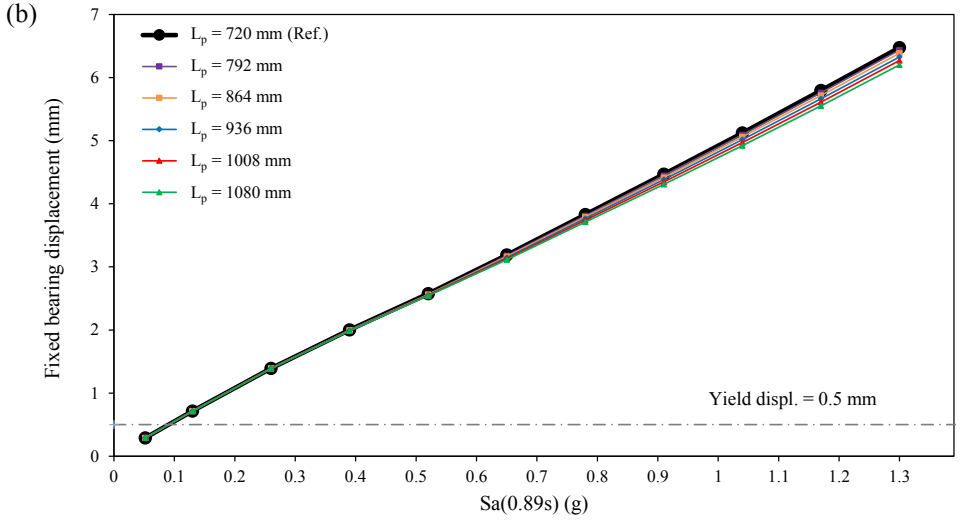

Figure 5.45 Maximum mean fixed bearing displacements according to different plastic hinge length: (a) Bridge #1; (b) Bridge #2.

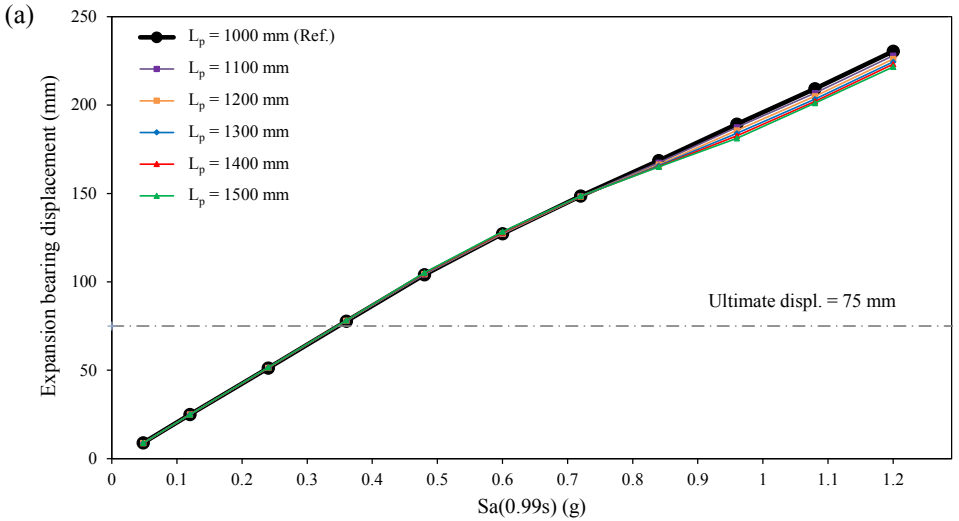

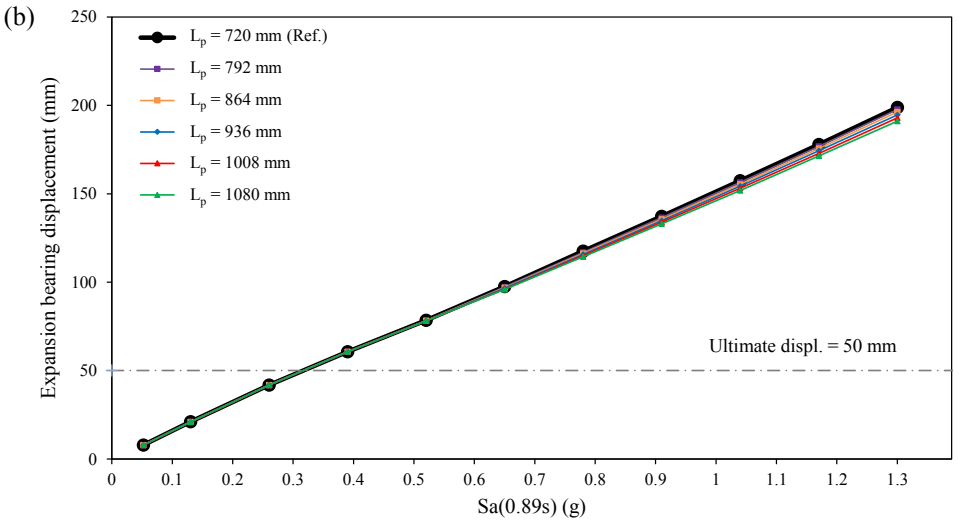

Figure 5.46 Maximum mean expansion bearing displacements according to different plastic hinge length: (a) Bridge #1; (b) Bridge #2.

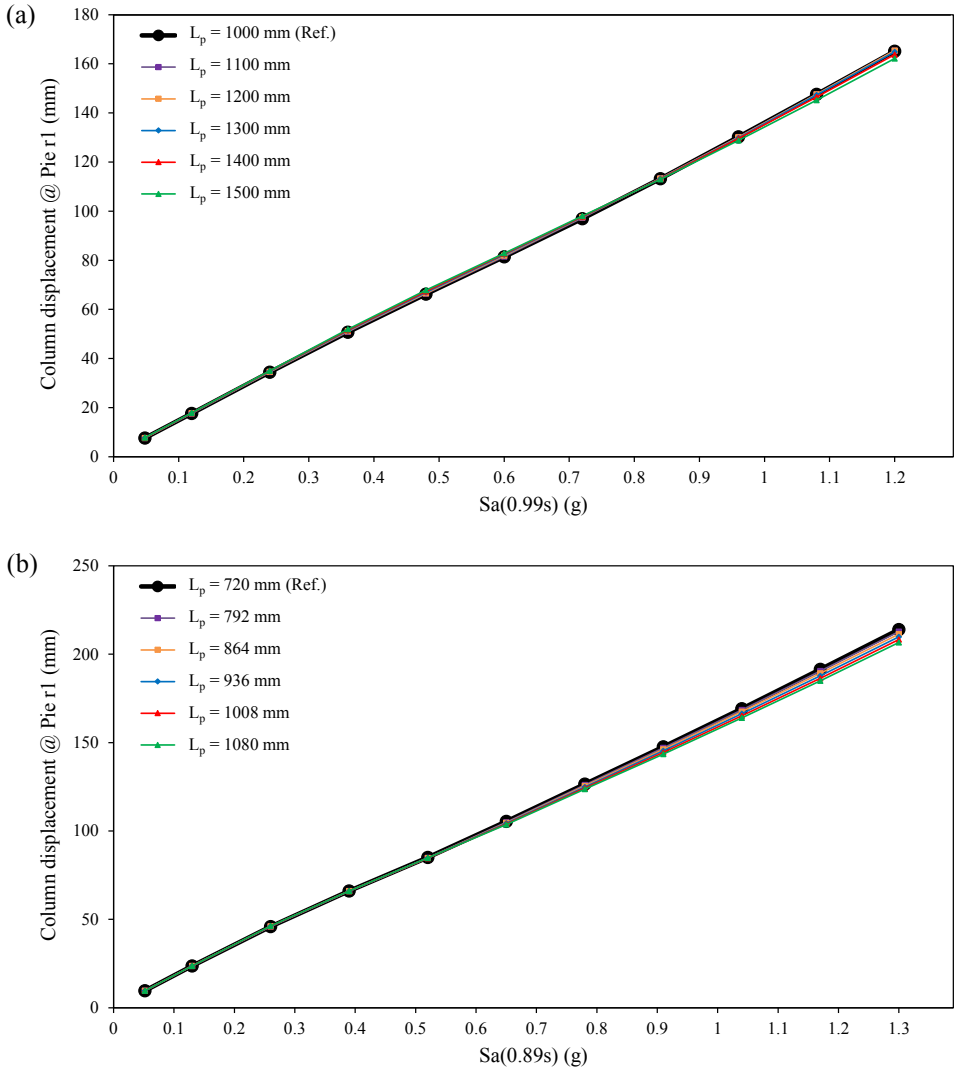

Figure 5.47 Maximum mean column displacements at pier 1 (fixed bearing) according to different plastic hinge length: (a) Bridge #1; (b) Bridge #2.

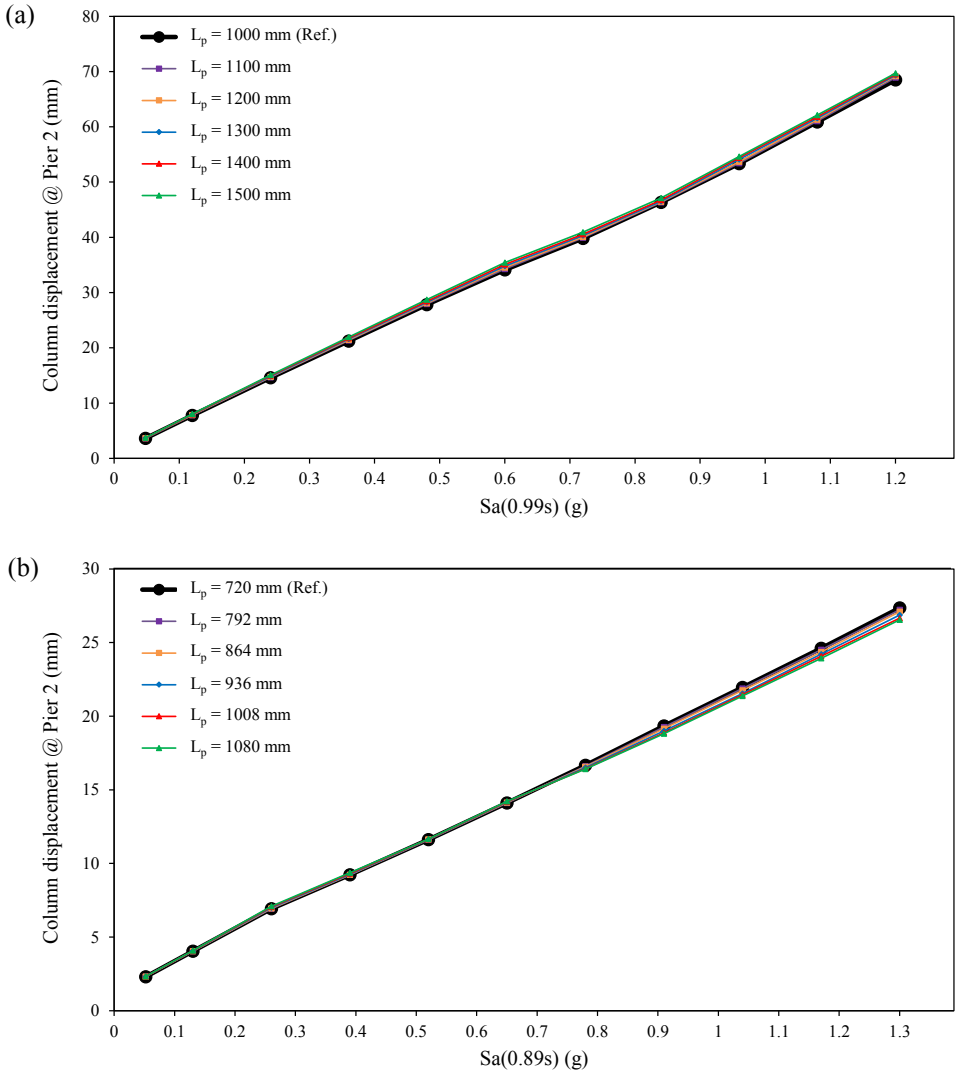

Figure 5.48 Maximum mean column displacements at pier 2 (expansion bearing) according to different plastic hinge length: (a) Bridge #1; (b) Bridge #2.

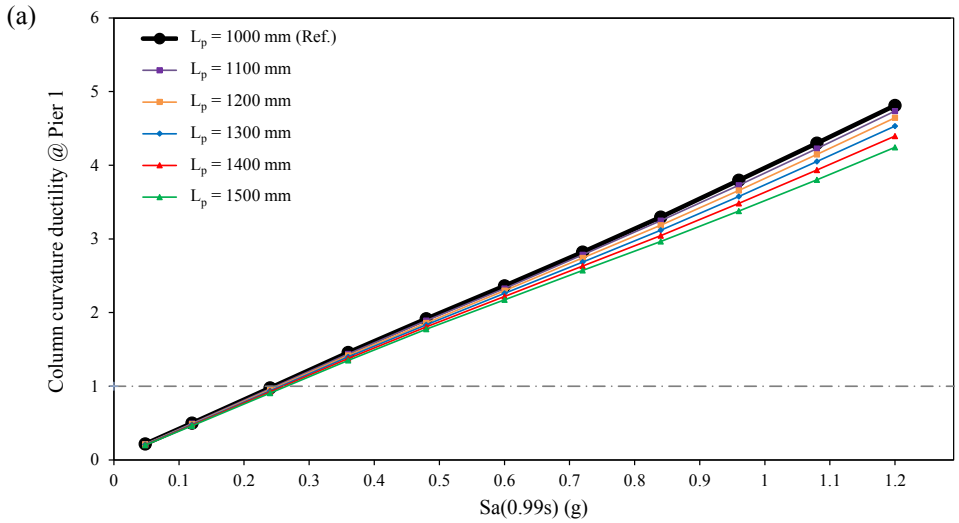

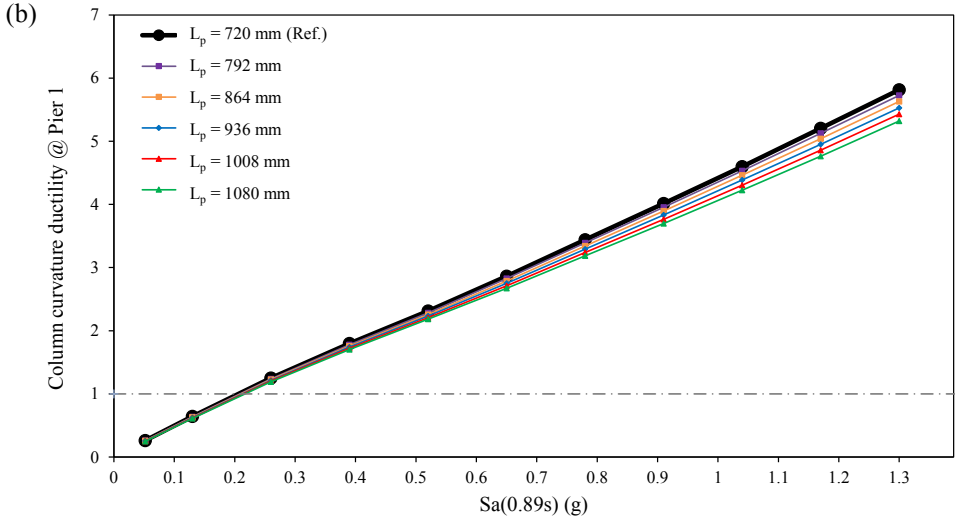

Figure 5.49 Maximum mean column curvature ductilities at pier 1 (fixed bearing) according to different plastic hinge length: (a) Bridge #1; (b) Bridge #2.

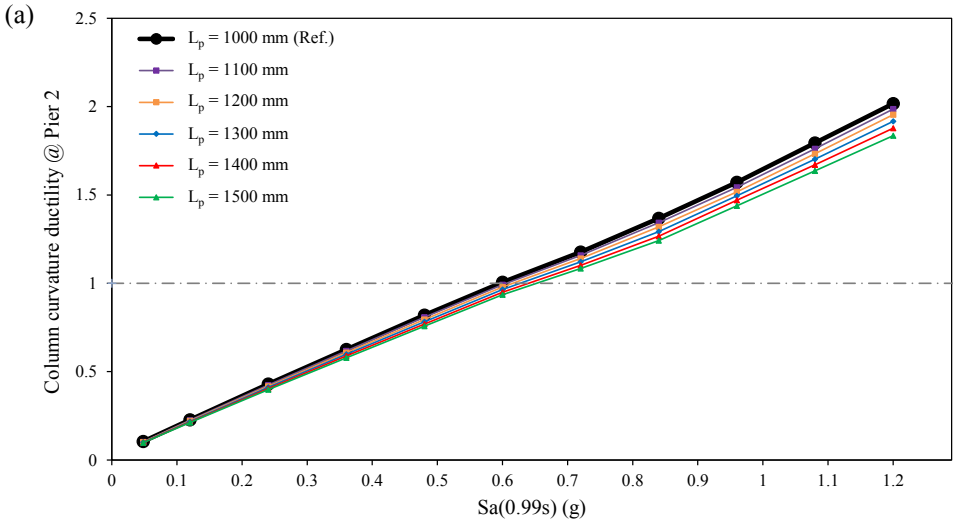

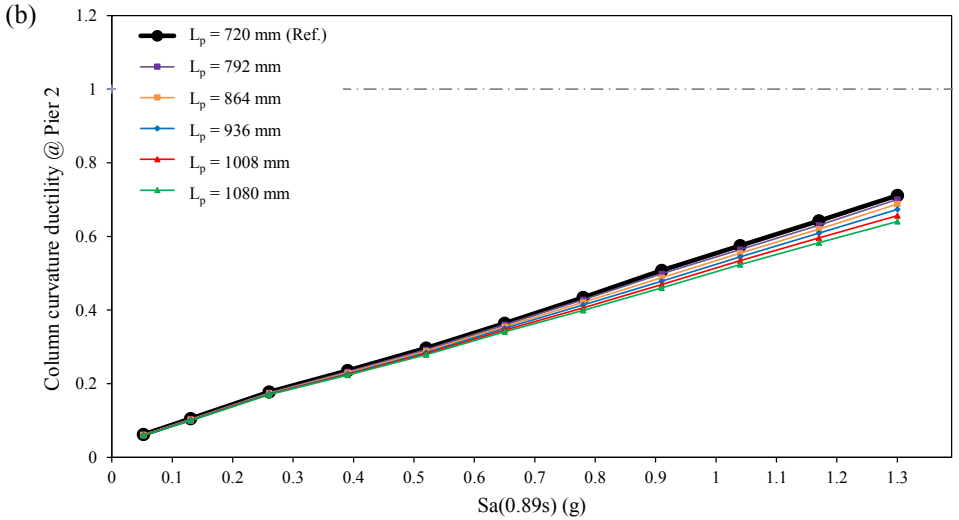

Figure 5.50 Maximum mean column curvature ductilities at pier 2 (expansion bearing) according to different plastic hinge length: (a) Bridge #1; (b) Bridge #2.

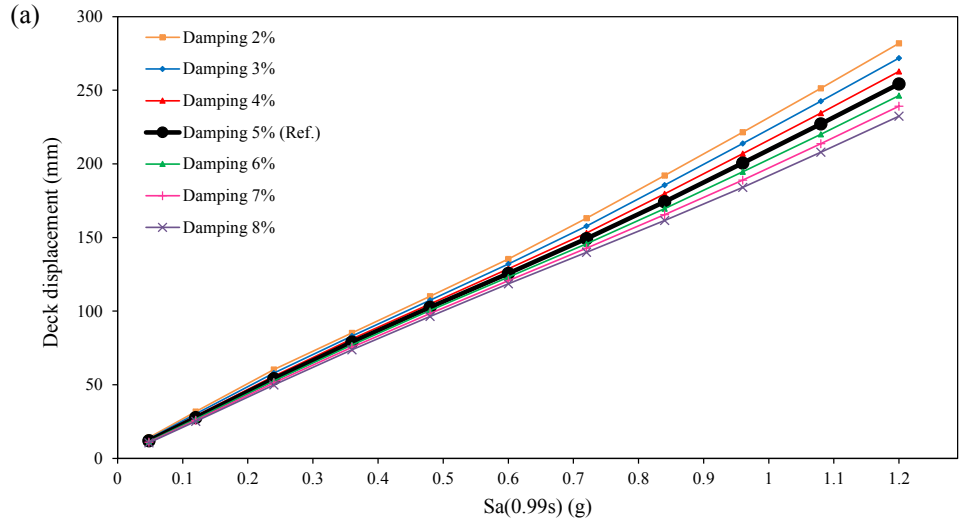

Figure 5.51 Maximum mean deck displacements according to different damping: (a) Bridge #1; (b) Bridge #2.

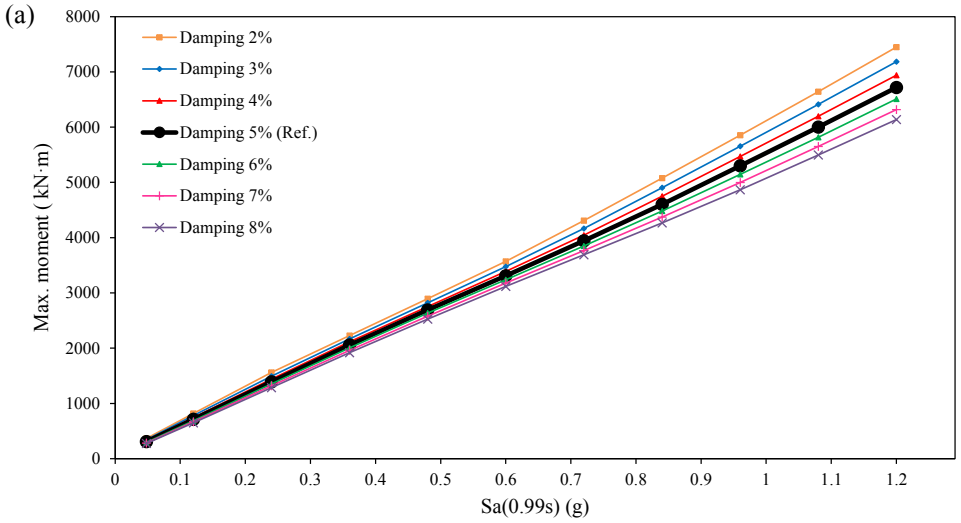

Figure 5.52 Maximum mean moments at the base of the column according to different damping: (a) Bridge #1; (b) Bridge #2.

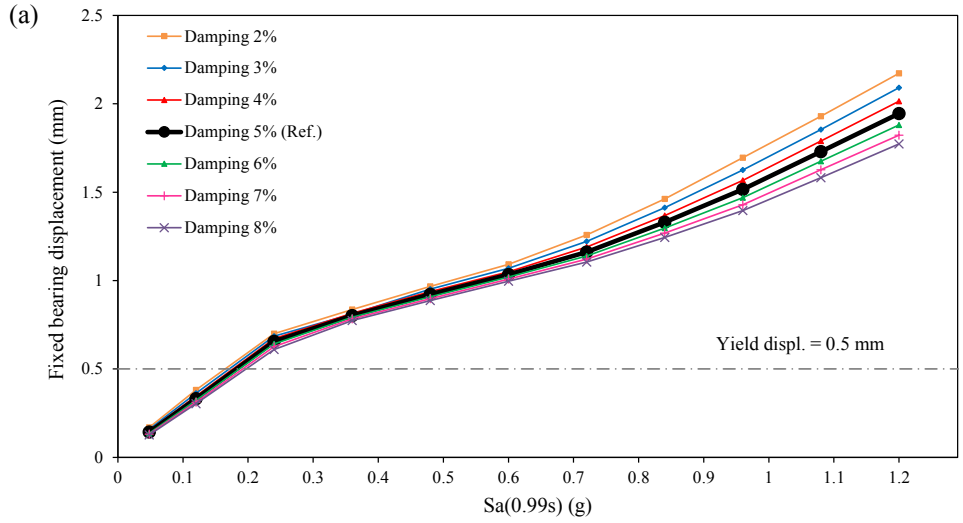

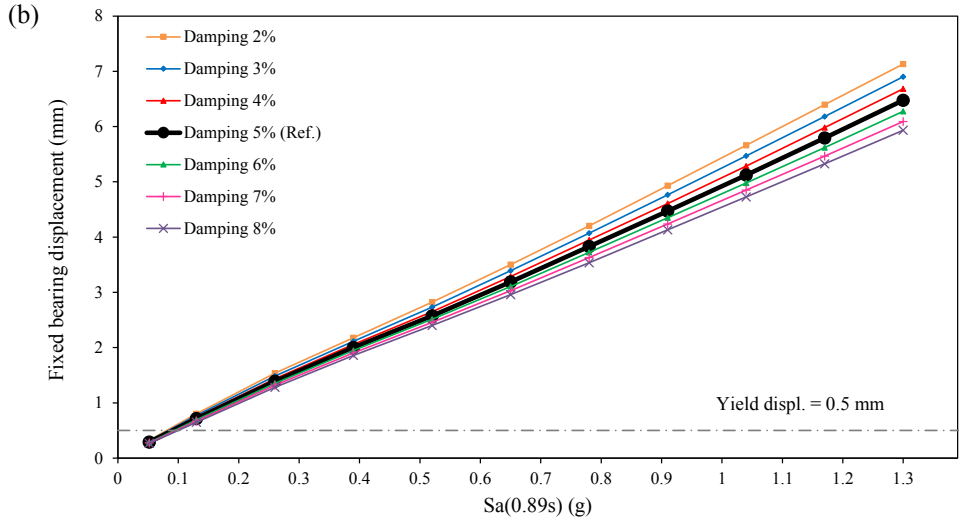

Figure 5.53 Maximum mean fixed bearing displacements according to different damping: (a) Bridge #1; (b) Bridge #2.

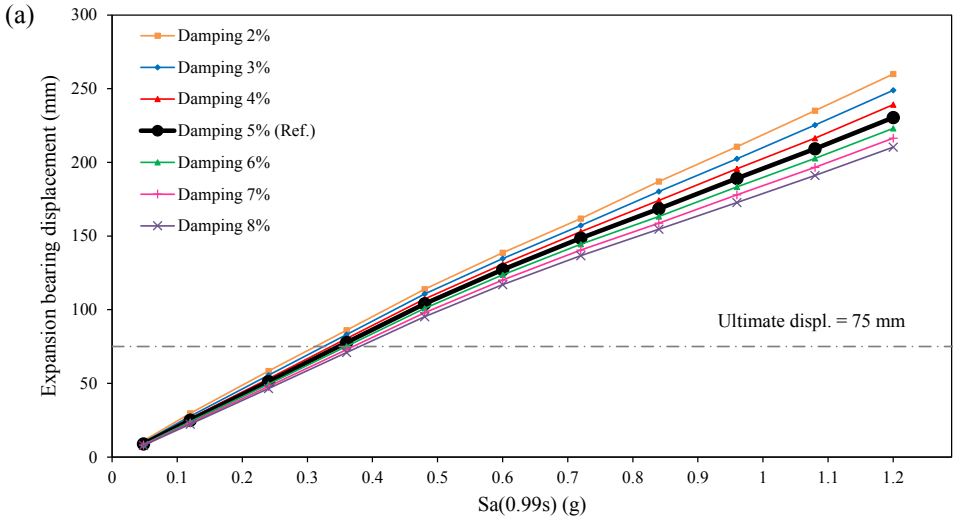

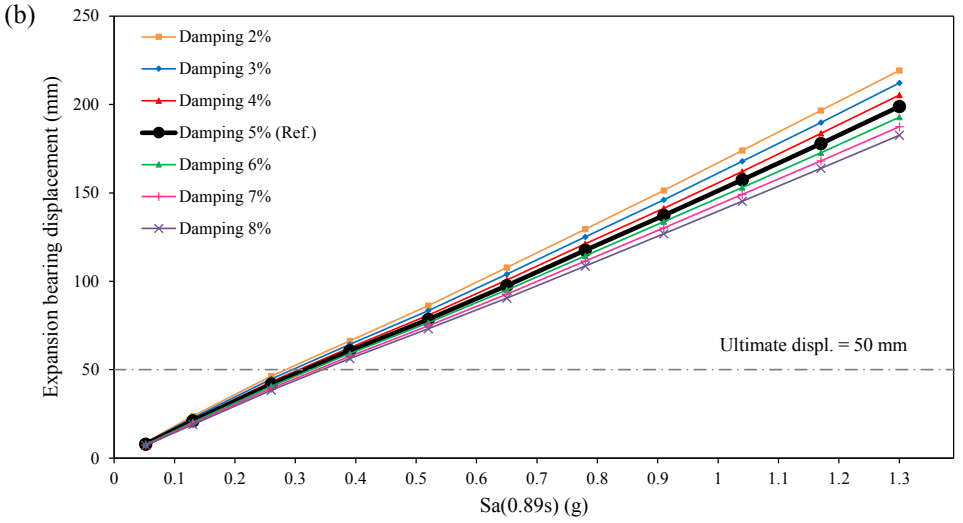

Figure 5.54 Maximum mean expansion bearing displacements according to different damping: (a) Bridge #1; (b) Bridge #2.

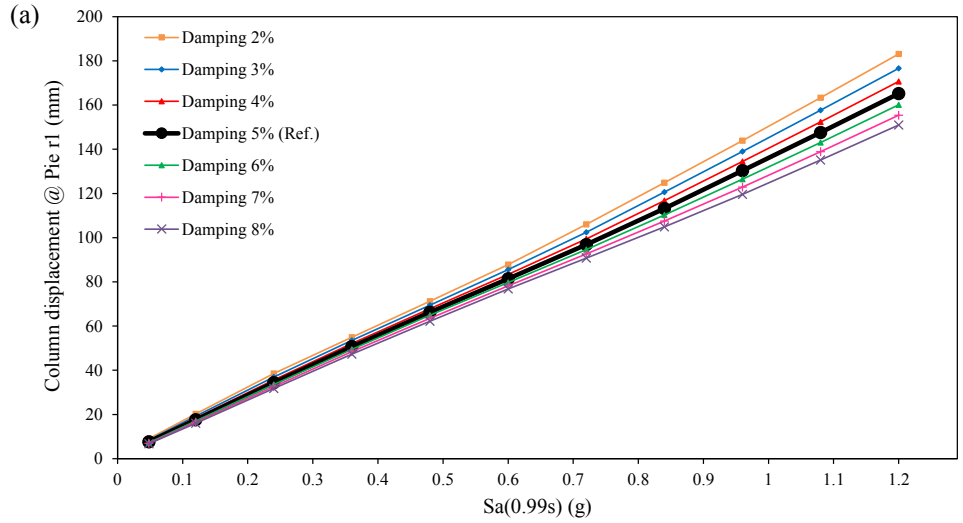

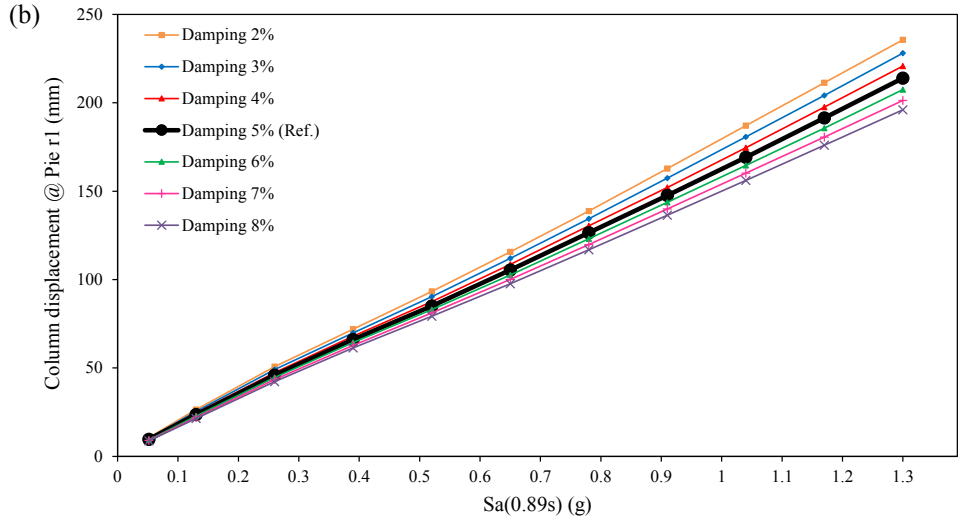

Figure 5.55 Maximum mean column displacements at pier 1 (fixed bearing) according to different damping: (a) Bridge #1; (b) Bridge #2.

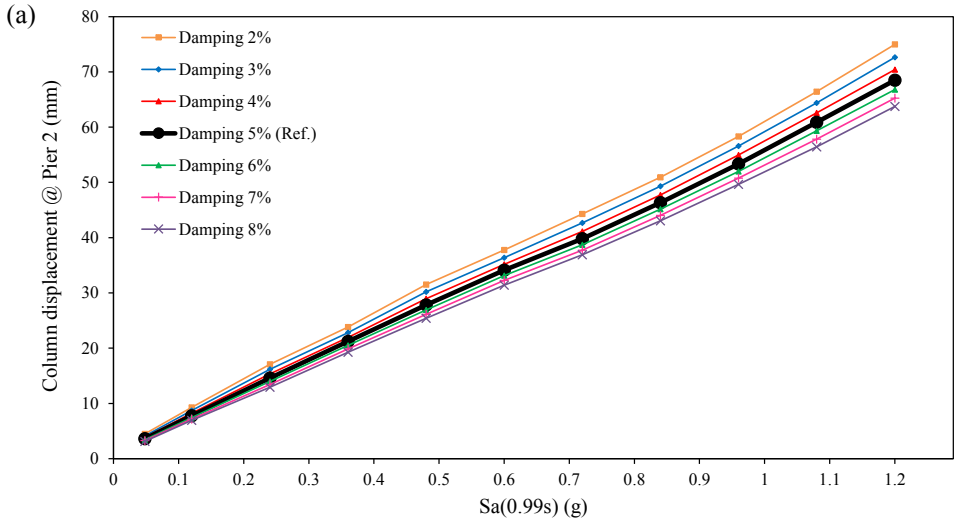

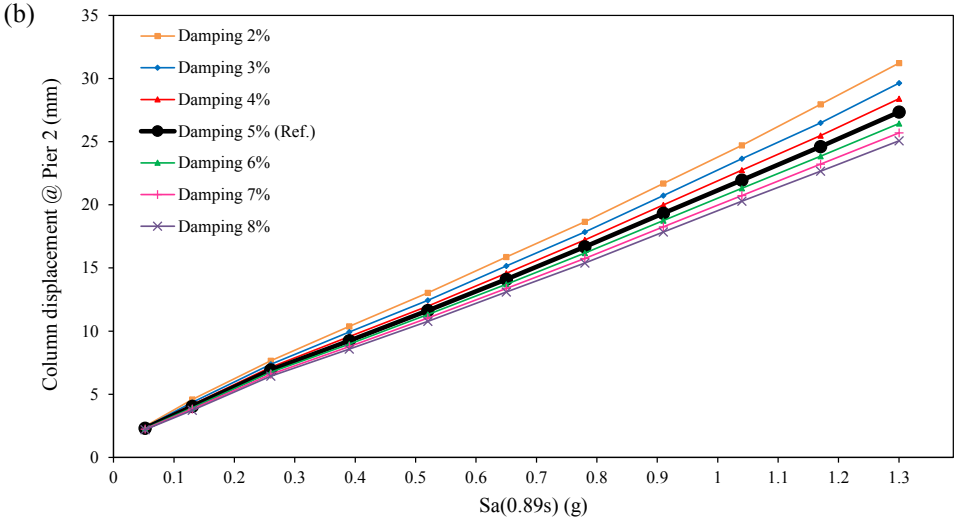

Figure 5.56 Maximum mean column displacements at pier 2 (expansion bearing) according to different damping: (a) Bridge #1; (b) Bridge #2.

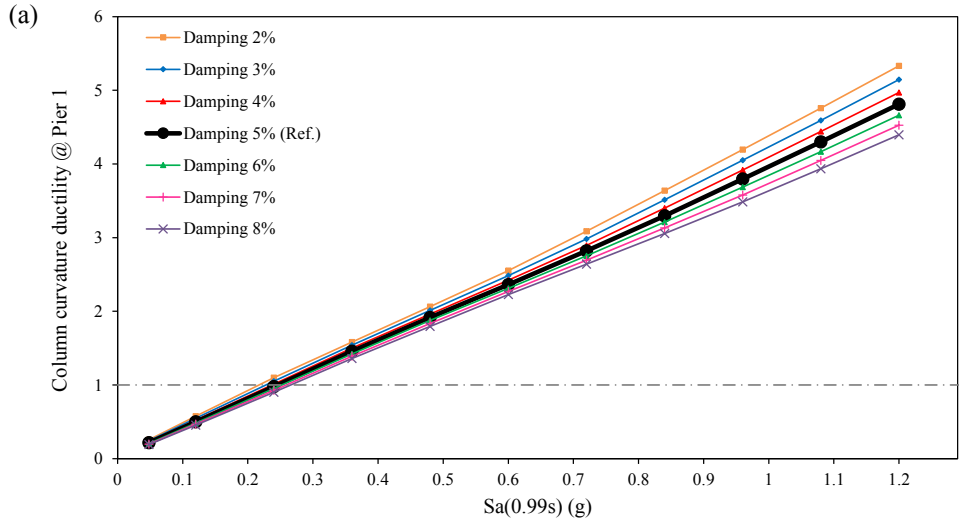

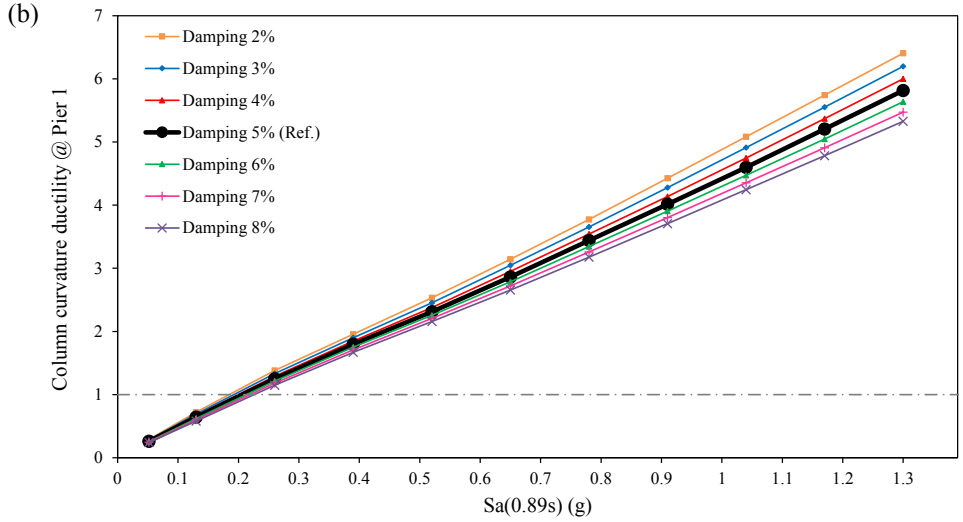

Figure 5.57 Maximum mean column curvature ductilities at pier 1 (fixed bearing) according to different damping: (a) Bridge #1; (b) Bridge #2.

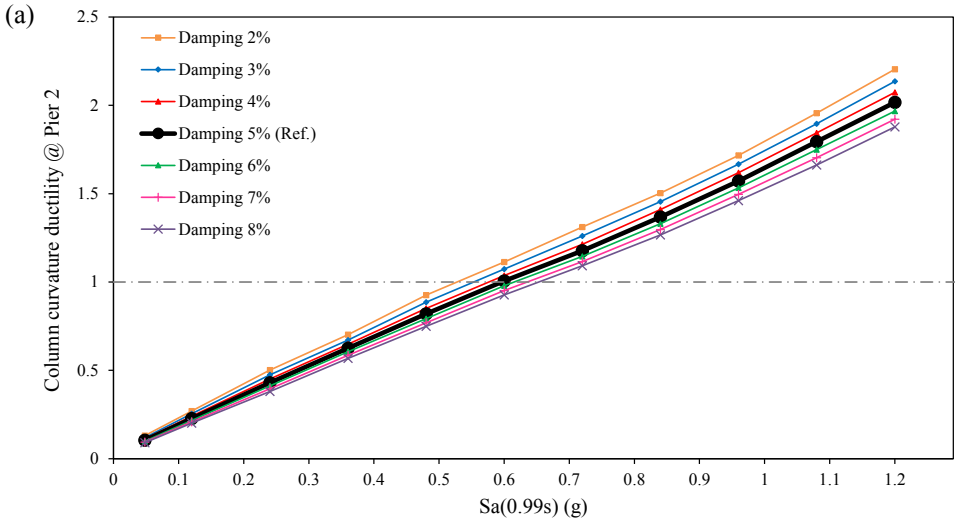

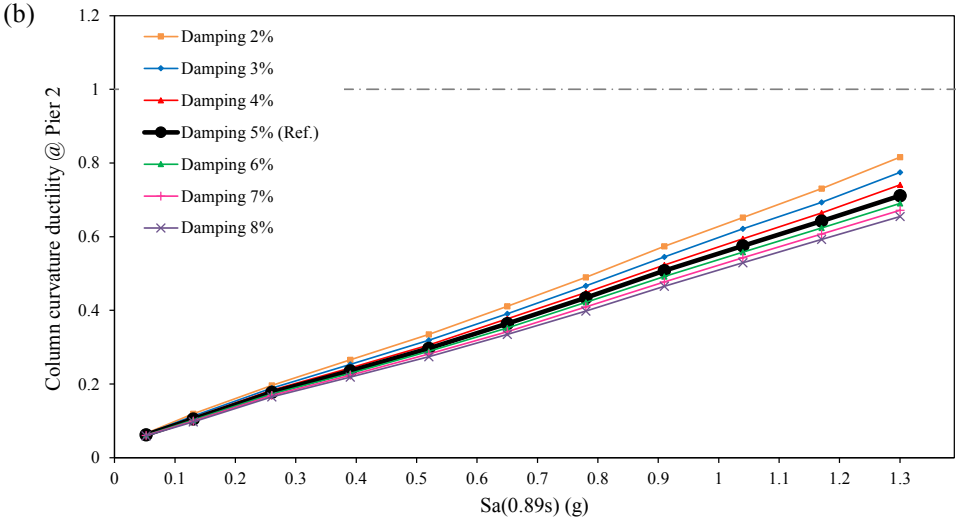

Figure 5.58 Maximum mean column curvature ductilities at pier 2 (expansion bearing) according to different damping: (a) Bridge #1; (b) Bridge #2.

Chapter 6

Discussion and Conclusions

6.1 Discussion

It has been reported that significant earthquakes could cause severe damage to bridges, such as, the 1995 M7.2 Kobe earthquake, the 1989 M7.8 Loma Prieta earthquake, etc. In addition, moderate earthquakes can also cause damage or even collapse of bridges or bridge components. One typical example is the M5.0 Val-des-Bois earthquake occurred about 60 km from Ottawa on June 23, 2010. A bridge embankment which close to the epicentre collapsed and three landslides were triggered in unstable soil deposits during this event.

The lessons from the past earthquakes lead to sustainable research on the seismic evaluation of bridges. Two methods are typically used for the study: one is deterministic approach which is applied to a specific bridge, the other is probabilistic approach which is used for the investigation of bridge portfolios. It has been noticed that earthquakes occurred quite often in the last several years. For example, 2010 M7.0 Haiti Earthquake, 2010 M8.8 Chile Earthquake, 2011 M9.0 Japan Earthquake (Tohoku), 2011 M7.2 Alaska Earthquake, and 2011 M7.6 New Zealand Earthquake. Given this, there is an urgent need to conduct seismic risk analysis on bridges on a large scale (i.e., a specific region or a city) in addition to a specific bridge due to the importance of bridges in a transportation system. It is necessary to mention herein that seismic risk assessment of bridge portfolios is needed in order to estimate the economic losses of the transportation system in a specific area due to potential future

earthquakes. The estimation will, in turn, help the government make an emergence plan should an earthquake happen. However, there is a big challenge for the study because the configuration of each bridge is unique in terms of the structural system (i.e., simply supported or continuous), type of the superstructure (i.e., slab-girder type, solid slab deck, single-cell box girder, multi-cell box girder, etc.), type of the foundation (i.e., shallow foundation, or deep foundation), number of spans, span length, height of the column, etc. Given this, the deterministic approach cannot be used for such study since it is not practical to conduct analysis on each bridge if one wants to investigate the seismic vulnerability of bridges in a large area. In another word, the probabilistic approach should be considered for the seismic evaluation of a large population of bridges. In order to use the probabilistic method to assess the seismic vulnerability of bridge portfolios in a specific zone, types of generic bridges shall be developed first, which based on the statistics analysis of the current bridge blocks in the zone with considered of the continuity of the structural system, number of spans, span length, type of the superstructure, type of the substructure. The features of each bridge within each group, e.g., the total length and width of the bridge, material properties (concrete strength and the yield strength of the steel bar), column height, weight of the superstructure, gap width, property of bearing including thickness of the bearing and stiffness of bearing and other uncertainties in the modeling are taken into account by using Monte-Carlo simulation. Since the structural engineers are not familiar with the Monte-Carlo method, this approach has not been used in practical applications, i.e., it is mainly used by researchers. In addition, uncertainties of the modeling parameters should also be considered in the seismic evaluation of a specific bridge using the deterministic method. It should be noted the seismic vulnerability of a bridge is typically represented by the fragility curves which show the damage probabilities of the bridge

at a series of seismic excitation levels for different damage states, such as, slight damage, light damage, extensive damage and complete damage (i.e., collapse). The fragility curves are further used to estimate the loss estimation due to potential earthquakes in the future.

In this study, effects of the uncertainties of the superstructure mass, concrete compressive strength, yield strength of the reinforcing steel, yield displacement of the bearing, post-yield stiffness of the bearing, plastic hinge length, and damping on the seismic response of bridges are investigated. For the purpose of study, two typical reinforced concrete highway bridges located in Montreal are selected. Nonlinear three-dimensional (3-D) models of the bridges are developed using SAP2000 for use in the analysis. The effects of each of uncertainties mentioned above are investigated separately by conducting time-history analyses of the bridge models. In total, 15 records from the earthquakes around the world are used in nonlinear time-history analysis. The selected records represent the characteristics of ground motions in eastern Canada. Among a number of response parameters from the analyses, the deck displacement, bearing displacement, column displacement, column curvature ductility, and moment at the base of the column are used to assess the effects of the uncertainty of the modeling parameter on the seismic response of the bridge.

6.2 Conclusions

The main conclusions of the study conducted in this thesis can be summarized as follows:

- **Effects of the superstructure mass**
    - Change of the superstructure mass by 30% causes the deck displacement to change about 10% at the seismic excitation level of $5.0Sa(T_1)$, in which $Sa(T_1)$

is the spectral acceleration at the fundamental period of the bridge based on the design spectrum at the bridge site. In addition, change of the deck displacement is proportional to the change of the superstructure mass. For example, the deck displacement will change about 5% if the superstructure mass changes 15%.

- The observations of the results of maximum bending moment in the column are similar to those of the deck displacement as described above.
- The effects of the superstructure mass depend on the type of the bearing, and the geometry of the bearing. More specifically, the superstructure mass has significant effect on the lateral displacement of the fixed bearing, and it has less effect on the expansion bearing.
- The superstructure mass does not have effect on the column displacement and column curvature ductility.

- **Effects of the concrete compressive strength**
  - The concrete compressive strength does not have effects on the deck displacement.
  - The concrete compressive strength does not have significant effects on the maximum bending moment in the column. The difference between the responses using the strengths of 30MPa and 40MPa (or 20 MPa) at the highest excitation level of $5.0Sa(T_1)$ is about 5%.
  - The concrete compressive strength does not affect the lateral displacement of the expansion bearing. However, it might have significant effect on the fixed bearing depending on the geometry of the bearing.

- In general, the concrete compressive strength does not affect the column displacement and column curvature ductility. However, for some bridge (e.g., Bridge #2), the concrete compressive strength could produce about 10% difference on the response corresponding to the concrete strengths of 20 MPa and 40 MPa.

- **Effects of the yield strength of the reinforcing steel**
  - The yield strength of the steel does not affect the deck displacement.
  - The change of the steel yield strength by 50 MPa would lead to 2% difference in the moment in the column. More specifically, the difference between the maximum bending moments in the column using the strength of 300 MPa (or 550 MPa) and 400 MPa is about 5% at the highest intensity level $5.0Sa(T_1)$ considered in the analysis.
  - The yield strength of the reinforcing steel does not affect the displacement of the expansion bearing. However, it decrease the displacement of the fixed bearing by 15% using the yield strength of 300 MPa with respect to that using the strength of 400 MPa.
  - The change of the yield strength of the steel bar has slight effect on the displacement of the column on which the fixed bearing is used. The approximate 7% difference in the column displacement where the expansion bearing is installed would expect at the lower excitation levels between $1.0Sa(T_1)$ and $3.0Sa(T_1)$.

- The yield strength of the reinforcing steel has significant effects on the column curvature ductility. The difference about 30% between the ductilities corresponding to the strengths of 300 MPa (or 550 MPa) and 400 MPa is observed in all the excitation levels used in the study.

- **Effects of the yield displacement of the bearing**

  - The change of the yield displacement of the bearing will not change the deck displacement, bending moment in the column, and bearing displacement.

  - The effect of the yield displacement of the bearing on the column displacement and column curvature ductility depends on the geometry of the bearing and the configuration of the bridge. For the two bridges considered in this study, the yield displacement of the expansion bearing does not affect the column displacement and column curvature ductility of bridge #1. However, it has significant effects on the Bridge #2. More specifically, the yield displacement three times the reference value would provide the response about 30% larger than the reference response at the excitation levels lower than $2.0Sa(T_1)$.

- **Effects of the post-yield stiffness of the bearing**

  - For the deck displacement, bending moment in the column, displacement of the fixed bearing, displacement and curvature ductility of the column under the fixed bearing, the response corresponding to the post-yield stiffness of the bearing of 0 is about 7% larger than the reference value using the post-yield stiffness of 0.3 times the initial elastic stiffness of the bearing. The post-yield

stiffness factors considered in the analysis, i.e., 0.3, 0.5, 0.7 provide very similar response.

- The post-yield stiffness of the bearing has significant effects on the displacement and curvature ductility of the column under the expansion bearing. Based on the results in this study, it is recommend to use factor of 0.4 to define the post-yield stiffness of the bearing.

- **Effects of the plastic hinge length**
  - The plastic hinge length does not affect the deck displacement, bearing displacement including both the fixed bearing and the expansion bearing, and column displacement.
  - The plastic hinge length affects the bending moment in the column and column curvature ductility, i.e., larger plastic length provides smaller response. It is found in this study that the plastic hinge length 1.5 times that determined according to the Code formula reduces the response by about 10%.

- **Effects of the damping**
  - Damping has more effects on the response at the lower excitation levels than on the higher, especially for the column displacement and column curvature ductility.
  - The 5% damping is appropriate for use in the analysis.

Based on the observations of this study as described above, the following recommendations are made for the evaluation of the seismic response of **existing** bridges,

1. Nominal superstructure mass is suitable for use in the analysis especially when the seismic excitations are about 1 to 2 times the design earthquake level. However, the difference on the response of about 10% would be expected at the extremely high intensity levels, such as, five times the design earthquake level.

2. The nominal concrete compressive strength of the substructure (i.e., column) is appropriate to assign as an input in the modeling, i.e., variations can be ignored.

3. Since the strain hardening of the reinforcing steel does not affect the bridge response, an idealized bilinear stress-strain curve for the steel is good enough for the analysis. It should be mentioned that the yield strength of the steel (i.e., f_y) has significant effect on the column curvature ductility. Therefore, attention must be given on the selection a suitable value for f_y for prediction of the column curvature ductility.

4. The yield displacement of the bearing shall be carefully selected in the analysis. Parametric study is suggested to conduct first in order to define a suitable value in modeling.

5. The post-yield stiffness of bearing should be taken as 0.3-0.4 times its elastic stiffness for modeling the plastic behavior of the bearing. The elastic-perfectly-plastic hysteretic loop shall not be used for modeling bearings.

6. It is appropriate to use the plastic hinge length determined using the code formula in the analysis.

7. The 5% damping is a reasonable value to be used in the analysis.

The suggestions of the use of the modeling parameters investigated in this study for the design of **new bridges** are given below,

1. In this study, it was found that both fixed bearing and expansion bearing yield at a relatively low excitation level which is less than the design earthquake level. Therefore, higher ductility should be considered in the design of bearings such that bridges could survive during strong earthquake events.

2. For the design purpose, it might be beneficial to consider smaller plastic hinge length on the column in order to achieve a higher ductility. This will, in turn, improve the performance of bridge against seismic loads.

6.3 Future Work

The research work presented in this thesis is focussed on two bridges located in Montreal which are representative of typical highway bridges in eastern Canada. This might limit the conclusions discussed in section 6.2. Given this, further research is needed as summarised hereafter:

- The research in this thesis is done using the structural models of reinforced concrete slab, and reinforced concrete slab-girder type bridges. Other types of bridges, such as, box girder bridges, shear-connected beam bridges, etc. need to be analyzed as well. In addition to concrete bridges, steel bridges shall be considered in order to understand the effects of uncertainty of modeling parameters on the seismic response of bridges.

- The bridges considered in this study are located in eastern Canada. Since the characteristics of ground motions in eastern Canada and western Canada are different, it is worth conducting a similar study on the bridges in western Canada.

- It would be very interesting to see how the uncertainties of modeling parameters considered in this study affect the fragility curves. The results of such study will help us eliminate the uncertainty of the modeling parameter which does not have significant effects on the fragility curves. This will simplify the probabilistic method or produce more stable results on the seismic response of a specific bridge using deterministic approach.

Refernces

AASHTO (2014). AASHTO LRFD Bridge Design Specifications, Customary U.S. Units, 7th Edition. American Association of State Highway and Transportation Officials, Washington, DC.

Abdel-Mohti, A. (2010). Effect of skew on the seismic response of RC box-girder bridges. Proceedings of the 9th US National and 10th Canadian Conference on Earthquake Engineering, Toronto, ON, Canada.

Adams, J., and Halchuk, S. (2003). Fourth generation seismic hazard maps of Canada: Values for over 650 Canadian localities intended for the 2005 National Building Code of Canada. Open File Report 4459, Geological Survey of Canada, Ottawa, ON, Canada.

Akogul, C., and Celik, O.C. (2008). Effect of elastomeric bearing modeling parameters on the seismic design of RC highway bridges with precast concrete girders. Proceedings of the 14th World Conference on Earthquake Engineering, Beijing, China.

ATC-32. (1996). Improved seismic design criteria for California bridges: Provisional recommendations. Applied Technology Council, Redwood City, CA.

Aviram, A., Mackie, K.R., and Stojadinovic, B. (2008a). Effect of abutment modeling on the seismic response of bridge structures. Journal of Earthquake Engineering and Engineering Vibration, 7(4): 395-402.

Aviram, A., Mackie, K.R., and Stojadinovic, B. (2008b). Guidelines for nonlinear analysis of bridge structures in California. PEER Report 2008/03, Pacific Earthquake Engineering Research Center, Berkeley, CA.

Avşar, Ö. (2009). Fragility based seismic vulnerability assessment of ordinary highway bridges in Turkey. Ph.D. Thesis, Department of Natural and Applied Sciences, Middle East Technical University, Ankara, Turkey.

Avşar, Ö., Yakut, A., and Caner, A. (2011). Analytical fragility curves for ordinary highway bridges in Turkey. Earthquake Spectra, 27(4): 971-996.

Baker, J.W., and Cornell, C.A. (2005). A vectored-valued ground motion intensity measure consisting of spectral acceleration and epsilon. Earthquake Engineering and Structural Dynamics, 34(10): 1193-1271.

Caltrans (2013). Seismic design criteria, version 1.7. California Department of Transportation, Sacramento, CA.

CHBDC (2006). Canadian Highway Bridge Design Code, CAN/CSA S6-06. Canadian Standards Association, Rexdale, ON, Canada.

Choi, E., DesRoches, R., and Nielson, B. (2004). Seismic fragility of typical bridge in moderate seismic zones. Engineering Structure, 26(2):187-199.

Cornell, A.C., Jalayer F., Hamburger, R.O. (2002). Probabilistic basis for 2000 SAC federal emergency management agency steel moment frame guidelines. Journal of Structural Engineering, 128(4):526-533.

DesRoches, R., Leon, R.T., and Dyke, S. (2003). Response modification of bridges. MAE Center Project ST-12, MAE report 30-08. MAE Center, Urbana, IL.

Dicleli, M., and Bruneau, M. (1995). Seismic performance of single-span simply supported and continuous slab-on-girder steel highway bridges. Journal of Bridge Engineering, 121(10): 1497-1506.

FEMA. (2003). Multi-hazard loss estimation methodology: earthquake model: HAZUS- MH MR3 technical manual. Federal Emergency Management Agency, Washington, DC.

FHWA. (2012). Manual for design, construction, and maintenance of orthotropic steel bridges, FHWA-IF-12-027. US Department of Transportation Federal Highway Administration, Washington, DC.

Fu, G. (2013). Bridge design and evaluation: LRFD and LRFR. John Wiley & Sons, Inc., Hoboken, NJ.

Heidebrecht, A.G., and Naumoski, N. (2002). The influence of design ductility on the seismic performance of medium height reinforced concrete buildings. ACI special Publications SP-197. American Concrete Institute, Farmington Hills, MI.

Hines, W.W., Montgomery, D.C., Goldsman, D.M., and Borror, C.M. (2003). Probability and statics in engineering, 4th Edition. John Wiley & Sons, Inc., Hoboken, NJ.

Huang, K. (2014). Minimum number of accelerograms for time-history analysis of typical highway bridges. M.A.Sc. Thesis, Department of Building, Civil, and Environment Engineering, Concordia University, Montreal, QC, Canada.

Hwang, H., Liu, J.B., and Chiu, Y.H. (2001). Seismic fragility analysis of highway bridges. Report No. MAEC RR-4. Center for Earthquake Research Information, University of Memphis, Memphis, TN.

Hwang, H., Jernigan, J.B., and Lin, Y.-W. (2000). Evaluation of seismic damage to Memphis bridges and highway systems. Journal of Bridge Engineering, 5(4): 322-330.

Kelly, J.M. (1997). Earthquake-resistance design with rubber, 2nd Edition. Springer, Part of Springer Science+Business Media, London, UK.

Mander, J.B., Kim, D.K., Chen, S.S., and Premus, G.J. (1996). Response of steel bridge bearings to the reversed cyclic loading. Technical Report NCEER-96-0014, National Center for Earthquake Engineering Research, University at Buffalo, State University of New York, Buffalo, NY.

Mander, J.B., Priestley, M.J., and Park, R. (1988). Theoretical stress-strain model for confined concrete. Journal of Structural Engineering, 114(8): 1804-1826.

McKenna, F., and Feneves, G.L. (2005). Open system for earthquake engineering simulation (OpenSees), 1.6.2 Edition. Pacific Earthquake Engineering Research Center, Berkeley, CA.

Melchers, R.E. (2001). Structural reliability analysis and prediction, 2nd Edition. John Wiley & Sons, Inc., West Sussex, England.

Miranda, E., and Aslani, H. (2003). Probabilistic response assessment for building-specific loss estimation. PEER 2003/03, Pacific Earthquake Engineering Research Center, University of California at Berkeley, Berkeley, CA.

Naumoski, N., Heidebrecht, A.C., and Rutenberg, A.V. (1993). Representative ensembles of strong motion earthquake records. EERG report, 93-1, Department of Civil Engineering, McMaster University, Hamilton, ON, Canada.

Naumoski, N., Heidebrecht, A.C., and Tso, W.K. (1988). Selection of representative strong motion earthquake records having different A/V ratios. EERG report, 88-01, Department of Civil Engineering, McMaster University, Hamilton, ON, Canada.

Nielson, B. G. (2005). Analytical fragility curves for highway bridges in moderate seismic zones. Ph.D. Thesis, Georgia Institute of Technology, Atlanta, GA.

Nielson, B.G. and DesRoches, R. (2006). Influence of modeling assumptions on the seismic response of multi-span simply supported steel girder bridges in moderate seismic zones. Engineering Structures, 28(8): 1083-1092.

Nielson, B.G., and DesRoches, R. (2007). Analytical seismic fragility curves for typical bridges in the central and southeastern United States. Earthquake Spectra, 23(3): 615-633.

NRCC (2010). National Building Code of Canada 2010, Institute for Research in Construction, National Research Council of Canada, Ottawa, ON, Canada.

Padgett, J.E. and DesRoches R. (2007). Sensitivity of seismic response and fragility to parameter uncertainty. Journal of Structural Engineering, 133(12):1710-718.

Pan, Y., Agrawal, A.K., and Ghosn, M. (2007). Seismic fragility of continuous steel highway bridges in New York State. Journal of Bridge Engineering, 12(6): 689-699.

Pan, Y., Agrawal, A.K., Ghosn, M., and Alampalli, S. (2010). Seismic fragility of multispan simply supported steel highway bridges in New York State. I: Bridge Modeling, Parametric Analysis, and Retrofit Design. Journal of Bridge Engineering, 15(5): 448-461.

Paulay, T. and Priestley, M.J.N. (1992). Seismic design of reinforced concrete and masonry buildings. John Wiley & Sons, Inc., Hoboken, NJ.

Pekcan, G., and Abdel-Mohti, A. (2008). Seismic response of skewed RC box-girder bridges. Proceedings of the 14th World Conference on Earthquake Engineering, Beijing, China.

Priestley, M.J.N., Seible, F. and Calvi, G.M. (1996). Seismic design and retrofit of bridges. John Wiley & Sons, Inc., Hoboken, NJ.

Shafiei-Tehrany, R. (2008). Nonlinear dynamic and static analysis of I-5 Ravenna Bridge. Ph.D. dissertation, Washington State University, Pullman, WA.

Shome, N. (1999). Probabilistic seismic demand analysis of nonlinear structures. Report RMS-35, RMS Program, Department of Civil and Environmental Engineering, Stanford University, Stanford, CA.

Tavares, D.H. (2011). Seismic risk assessment of bridges in Quebec using fragility curves. Ph.D. Thesis, University of Sherbrooke, Sherbrooke, QC, Canada.

Tavares, D.H., Padgett, J.E., and Paultre, P. (2012). Fragility curves of typical as-built highway bridges in eastern Canada. Engineering Structures, 40: 107–118.

TNZ (2003). Bridge Manual, 2nd Edition. Transit New Zealand, Wellington, New Zealand.

Waller, C.L. (2011). A Methodology for probabilistic performance-based seismic risk assessment of bridge inventories. M.A.Sc Thesis, Department of Civil and Environmental Engineering, Carleton University, Ottawa, ON, Canada.

Wilson, J.C., and Tan, B.S. (1990). Bridge abutments: formulation of simple model for earthquake response analysis. Journal of Engineering Mechanics, 116(8): 1828-1837.